LEWIS-GRANT

original art
Reproducible
Copy
143 P.

IN-14857

AAE

AERONAUTICAL AND ASTRONAUTICAL

ENGINEERING DEPARTMENT

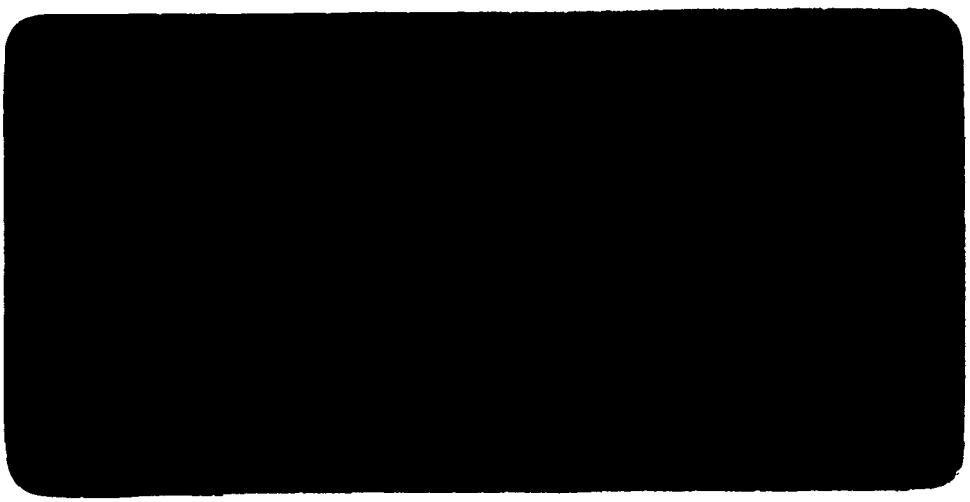

(NASA-CR-177132) THE BEHAVIOR OF FUEL-LEAN PREMIXED FLAMES IN A STANDARD FLAMMABILITY LIMIT TUBE UNDER CONTROLLED GRAVITY CONDITIONS Final Report, Jan. - Dec. 1985 (Illinois Univ.) 143 p HC A07/MF A01 G3/25

N86-28139

Unclas 43484

ENGINEERING EXPERIMENT STATION, COLLEGE OF ENGINEERING, UNIVERSITY OF ILLINOIS, URBANA

Aeronautical and Astronautical Engineering Department
University of Illinois Urbana, Illinois

Technical Report AAE 86-3
UILU ENG 86-0503

The Behavior of Fuel-Lean Premixed Flames in a Standard Flammability Limit Tube Under Controlled Gravity Conditions

by

Brian L. Wherley and Roger A. Strehlow
Aeronautical and Astronautical Engineering Department
University of Illinois at Urbana-Champaign

Final Report
NASA NCC 3-35
for the period
January 1985 through December 1985

Grant Monitor
Kurt Sacksteder

July 1986

Abstract

Fuel-lean flames in methane-air mixtures from 4.90 to 6.20 volume percent fuel and propane-air mixtures from 1.90 to 3.00 volume percent fuel were studied in the vicinity of the limit for a variety of gravity conditions. The limits were determined and the behavior of the flames studied for one g upward, one g downward, and zero g propagation. The one g upward and downward propagating flames were observed in ground tests while zero g was achieved in the NASA Lewis Airborne Research Facility, a modified Lear jet Model 25, by flying along Keplerian trajectories. This provided approximately 20 seconds of zero g. Gravity conditions were also varied in constant increments from 0.0 to 2.0 g's for upward propagation and continuously from 0.0 to 2.0 g's for upward and downward propagation. The flammability limit apparatus was designed to fit into two standardized aluminum racks, one containing a carrousel of eight shortened (0.71 meter) SFLT's. These were filled on the ground with mixtures of methane or propane and air and ignited at the open end of the tube in flight under the desired gravity conditions. Photographic data were collected using two 16 mm movie cameras mounted in the other rack, which also contained an automatic sequencing system to properly synchronize starting the cameras, opening of the tube, firing of the igniter, and, finally, to shut down all equipment when the experiment had been completed.

Photographic records of all flammability tube firings were obtained. The structure and behavior of these flames have been detailed including the variations of the curvature of the flame front, the skirt length, and the occurrence of cellular instabilities with varying gravity conditions.

The effect of ignition energy was also discussed. A survey of flame speeds as a function of mixture strength was made over a range of lean mixture compositions for each of the fuels studied. The results are presented graphically with those obtained by several other researchers. The flame speeds for constant fractional gravity loadings have been plotted as a function of gravity loading from 0.0 up to 2.0 g's against flame speeds extracted from the transient gravity flame histories for corresponding gravity loadings. Also, the effects of varying gravity conditions on the extinguishment process for upward and downward propagating flames were investigated. Flame propagation was initiated in zero gravity for a sufficiently lean fuel-air mixture; then the gravity loading was increased to roughly 2.0 g's, the flame extinguishing in the process.

Acknowledgements

I would like to thank the people at NASA Lewis Research Center in Cleveland, Ohio, for the support they provided in the air and on the ground. I have never had the pleasure of working with a finer or more professional group of people. Special thanks to Eric Neumann whose assistance expedited this research and made possible collection of more data than had originally been anticipated.

The Pilots
Bill Rieke
Earl Boyer
Bob McKnight

The Ground Crew
Bill Bohrer
John Johnson
Regina Kelly

Grant Monitor and Technical Advisor
Kurt Sacksteder

Operations Personnel
Eric Neumann
Ray Sotos

Photographic Consultant
Dave Clinton

Electrical Technicians
Eiter Reyes
Don Rhodes

Clerical Personnel
Gerry Ziemba
Sally Harrington

Preface

The first portion of this thesis is devoted to a description of the experimental apparatus used in this study. The methods used in calibrating the equipment have been discussed, and step-by-step procedural information has been provided. Also, the performance of this equipment has been evaluated with recommendations for improvements. This material has been extensively detailed to serve as a guide to any researcher who might be using the same apparatus in the future. Lastly, a complete record of all photographic data, intended as an index for NASA, catalogues each result of every tube firing according to the reel of film on which it appears and the order of its appearance on that reel.

Table of Contents

List of Tables

List of Figures

Nomenclature

Letters

A	Amperes
A	area, cm^2
ac	alternating current
C	capacitance of a condenser, Farads
DPM	digital panel meter
dc	direct current
f_i	statistical frequency of occurrence of the ith experimental measurement
$f(x,y)$	any function of variables x and y
g	gravity
Hz	Hertz, sec^{-1}
J	total of independent variables
M	mixture composition, volume % fuel
m	mean value
n	number of moles of gas
n	nth term in series
p	absolute pressure, mm Hg, kPa, psia
p_i	partial pressure of the ith species, mm Hg, psia
Q	volume flow rate, cm^3/sec

$\mathscr{R}$	universal gas constant
SFLT	standard flammability limit tube
S_b	flame speed, cm/sec
S_u	burning velocity, cm/sec
s_x	standard deviation in measurement x
s_y	standard deviation in measurement y
s_u	standard deviation in result u
T	absolute temperature, K
t	time, seconds
U	energy, Joules
u	result variable
V	Volts
V	voltage, Volts
V	volume, cm^3
w_i	statistical weight of the ith measurement
w_i	uncertainty interval for the ith measurement
x, y	independent variables
x_i, y_i	ith measurement of independent variables x and y

Greek Letters

δ	incremental value
μF	capacitance, microfarads

Subscripts

Act	actual
Avg	average
Obs	observed
STP	standard temperature and pressure
i	ith species
i	running index
j	running index
x, y	independent variables
u	result variable

Math operators

Δ	incremental change in property
Σ	summation sign
d	differential
∂	partial differential
$\equiv$	identity symbol

Introduction

For any given fuel-oxidizer system there is a range of composition over which these mixtures can sustain flame propagation. At the extremes of this range are the fuel-lean and fuel-rich flammability limits characterized by a fuel-to-oxidizer ratio less than stoichiometric and greater than stoichiometric, respectively. The limit mixture compositions for a given system are determined using a standard flammability limit tube (SFLT) of two inches (51 millimeters) inside diameter and from four to six feet (1.22 to 1.83 meters) long. Such a tube has one closed and one open end and, when filled with a flammable mixture, is ignited at the open end. The tube orientation may be such as to produce a flame that propagates either upward or downward in the Earth's gravitational field. Thus, there exist both upward and downward limits of propagation for fuel-lean and fuel-rich flames. The exact values of these limits can be influenced by the temperature and pressure of the mixture, gravity, the test apparatus geometry, combustion instabilities and, for rich mixtures, the formation of soot. How these factors affect the limit values is not completely understood. Limit flames are weak, propagating with extremely low flame speeds, and they are most strongly influenced by gravity-induced buoyancy effects. The interaction of the hot, less dense product gases with the cool, denser unburned mixture can act to stabilize or destabilize the flame front, depending on whether the flame is moving with the induced flow or against it. Hence, experimentally determined values of the limit mixture composition for a given fuel-oxidizer system are typically quite different for upward and downward propagation. Because of the profound effect that gravity has on limit flame behavior, it was

selected as the parameter to be varied in this study, keeping the remaining variables as constant as possible.

2 Experimental Facility, Apparatus and Procedure

2.1 NASA Lewis Airborne Research Facility

The variable-gravity experiments were performed in NASA Lewis Research Center's Airborne Research Facility. This is a Lear jet Model 25 business jet that has been modified internally to carry racks to contain the research apparatus (see Figure 2-1). The cabin layout has been changed to accommodate three researchers and the experimental racks. These racks are mounted on twin rails fixed to the left side of the cabin floor as illustrated in Figure 2-2. In addition, electric power is provided to the apparatus in a variety of direct and alternating current/voltage combinations. Instrumentation on board the aircraft that is important to the researcher includes a three axis accelerometer package, mounted aft of the rear bench seat, as well as an analog device that recorded the X, Y, and Z components of acceleration as a function of time on photosensitive paper ("Visicorder"). The cabin was darkened completely to facilitate collection of photographic data because of the very low luminosity of the near-limit flames.

The variable gravity conditions were, in large part, achieved by flying along a Keplerian trajectory or modified version of it for each experiment. Prior to the series of experiments conducted in this study, an upgraded accelerometer package was installed in the aircraft. The X, Y, and Z components of acceleration were displayed using three digital panel meters (DPM's), and this information was recorded on the 16 mm film with the image of the flame. In addition to the accelerometers, an upgraded display that provides the pilot with vertical and

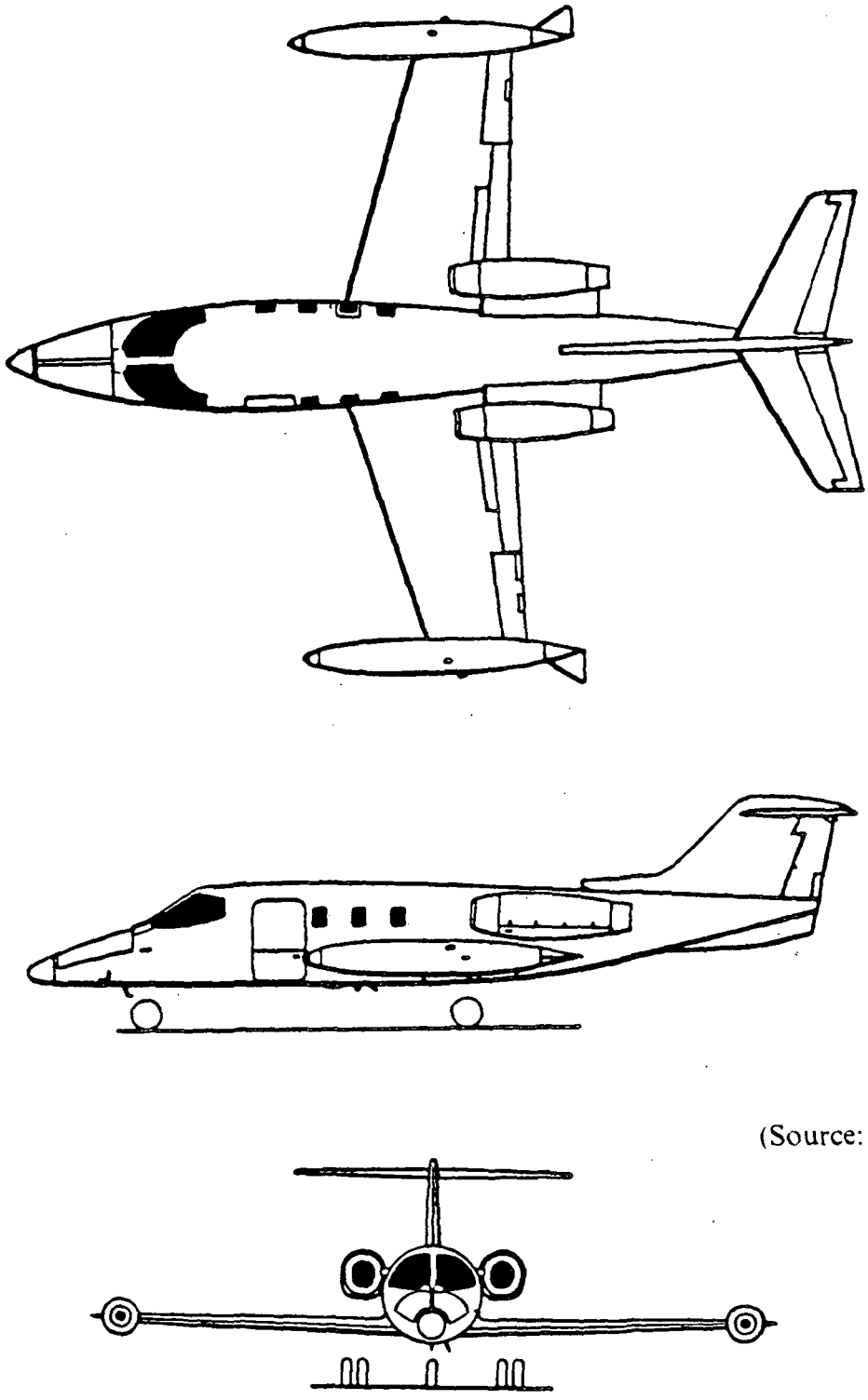

(Source: Ref. 1)

Figure 2-1. The NASA Lewis Airborne Research Facility. A three-view drawing of the Lear jet Model 25.

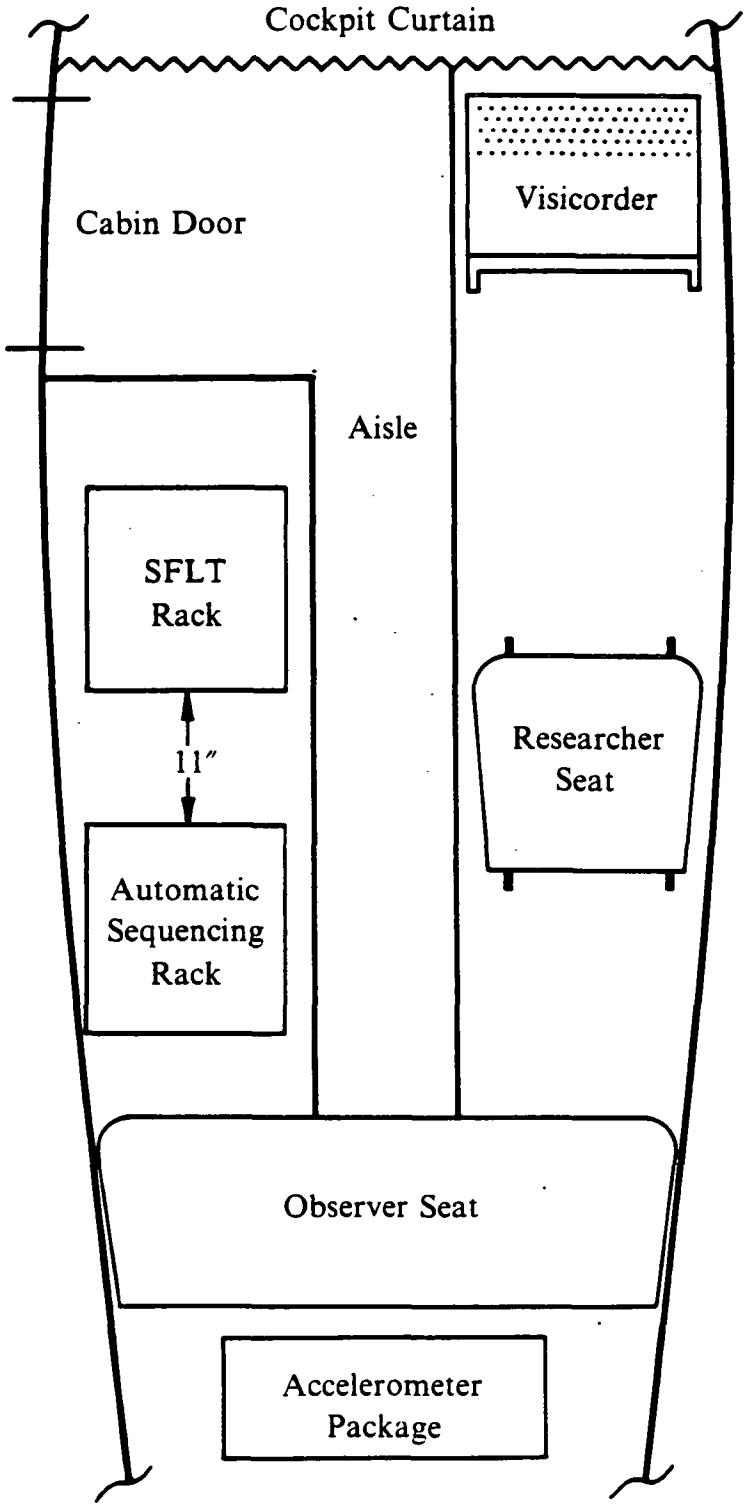

Figure 2-2. Aircraft cabin layout. The plan view of the modified Lear jet cabin showing the proximity of the researcher to the research equipment.

lateral acceleration information was installed in the cockpit. The importance of this display is that it permits the pilot to fly the aircraft at a constant fractional gravity loading, as well as at the zero gravity that was previously attainable. Furthermore, it allows these gravity conditions to be maintained more accurately over a greater portion of the trajectory, providing an excellent opportunity to conduct experiments at a number of gravity loadings. The difference between the actual acceleration the aircraft is undergoing and the desired acceleration is indicated by light-emitting diodes (LED's), which have been represented in the diagram of the cockpit display in black by the rectangles, the four arrows, and the central circle (see Figure 2-3). The Z axis has an expanded section that covers −0.015 g to +0.015 g, distinguishable by the larger rectangles. The shaded area in the center covers −0.01 g to +0.01 g. For a given setting, the pilot applies aerodynamic control so that the center LED is the only one that remains lit. This corresponds to zero acceleration in the aircraft's lateral, or Y, axis and the desired g loading in the normal, or Z, axis (parallel to the longitudinal axis of the SFLT). A separate display similar to this provides longitudinal, or X, axis acceleration information to the copilot who is responsible for maintaining a zero thrust axis using appropriate throttle control (zero acceleration in the X axis). A switch is provided on this display to select the desired constant fractional gravity loading: 0.00, 0.10, 0.17, 0.25, 0.33, 0.50, 0.75, 1.00, or 1.50 g's. A total of 20 seconds of zero or partial gravity is available to the researcher. The probability that 10 seconds of this time will be within ± 0.01 g of the nominal value for the pitch, or Z, axis is 80%, depending strongly on the atmospheric conditions and on the skill of the pilots. Usually, the lateral and longitudinal accelerations are also within these limits. However, small fluctuations in the g loading inevitably result and shall be referred to hereafter as g-jitter. G-jitter is characterized by relatively small random g fluctuations around the nominal value. The data collected confirmed that the lateral and longitudinal accelerations were quite small, typically well below 0.01 g, and as such did not contribute noticeably to the motion of the flames along the axis of the tube. Thus, only the effects of varying the gravity loading in the direction of the tube axis were reported.

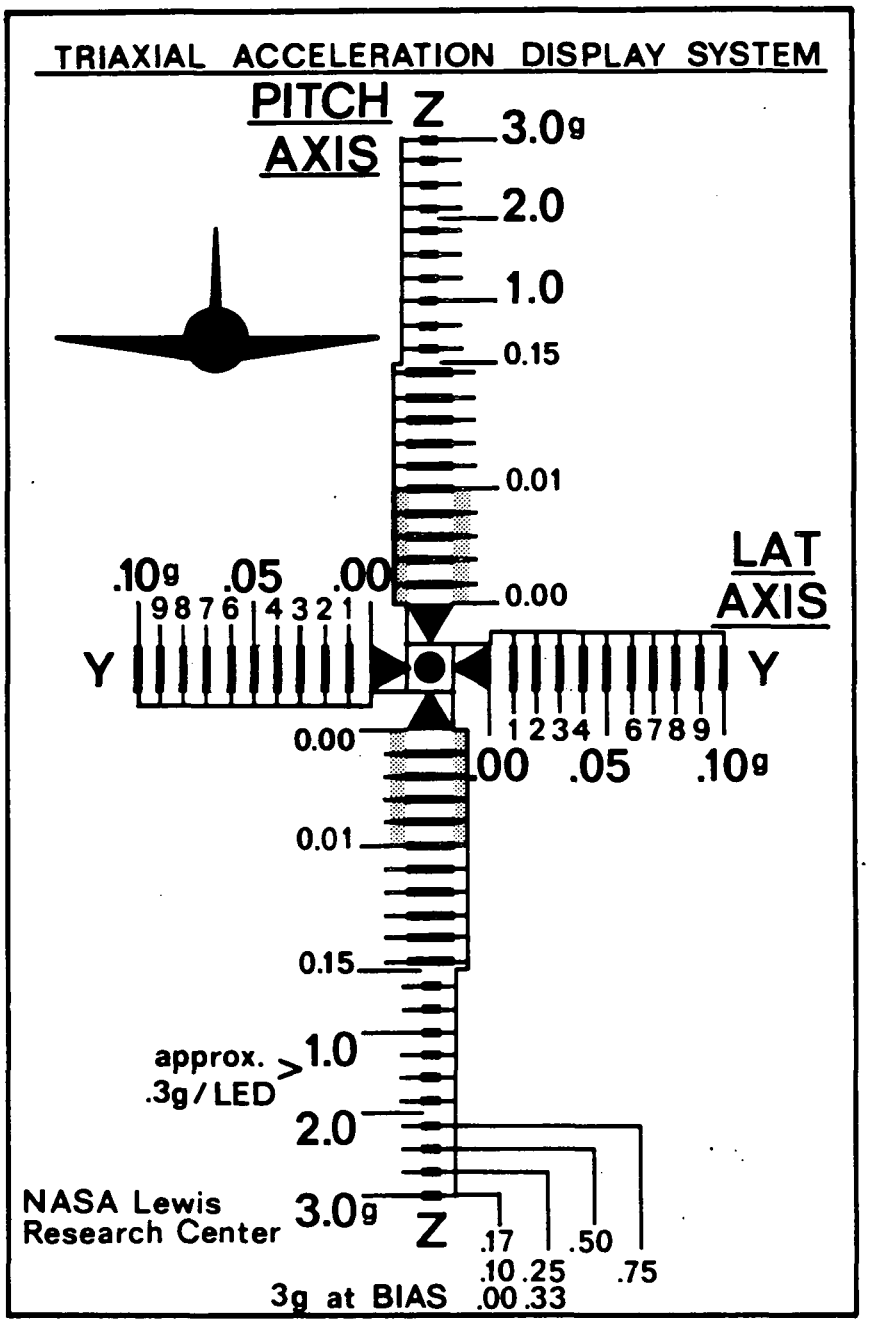

Figure 2-3. Triaxial Acceleration Display System.

It should be noted that during some of the trajectories flown at gravity loadings other than zero and one g, the actual gravity loadings as displayed by the DPM's contained within the experimental rack were consistently different than the nominal values expected. This was attributed to the use of a new, more sensitive cockpit accelerometer display that was essentially being flight tested during this time and may have been the result of incorrect biasing of the substitute device. This presented no problem. In the analysis of all data, the DPM readings were the values used. The factor to convert the DPM readings to engineering units was 2.47 Volts/g. The panel meter readings depended linearly on the gravity loading.

2.2 Flammability Limit Apparatus

The overall design of the flammability limit apparatus study was determined by four major factors:

- The apparatus had to fit within standardized equipment racks.
- Provisions for photographing the flames had to be made.
- The flammability limit tubes had to safely contain the flammable mixtures of gases at all times, especially during the combustion process.
- The entire operation of the apparatus had to be as automatic as possible since the researcher had to remain securely belted in a seat during a trajectory.

2.2.1 Standard Equipment Racks:

First, the complete flammability limit apparatus had to be designed to be compatible with standardized research equipment racks constructed by NASA for use in the Lear jet. These racks are of riveted aircraft aluminum sheet and angle construction measuring 24 x 21 x 36

inches, length, width, and height, respectively. To meet the dimensional requirements of the racks, the standard 51 mm-diameter flammability limit tube was shortened from 1.83 meters in length to 0.71 meters. In addition, the racks with the equipment installed, as well as the equipment itself, had to withstand specified load factors without producing yield stresses in the materials used. These load factors are as follows [2]:

Load Factor	Load Direction
9.0 g	Forward
1.5 g	Aft
2.0 g	Upward
7.0 g	Downward
1.5 g	Lateral

Reference [2] may be consulted for further specifications of the Lear jet and its capabilities.

2.2.2 Photographing the Flames:

In addition to determining the variation of the lean limit with gravity, an important facet of this study was to collect data on changes in the behavior of the flame itself. This included analyses of the flame shape and the flame speed, and observation of any manifestation of combustion instability and of the extinguishment process itself. The device chosen to record all of this information was a 16 mm movie camera operated at 24 frames per second. To obtain images of the flames that were as large as possible, to provide the necessary detail of flame structure and to collect as much light as possible, two movie cameras were used, each fitted with an f 1.8 lens. The two cameras were positioned one directly above the other so that one camera covered the top two-thirds of the SFLT and the other covered the bottom two-thirds of the SFLT. Their fields of view overlapped at the middle one-third of the tube. Each camera was loaded with a 200 foot roll of Eastman Ektachrome high speed, 7250 Tungsten, VNX 430, ASA

400, Video News film perforated along both edges, catalog number 121 8684. Because of the low luminosity of the limit flames, the film was forced processed one f-stop to enhance the photographic images. Even using forced processing, some flames were all but invisible on the film. The cameras operated on 28 V dc power at a continuous current of 2 A each (4 A total) with a starting current of 5 A each (10 A total). The system was also equipped with two small incandescent lights that illuminated the tube and its information placard immediately prior to a firing. The illumination occurred during the starting period for the cameras before their speed had stabilized and provided a record of the tube number, time of day (A.M. or P.M.), date, and the gravity conditions investigated. This information could be matched to the log that specifies the mixture that each tube contained and the results of each firing.

Also located for inclusion in the photographic record are three digital panel meters (DPM's) that display the three-axis accelerometer output in Volts and one that displays the cabin pressure in units of psia. Since the analyses were directed toward determining the influence of gravity along the tube axis (Z-axis), the DPM's were arranged vertically along the length of the SFLT (see Figure 2-4) with the Z-axis display located so that it would be photographed by both cameras.

2.2.3 The Standard Flammability Limit Tubes:

Because of the unacceptable risk involved with operating a filling system on board the aircraft, and also considering the limited time available to the researcher during flight, it was necessary to design the apparatus to contain multiple flammability limit tubes that could be filled with different mixtures on the ground prior to take-off. Practicality dictated that the two cameras be located in a fixed position while the SFLT's were assembled in a carrousel arrangement supported between two plexiglas rings that rotated on "lazy-Susan" bearings. These shortened SFLT's were constructed from clear 0.125-inch-wall plexiglas tubes. The closed end of each tube was fitted with a plexiglas cap held in place securely by four allen-head screws and

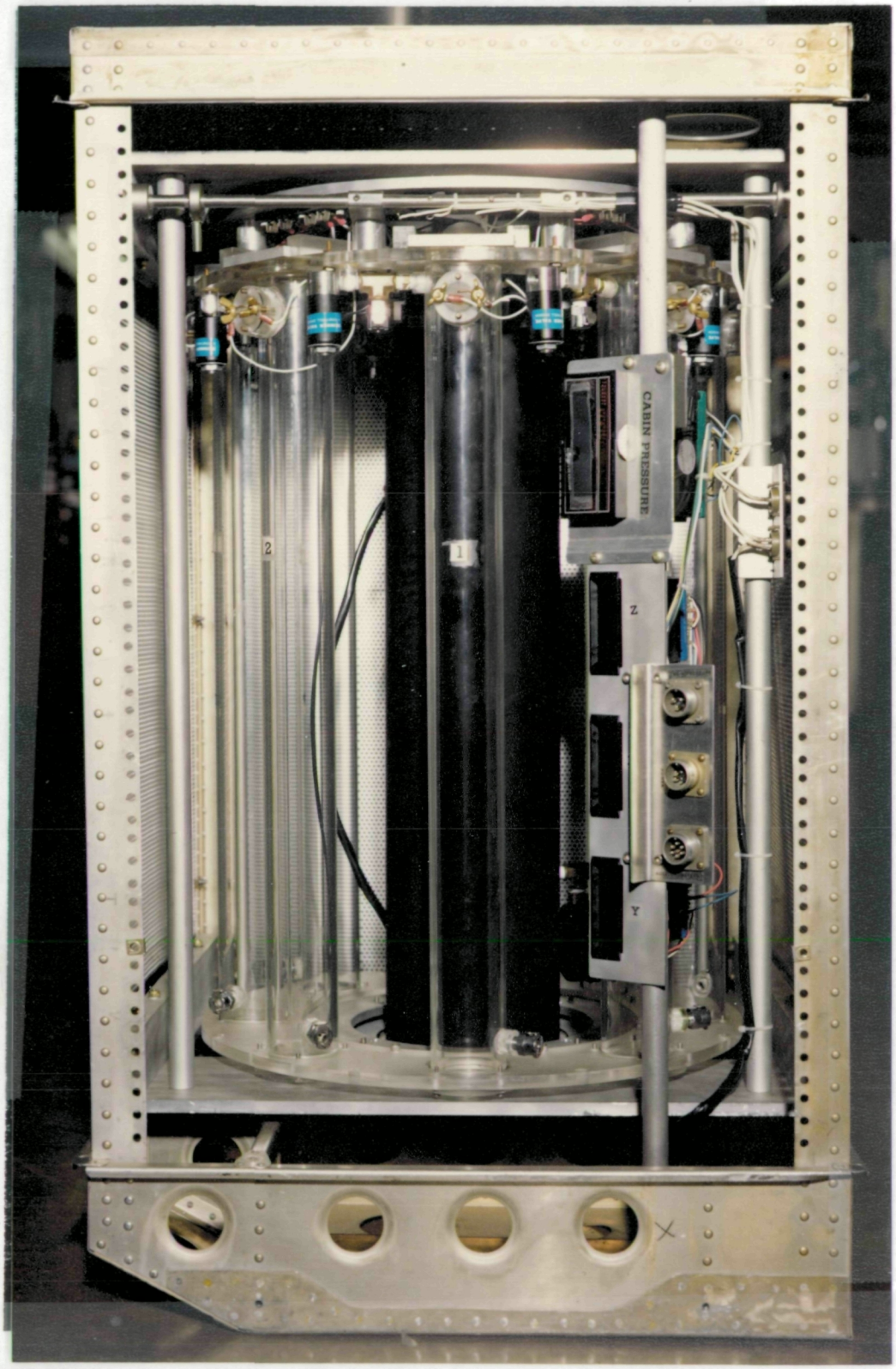

Figure 2-4. The flammability limit apparatus. A photograph of the complete flammability limit apparatus installed in the NASA rack. The eight-tube carrousel has been inverted in the NASA rack for downward propagation studies and the number one tube is in firing position. Note the DPM's and the cabin pressure display to the right of the number one tube.

sealed with an O-ring. Removal of this cap permitted cleaning of the tube between firings. The other end of the SFLT was equipped with a sliding, O-ring sealed, aluminum plate valve that kept the tube closed until it was fired. The operation of this valve is detailed in Figure 2-5. Examination of the figure reveals that the sliding plate valve has a slot machined on its underside that engages the plunger of a pneumatic cylinder. This plunger is driven by a high pressure air tank mounted in the center of the carrousel. The tank is fitted with a quick-disconnect socket for filling and a Bourdon-tube pressure gauge. The pneumatic cylinder was found to operate most effectively when the tank pressure was maintained between 25 and 40 psig. Air flow from the tank to the pneumatic cylinder was controlled by a solenoid valve. Activating the solenoid valve extended the plunger, forcing open the sliding plate valve that seals the SFLT. At the end of a tube firing, the solenoid valve closes, shutting off air from the tank and venting the air in the pneumatic cylinder to the atmosphere. Venting the air allows the piston to return to its original position under spring tension.

Each SFLT is fitted with two quick-disconnect sockets, at opposite ends of the tube, to allow purging of the air from the SFLT during filling. Also near the open end of the tube, a short plexiglas collar is cemented to the exterior of the tube. A 0.625-inch-diameter hole has been bored through this collar and the tube wall. An O-ring sealed plexiglas plug containing two copper leads bridged by a coil of nichrome wire serves as the igniter and is inserted into this hole before filling the SFLT. The coil is coated with a solution of nitrocellulose in acetone and allowed to dry before installation. The energy released by combustion of the nitrocellulose, when a capacitor is discharged across the coil, is more than sufficient to consistently ignite limit and near-limit mixtures. Once a SFLT is in firing position, a locking lever is manually rotated, thereby aligning and securing the tube in that postion and simultaneously engaging two sets of knife switches. These knife switches provide power to the microswitch on each SFLT that controls the igniter. The sliding plate valve triggers the microswitch upon reaching the fully open position so that ignition can occur only when the desired tube is locked in firing position

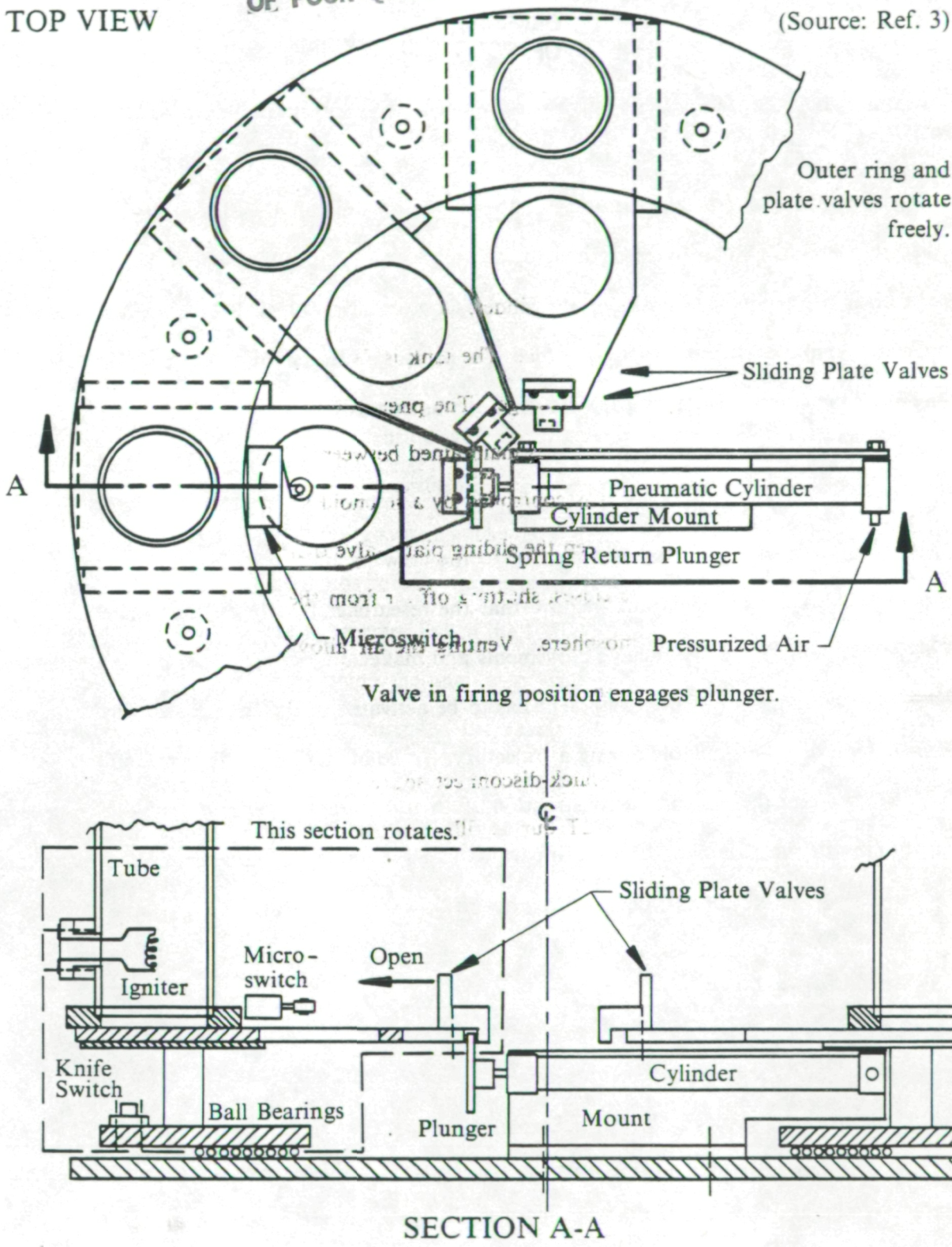

Figure 2-5. Sliding plate valve detail. The entire outer ring assembly rotates allowing the plunger to engage only one sliding plate valve at a time.

and only when the sliding plate valve is fully open. This precludes any possibility of firing a closed tube. The knife switches also control power to the solenoid valve that opens just before firing to equalize the internal pressure of the tube with the cabin pressure. The SFLT's were filled to a pressure slighty greater than the cabin pressure at altitude so that no air entered the tube prior to opening the sliding plate valve, and to ensure outward flow when the tube was opened. Venting was necessary to reduce this pressure differential and prevent unsteady behavior of the column of gas in the tube when it was opened.

2.2.4 The Automatic Sequencing System:

To prevent injury to the researcher or to the crew members of the Lear jet during a trajectory, NASA safety regulations require that the researcher remain securely belted in a seat. This severely limits the researcher's movements and makes only minor manual operations practical. Furthermore, all of the equipment has to be activated in the correct sequence within the limited span of time available during a trajectory. In combination, these two factors were sufficient to warrant the design and construction of an automatic sequencing system to control the functioning of the flammability limit apparatus (see Figure 2-6). This system had to perform several tasks for each tube firing including operation of the following:

- timer motor power
- automatic cycle indicator light
- 16 mm movie cameras and timing light generator
- photographing lights
- tube pressure equalization valves

- pneumatic plunger solenoid valve

The heart of the automatic sequencing system is the timer box. This controller is mechanical rather than electronic to make repairs while at the hangar as simple as possible. The timer box consists of an axle that has affixed to it six evenly spaced 5.0-inch-diameter, 0.25-inch-thick aluminum cams held fast by allen-head set screws. The perimeter of each cam has been machined so that the radius of the disk is reduced over a predetermined arc length. Six microswitches are mounted along the inside wall of the timer box positioned so that one switch engages the edge of one cam. Presently, only four of the six microswitches are being used to operate the automatic sequencing system. The axle is driven at two revolutions per minute by a 115 V ac motor. As the cams rotate, the microswitches are held in the "ON" position along raised portions of the disk perimeters and in the "OFF" position where the disk perimeters have been machined away. By varying the angular position of these cams with respect to the axle and the length of their raised portions, the relative triggering of the desired events by the microswitches can be controlled.

The timer box, movie cameras, timing light generator, ignition system, and pressure transducer are all mounted in a standard Lear jet equipment rack. A control panel has been installed in this rack within easy reach of the researcher. Mounted in this panel (see Figure 2-7) is a single-pull double-throw master switch that controls the 28 V direct current, as well as the 115 V, 60 Hz, alternating current to all electrical components contained within the racks except for the DPM's and the digital pressure transducer with its display, which are each controlled by separate power switches. When the master switch is in the "ON" position, two red indicator lights, one for each voltage/current combination, remain lit. Fuses of 1 A for the 115 V line and 10 A for the 28 V line have been installed adjacent to the indicator lights. Red indicator lights and line fuses are also provided for the DPM's and the pressure transducer. In addition to controlling power to the automatic sequencing system, turning on the master switch energizes

the ignition system. This is the only electrical system not directly controlled by automatic sequencing. The ignition system consists of a 38,000 μF capacitor in series with a 100 Ω high power resistor to limit the current flow to the capacitor, a small dc voltmeter, and a nichrome coil igniter. The value of the capacitance was selected based on tests with the igniters which showed that it provided a discharge that was strong enough to ensure ignition without burning out the nichrome wire coil. The capacitor/resistor combination is charged from the 28 V dc supply and has a charging time constant of approximately 15 seconds which is adequate to fully charge the capacitor in the time between tube firings. A voltmeter mounted near the top of the control panel is used to monitor its state of charge. Shielded wire is attached to the terminals of the capacitor and connected by a cannon plug to the SFLT rack. From this junction, the lines are connected through the knife switches, that engage only the tube in firing positon, to a microswitch that can close the ignition circuit across the igniter coil. With the desired tube selected and securely locked into firing position, the system is ready for an automatic sequencing cycle.

The number one disk on the timer axle controls power to the timer motor itself. To initiate a firing sequence, a hand-held push-button switch is depressed for approximately 1 second. In 1 second, the number one disk has rotated sufficiently to engage the corresponding microswitch and maintain power to the timer motor without further researcher intervention. An orange light is used to indicate that an automatic sequencing cycle is in progress. The precise order in which the equipment is activated and the duration of its operation are given for each piece of equipment as a function of the particular cam that controls it in Figure 2-8.

The entire experimental set-up is brought up to functional status by turning on the master power switch, the DPM power, and the pressure transducer power. This activates the timing light generator and, also, the ignition system capacitor begins to charge. Once the automatic sequencing switch has been depressed and held for the required 1-second interval, the

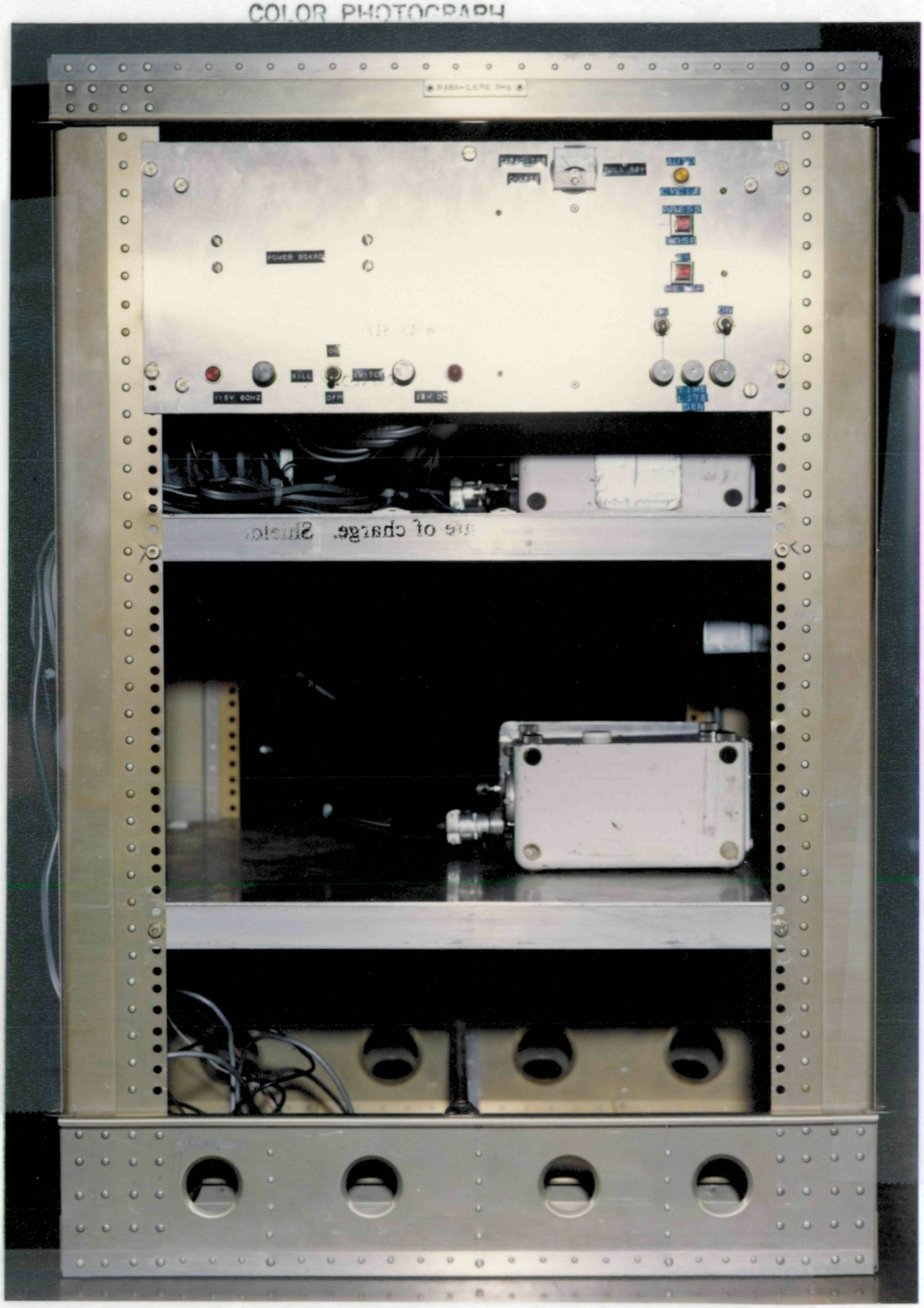

Figure 2-6. The automatic sequencing system. A photograph of the automatic sequencing system components installed in the NASA rack showing the control panel layout. and the two 16 mm movie cameras.

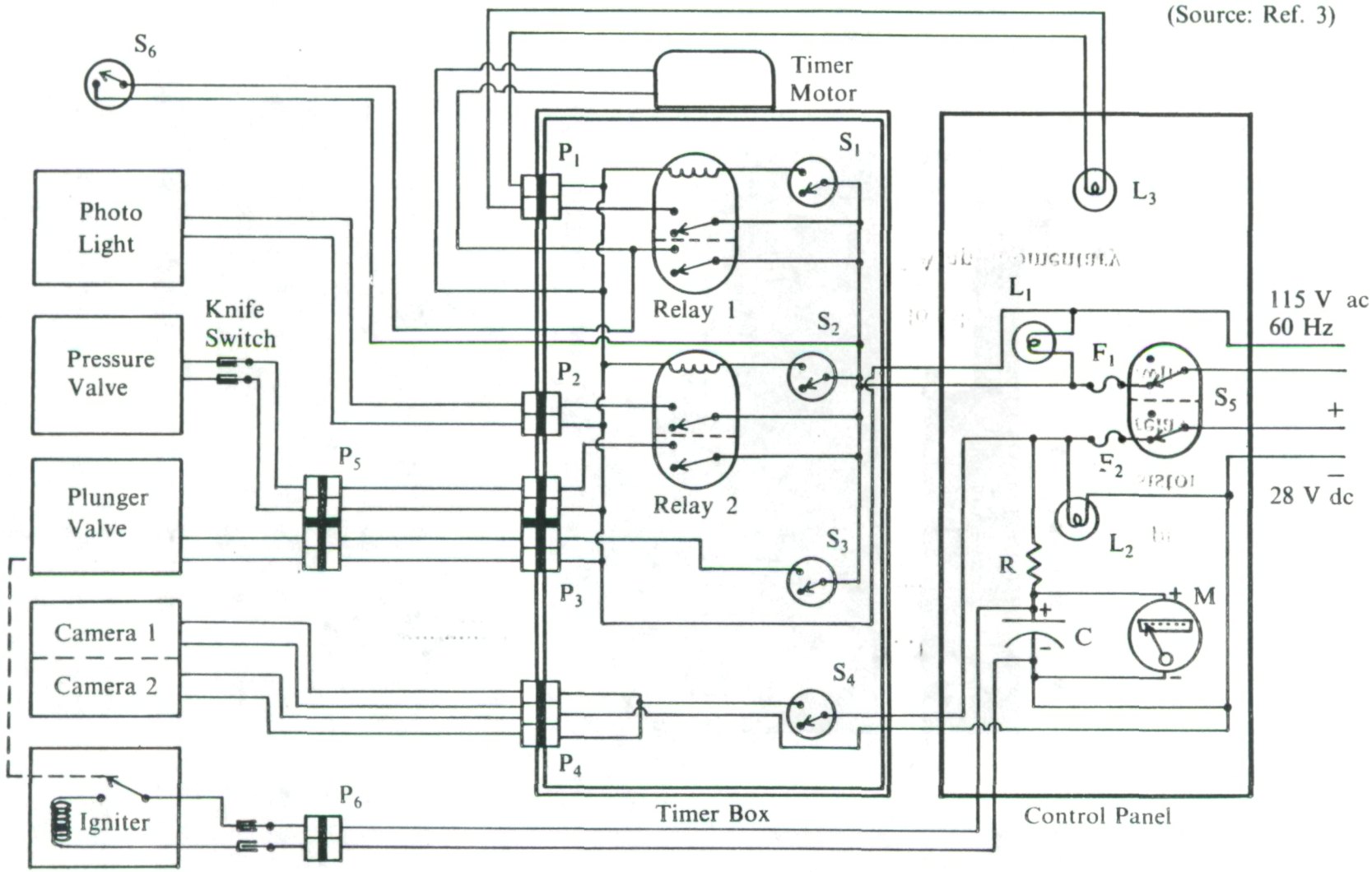

Figure 2-7a. Automatic sequencing system timer unit electrical diagram.

C.....38,000 Microfarad capacitor

F_1.....0.5 Amp, 115 Volt fuse

F_2.....10 Amp, 28 Volt fuse

L_1, L_3.....115 Volt indicator lights

L_2.....28 Volt indicator light

$P_1 - P_6$.....Cannon plug; 2,4,3 pins

R.....100 Ohm resistor

Relays 1 & 2.....10 amp contact relays

$S_1 - S_4$.....15 Amp, single-pull double-throw microswitch

S_5.....15 Amp, double-pull double-throw microswitch

S_6.....5 Amp momentary switch

(Source: Ref. 3)

Figure 2-7b. Description of automatic sequencing system timer unit electrical components.

orange indicator light signals that the firing sequence is in progress and it remains on for the duration of the sequence. At 1 second, the solenoid valve that equalizes the SFLT internal pressure with the pressure in the aircraft cabin opens for 1 second. Also, at this time, the 16 mm movie cameras are started and the incandescent light is activated for a 1-second interval to photograph the tube number, date, flight and gravity conditions being investigated as written on an information placard located near the DPM's. At 5 seconds, both camera motor speeds have stabilized, and the solenoid valve that activates the pneumatic cylinder is opened. The plunger forces open the sliding plate valve at the bottom of the tube in firing position. When the sliding plate valve reaches the fully open position, the ignition circuit microswitch is triggered, allowing the capacitor to discharge through the igniter, possibly resulting in a propagating flame. At 24 seconds, after even the slowest flame would have propagated the length of the tube, the cameras shut down and in 1 second more, the sliding plate valve closes. The timer box then shuts down and the cycle has come to its conclusion. Another tube may then be selected for firing, manually rotated into position, and locked in place.

2.3 Gas-Mixing System and Calibration

The calibration of the rotameters used in the mixing system was the first and one of the most important pieces of work to be completed for this project. The credibility and accuracy of the data collected depend upon the exact degree of confidence with which a given flow rate is known. Because the flow rates of the mixing system are determined by the differential between the upstream and downstream pressures, the apparatus has been configured with an upstream and a downstream pressure gauge for both the fuel and air rotameters (see Figure 2-9). As an example, consider the calibration of the air rotameter.

To calibrate the air rotameter, it was first necessary to select appropriate upstream (supply) and downstream (back) pressures capable of providing the required flow rates over a suitable

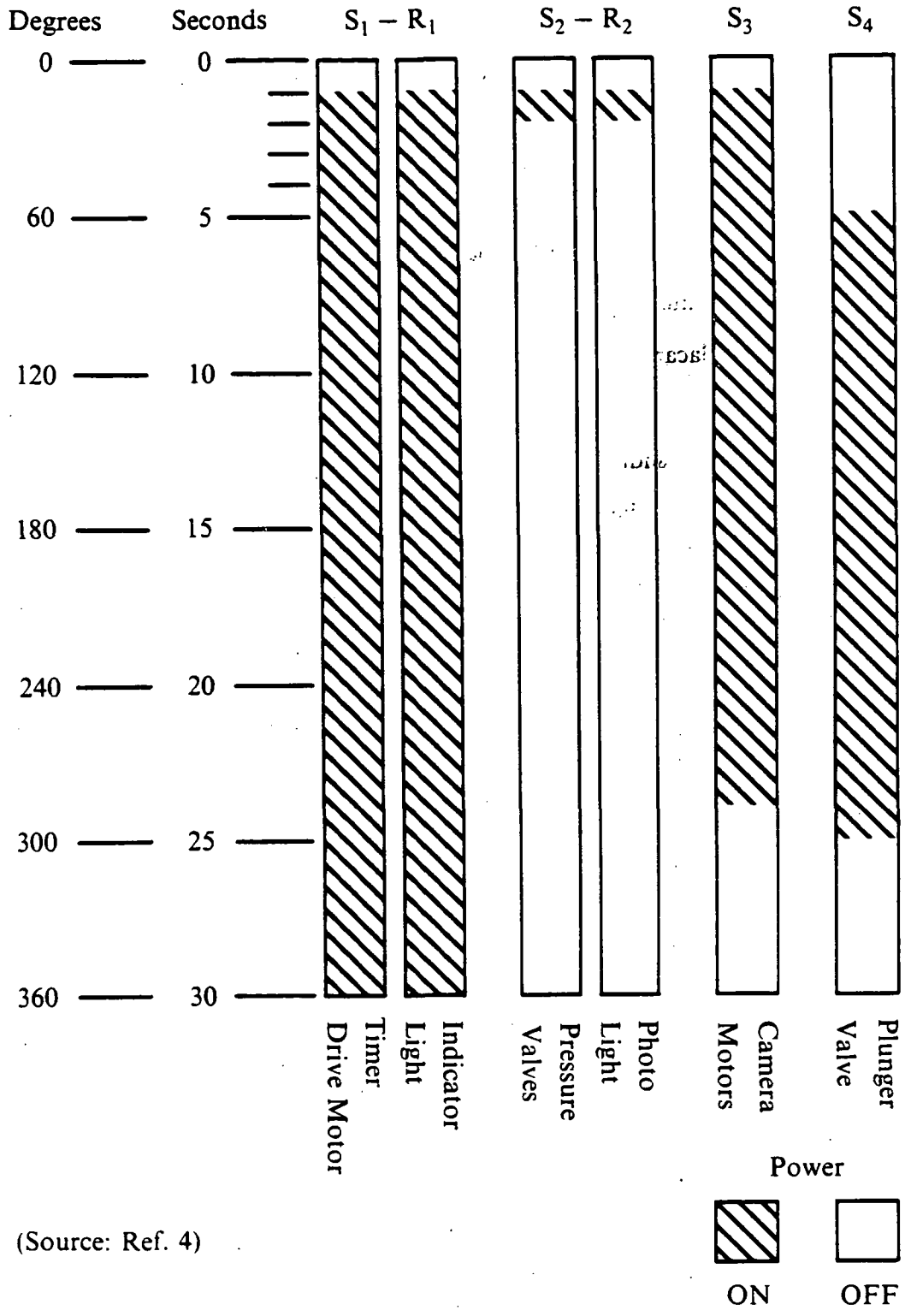

(Source: Ref. 4)

Figure 2-8. Detail of the timing sequence. The duration of operation of each automatic sequencing system component is given in units of time and in units of angular displacement of its governing cam.

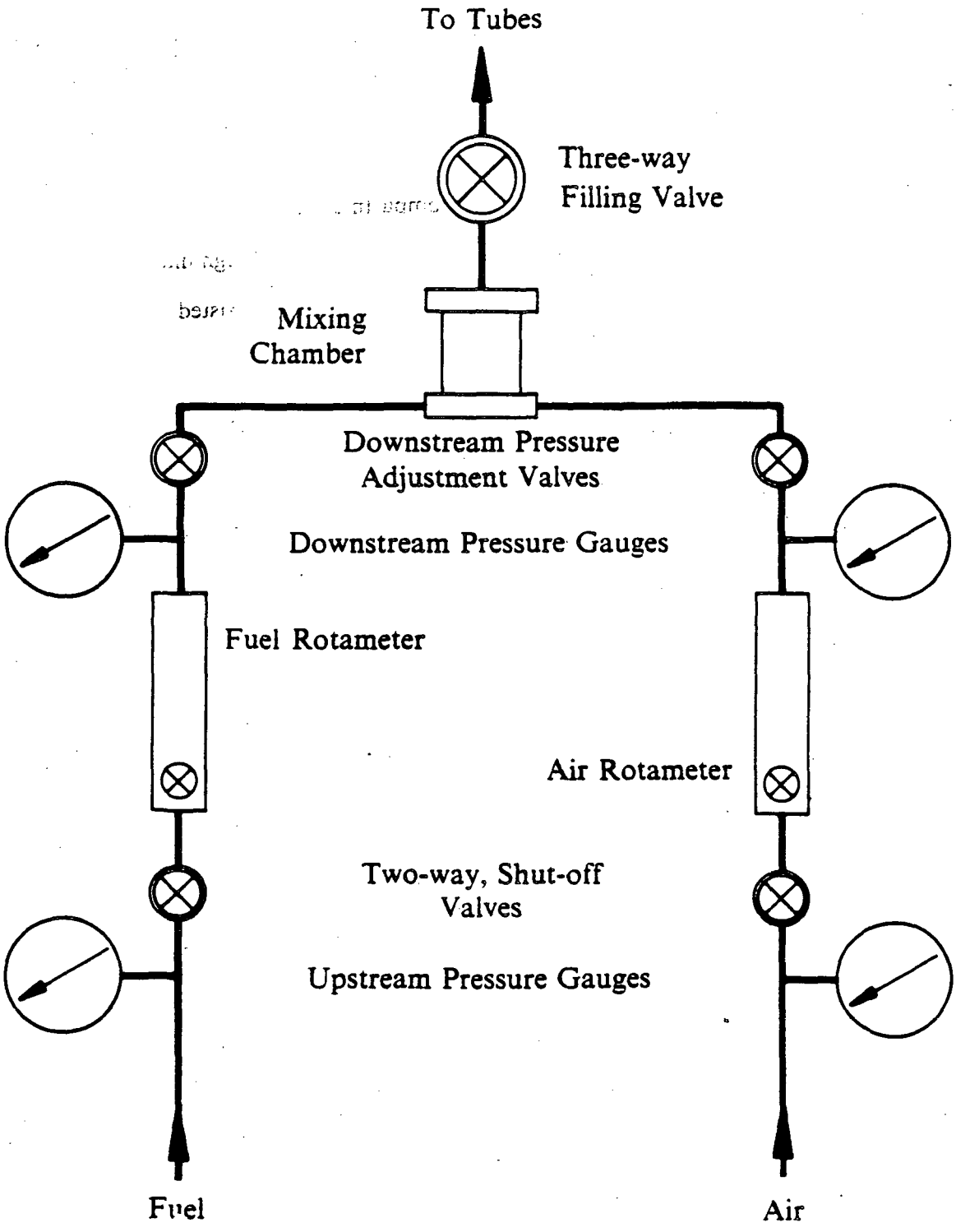

Figure 2-9. Gas-mixing system schematic. Note the upstream and downstream pressure adjustment valves.

range of the rotameter scale. The flow rate for the air rotameter was largest and, consequently, determined the supply pressure, which was limited only by the structural integrity of the plexiglass mixing chamber. An upstream pressure of 25.0 psig was found to meet these criteria. The mixing chamber itself contained two compartments. The first was a swirl chamber into which the streams of fuel and air were injected tangentially through diametrically opposed ports. The swirl chamber emptied into a second compartment that consisted of a chamber packed with coarse stainless steel wool to enhance mixing and dampen nonsteadiness of the flow. The air flow rate also determined the maximum allowable downstream pressure. A suitably small value that met the flow rate requirements was found to be 15.0 psig. This value also had to be large enough to absorb the greatest downstream pressure offered by the SFLT's, which was observed when filling all eight SFLT's simultaneously. In this manner, the rotameters could be calibrated over a range of settings at constant upstream and downstream pressures, ensuring consistent flow rates regardless of variations in the downstream flow impedance with different tubes or combinations thereof. With suitable upstream and downstream operating pressures determined, the pressures were set dynamically and maintained during the calibration and filling processes within specified limits. The calibration rig consisted of a 2,000 cm^3 graduated cylinder filled with water and inverted. It was held in position several centimeters off the bottom of a water tank by a clamp attached to a ring stand. Also attached to the ring stand was a plexiglas box containing a glass prism held at the level of the water so that the line of meniscus in the graduated cylinder could be read easily and accurately. To calibrate the rotameters, the mixing system was operated separately for each individual gas tested. Each rotameter was calibrated over a range of settings that bracketed the flow rates required to produce the desired range of mixture compositions. The rotameters were read from the top of the spherical float rather than the center to minimize reading error. With the three-way valve set on "FILL", the metered gas was bubbled into the inverted graduated cylinder for an interval of time that was measured by a hand-held digital stop watch. The graduated cylinder was then checked for its vertical alignment and the height of the cylinder was adjusted so that the meniscus of the column of water

in the cylinder coincided with the level of the water in the tank. This eliminated the need for correcting for the height of the column of water. This method was subject to a certain amount of precision error due to the difficulty inherent in starting the watch at the same time the tube was placed under the graduated cylinder and stopping the watch when the tube was removed from beneath the graduated cylinder. To reduce this precision error, multiple readings were taken for each rotameter setting. These data were reduced and used to construct a plot of the volume flow rate versus rotameter setting. This was always found to yield a straight line and an analytical expression was easily determined. The exact method of flow rate data reduction is summarized by the following example calculations:

Table 2-1. Air rotameter flow rate calibration data.

Trial Number	Air Rotameter Setting (Steel Float)	Filling Time (seconds)	Observed Volume (cm^3)	Uncorrected Flow Rate (cm^3/sec)
1	60.0	11.51	1840	159.86
2	60.0	10.46	1645	157.26
3	60.0	11.89	1880	158.12
4	60.0	11.58	1825	157.60
5	60.0	12.09	1910	158.00

where

upstream pressure = 25.0±0.10 psig

downstream pressure = 15.0±0.05 psig

ambient temperature = 69.1 °F

water temperature = 68.8 °F (20.44 °C)

barometric pressure = 29.272 in (743.51 mm Hg).

Assuming that the air in the graduated cylinder was saturated with water vapor, the partial pressure of water vapor is 18.02 mm Hg [5] and Dalton's Law of partial pressures yields

$$p_{\text{Total}} = \sum_{i=1}^{n} p_i = p_{H_2O_{\text{Gas}}} + p_{\text{Air}} \qquad [2\text{-}1]$$

$$p_{\text{Air}} = p_{\text{Total}} - p_{H_2O_{\text{Gas}}}$$

$$= (743.51 - 18.02) \text{ mm Hg}$$

$$= 725.49 \text{ mm Hg}$$

where p is the gas pressure. The Ideal Gas Law is applied to determine the actual flow rate.

$$pV = n\mathcal{R}T \qquad [2\text{-}2]$$

where p is the gas pressure, V is the volume of gas, n is the number of moles of gas, $\mathcal{R}$ is the universal gas constant and T is the gas temperature. Equation [2-2] can be used to determine the actual volume of air occupying the measured, or observed, volume in the graduated cylinder and, therefore, the actual flow rate.

$$p_{\text{Observed}} V_{\text{Observed}} = n\mathcal{R}T_{\text{Observed}}$$

and

$$p_{\text{Actual}} V_{\text{Actual}} = n\mathcal{R}T_{\text{Actual}} .$$

Then

$$\frac{p_{\text{Obs}} V_{\text{Obs}}}{p_{\text{Act}} V_{\text{Act}}} = \frac{T_{\text{Obs}}}{T_{\text{Act}}} = 1 .$$

$$V_{Act} = \frac{p_{Obs} V_{Obs}}{p_{Act}} \qquad [2\text{-}3]$$

In a similar fashion, the actual volume of air determined by Equation [2-3] can be related to standard conditons (STP).

$$\frac{p_{Act} V_{Act}}{T_{Act}} = \frac{p_{STP} V_{STP}}{T_{STP}}$$

Rearranging yields

$$V_{STP} = \frac{p_{Act} V_{Act} T_{STP}}{p_{STP} T_{Act}}$$

and substituting for observed conditions,

$$V_{STP} = \frac{T_{STP} p_{Obs} V_{Obs}}{p_{STP} T_{Act}}, \qquad [2\text{-}4]$$

where, for the air flow rate calibration,

T_{STP} =273.15 K $\qquad$ T_{Act} =293.44 K

p_{STP} =760.0 mm Hg $\qquad$ p_{Act} =743.51 mm Hg.

Therefore,

$$V_{STP} = 0.888 V_{Obs}.$$

In general, the average flow rate is given by

$$Q = \frac{V_{Displaced}}{\Delta t_{Filling}}, \qquad [2\text{-}5]$$

where t is the time elapsed during filling of the graduated cylinder. Thus,

$$Q_{STP} = 0.888 Q_{Obs} .$$

For the air flow rate calibration,

$$Q_{STP_{Avg}} = 140.47 \text{ cm}^3/\text{sec}$$

at the given rotameter setting at STP. These calculations were carried out for a range of air rotameter settings. Correcting the flow rate calibration data to standard conditions was necessary because the fuel and air rotameters were calibrated on different days at different ambient conditions. If the uncorrected flow rates were used to calculate the mixture compositions as a function of rotameter setting, these compositions would have been different when the rotameters were operated at the same ambient conditions (during filling of the SFLT's) because of the dependence of the volume flow rate on temperature and pressure. Since the Ideal Gas Law shows that this dependence on temperature and pressure is the same for each gas, by correcting the calibration volume flow rates to specific conditions (for example, STP), the volume ratio of fuel to air and, therefore, the mixture compositions would always remain constant for given rotameter settings, regardless of variations in ambient conditions during the filling process.

This exact procedure was duplicated for each of the fuels used except that the glass float (of lower density, thus, giving greater flow rate resolution) was used and the calibration was conducted in an extremely well-ventilated area. Calibration of the fuels required extreme caution because pure methane is odorless, colorless, and tasteless; and pure propane has only a slight odor. Plotting the average fuel flow rates as a function of the rotameter setting yielded a linear relationship as shown in Figures 2-10 and 2-11. The analytical expression for this dependence was easily obtainable in each case using a linear regression program on a hand calculator. The proper air rotameter settings for the prescribed upstream and downstream pressures that yield lean-limit mixtures when used with the corresponding fuel flow rate curve have been

noted in each figure. Using the fuel and air flow rate calibration curves, the desired mixture compositions are obtained using the following relation:

$$M = \text{volume \% fuel composition} = \frac{Q_{\text{Fuel}}}{Q_{\text{Fuel}} + Q_{\text{Air}}} \qquad [2\text{-}6]$$

Typically, one air flow rate is chosen and the desired range of mixture compositions is obtained by varying the fuel flow rates only. The necessary fuel flow rate may be determined from the above expression, and this flow rate related to the fuel rotameter setting through the linear relation obtained from the calibration. A table can be set up for easy reference that lists appropriate fuel and air rotameter settings for desired mixture compositions.

During the course of the flow rate calibration equipment set up, a number of leaks were detected in tubing connections and in the mixing chamber itself. These leaks were corrected by tightening or resealing the connections and by the construction of an improved mixing chamber. It is obvious that the system must be leak free to produce mixtures accurately and precisely, but it is emphasized here for those who may utilize this equipment in future research that checking the mixing system for leaks should be the first task to be completed prior to calibrating the rotameters. It should be executed in a thorough manner and checked periodically thereafter.

2.4 Tube-Filling Procedure

Filling of the SFLT's was accomplished on the ground prior to a scheduled flight with the test rack removed from the aircraft and transported to a safe location within the hangar as designated by the NASA Lewis Safety Committee. The mixing system could be linked to any SFLT or series of them via 0.125-inch tygon tubing and quick-disconnect fittings. A tygon tube, fitted at each end with an O-ring sealed quick-disconnect plug, joined a socket in the mixing system to a socket cemented into one end of the plexiglas SFLT wall. Another socket at the

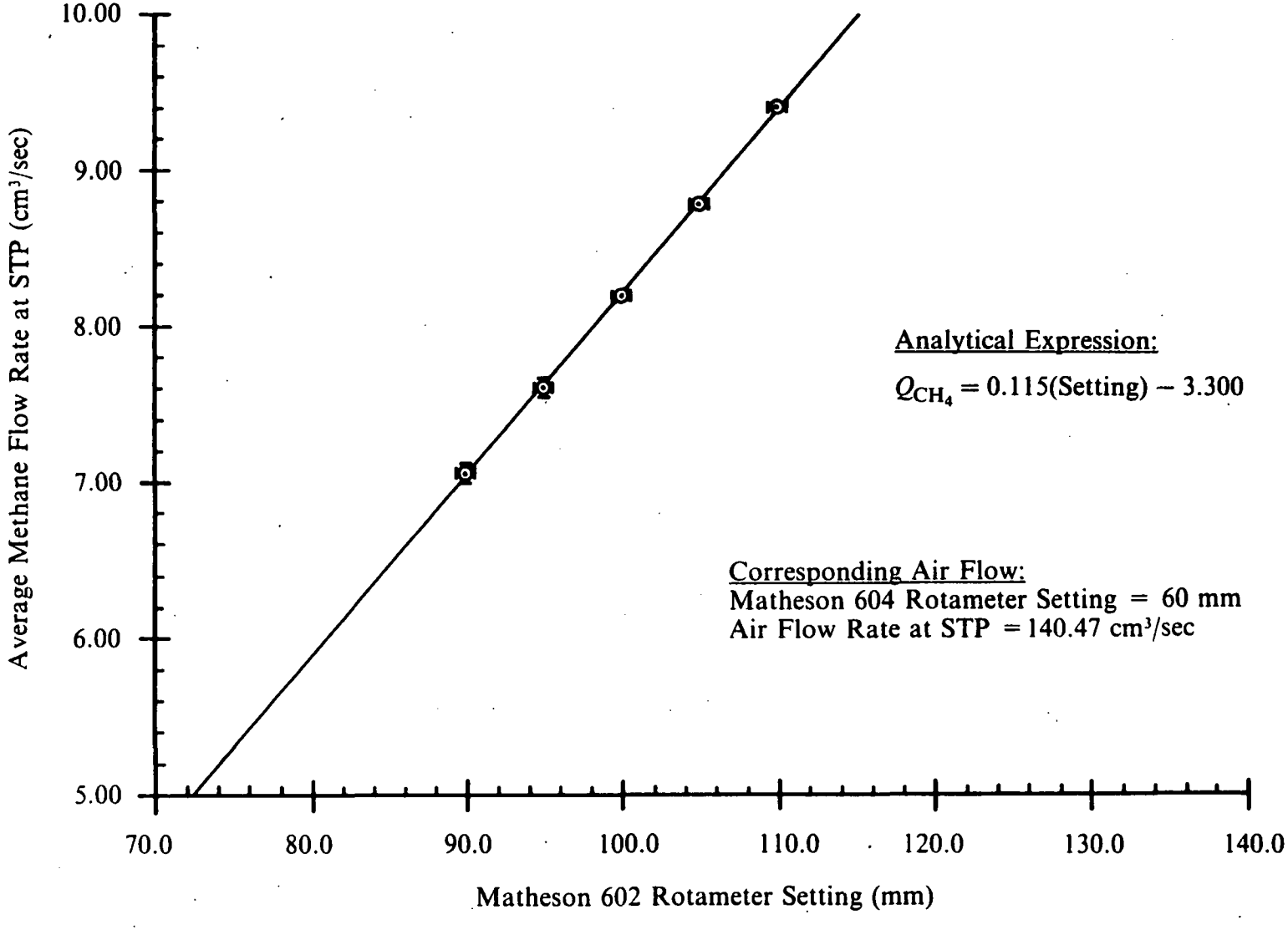

Figure 2-10. Methane flow rate calibration curve. Flow rate calibration curve of methane gas for Matheson #602 rotameter tube. The calculated errors in the flow rates are represented by bars for each point.

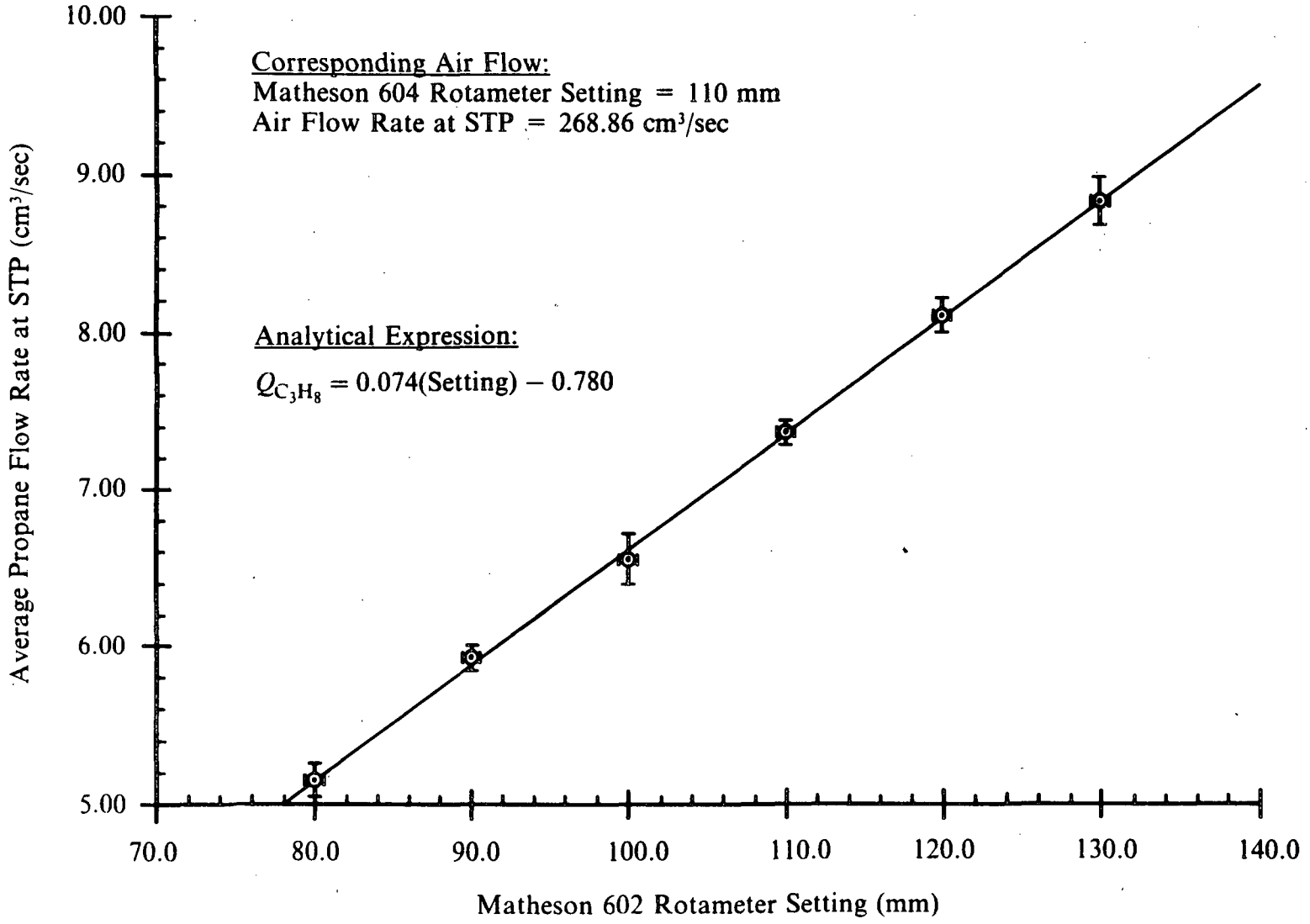

Figure 2-11. Propane flow rate calibration curve. Flow rate calibration curve of propane gas for Matheson #602 rotameter tube. The calculated errors in the flow rates are represented by bars for each point.

opposite end of the SFLT could then be connected to other plexiglas tubes using tygon patch hoses, or it could be vented outside the hangar. Unless a patch hose has been installed, an SFLT is vacuum tight. A ground-based flammability limit tube was also included as the last tube in the filling circuit. This tube was fired to check the mixture composition in the tube or tubes just filled. By noting the tip speed of the flame for one g upward propagation, the mixture composition could be verified by comparison to reference flame speeds for one g upward propagation.

To initiate the filling sequence, it was first necessary to select the appropriate fuel and air rotameter settings for the desired mixture composition. It was easiest to set each rotameter separately. As an example, consider setting of the air flow rate. Two-stage regulators were used at the supply tanks to provide essentially constant upstream pressure. Next, the air supply valve was opened and the two-stage regulator was set statically (no flow) at 25.0 psig. Then, the two-way air shut-off valve on the mixing system was set to "ON" while the three-way filling valve was set to the "EXHAUST" position. The air rotameter and downstream pressure valves were adjusted alternately until the rotameter setting was as desired and the downstream pressure was 15.0 psig. Lastly, the upstream pressure was rechecked and set dynamically to 25.0 psig. It was occasionally necessary to repeat this procedure to obtain the desired rotameter readings, upstream, and downstream pressures. Having achieved the proper air flow rate, the air was shut off and the fuel flow rate was set in exactly the same manner. Both fuel and air could then be turned on and the three-way valve set to "FILL". Final adjustments were made to the two rotameters and the four pressure gauges to the tolerances listed in Section 3.2. Roughly 30 seconds were required for the readings to stabilize which added to the difficulty of simultaneously maintaining these six readings within the above tolerances. Each pressure and flow rate, of course, influenced the others as they varied, making it necessary to continously monitor these readings during filling. In order to purge the air in the SFLT's, the mixing system was operated for a period of time that permitted the passage ten system volumes; that is, if eight tubes were filled, a volume of mixture equivalent to eighty tube volumes was passed through the system.

Safety regualtions required that the excess gas resulting from the filling process be vented outside the hangar. During the setting of the each rotameter, the three-way valve of the mixing system was set to "EXHAUST", which routed the flow through a standard compressed-air hose that was connected to an exhaust port installed in the hangar door. When the rotameter and pressure readings were steady, the three-way valve was switched to "FILL." The mixing system was attached to the desired SFLT via the tygon tubing. Similar tubing was connected from the exhaust port of the last SFLT to be filled to the exhaust port in the hangar wall. Lastly, the three-way valve could be completely turned off at the conclusion of a tube filling. Proceding in this manner, none of the flammable mixture was allowed to escape within the hangar. Once the tubes were filled and their compositions checked by performing the ground-based test-tube firings, the filled rack of flammability limit tubes could be loaded onto the aircraft.

2.5 In-Flight Procedure

After the filling of the rack and the ground tube test firing(s) have been completed, the two equipment racks are loaded onboard the aircraft and secured to two parallel I-section rails that are fastened to the floor of the left side of the cabin. The automatic sequencing rack mounts aft with the cameras facing towards the nose of the aircraft. The flammability limit rack mounts forward of this at a distance of 11 inches, rack to rack, such that the tube in firing position lies in the focal plane of the cameras. The researcher is seated alongside both racks where the control panel switches are accessible and the indicator lights are readily visible. The flammability limit tube carrousel is manually rotated, and the locking lever that secures it is operated with the researcher's left hand.

Once airborne, the Lear jet must be flown to restricted airspace over Wright-Patterson AFB in Dayton, Ohio, before the trajectories can be executed. In the restricted area, the aircraft is monitored by ground-based radar for the duration of the flight. Communication between the

pilot, copilot, and researcher is maintained throughout the flight with head sets via a two-way intercom. When nearing the restricted airspace, the cockpit curtain should be closed in preparation for filming. During a trajectory, the researcher must remain belted to his seat. The researcher should also wear safety goggles while an experiment is in progress. Next, all control panel power is switched on. For the actual test under normal conditions,the researcher should check the power indicator lights to confirm that research power is available and the voltmeter to be sure the capacitor is fully charged. Now, the desired tube can be selected and locked in place, ready for firing and the window shades are closed, darkening the cabin for filming. At this point, the copilot switches on the photosensitive-paper recorder and the trajectory is initiated. On receiving notification from the pilot that the desired gravity conditions have been achieved, the researcher presses and holds the button to start the automatic sequencing. The results of the tube firing are then noted and logged. Once the sequencing cycle is completed, the locking lever is disengaged, the carrousel rotated to bring the next tube into firing position, and the locking lever then re-engaged.

In the event of an emergency involving the experimental apparatus, the researcher must first shut off power to all system components using the master switch. The crew must then be informed of the emergency situation. If safety permits, the cannon plugs should be disconnected and electrical power resumed to complete only the sequencing of the timer motor. Finally, the feasibility of correcting the malfunction in flight and continuing the planned experiments should be assessed. The researcher must be in good health and pass the equivalent of a Class III flight physical. The researcher is also required to complete a one-day high-altitude-passenger training course. In the event of an aircraft emergency, the power to the experimental apparatus should again be shut off; and the Lear jet emergency procedures should be followed. Instruction in the use of oxygen equipment and other pertinent information will have been covered in high-altitude-passenger training.

3 Data Analysis and Results

3.1 Research Summary

The primary purpose of this research was to investigate the limit behavior of fuel-lean hydrocarbon-air flames under variable gravity conditions. First, the methane-air system was chosen for study to confirm and complement the results obtained previously by Noe [4] for the same flammability limit apparatus and because of the extensive body of experimental data that has been collected by other researchers and is available for comparison. During the research conducted by Noe, cellular instabilities were frequently observed for methane-air flames near the fuel-lean limit. This is a thermodiffusive instability that occurs because of preferential diffusion of the lighter fuel toward the reaction zone of the flame. For comparison purposes, a thermodiffusive-stable fuel-air system was also studied. The heavier-than-air hydrocarbon, propane, was chosen and tested in a set of experiments that duplicated the gravity conditions studied for the methane-air mixtures. Comparison of the results obtained for both fuel-air systems permitted investigation of the effects of cellular instability on the limit behavior of the methane-air flames. The methane and propane used for these experiments were research grade (99.97% purity). Bottled, dry, compressed air was used to mimimize contaminants and supply-pressure fluctuations that would reduce the accuracy of the mixture compositons produced by the continuous-flow mixing system. Mixture compositions investigated ranged from 4.90 to 6.20 volume percent methane and from 1.90 to 3.00 volume percent propane. Because of the limited availability of the Lear jet facility, richer mixtures were not investigated.

In the discussion of the results, all mixture compositions will be expressed as volume (or mole) percent fuel and will be denoted simply by the percent (%) fuel.

The fuel-lean limits were evaluated for one g upward, one g downward, and zero g propagation. In addition, the Lear jet facility allowed the study of near-limit flames under constant fractional g loadings, as well as time varying g loadings from 0.0 to +2.0 g's and, by inverting the apparatus within the NASA Lewis rack, from 0.0 to −2.0 g's. The flame structure, flame speeds and extinguishment processes for all gravity conditions will be discussed.

3.2 Mixing System Error Analysis

It is of the utmost importance to know the uncertainties in the mixture compositions if sensible interpretations of the data are to be made. Consequently, the fuel and air rotameters were calibrated for the prescribed upstream and downstream pressures prior to this research. Precautions were taken to reduce errors as much as possible, but instrument error and human error could not be completely eliminated. These errors will now be analyzed to determine their combined effect, which will be expressed as an uncertainty in the final mixture composition. The experimental errors present in this study have been divided into two categories:

1. Random Errors

- Upstream and downstream pressure fluctuations.
- Nonsteady position of the rotameter float.
- The precision of the rotameters, pressure gauges, stop watch and thermometer.

- Human error in reading the gauges, rotatmeters, thermometer, or the volume of gas in the graduated cylinder and in timing each filling of the graduated cylinder.

2. Systematic Errors

- Accuracy of the pressure gauges, rotameters, stop watch, thermometer and the graduated cylinder.
- Instrument hysteresis.
- Thermal expansion of the rotameter float and tube.
- Variation of the ambient pressure and temperature during calibration of the rotameters.
- Leaks in the mixing system.
- Dissolution of the gases in the water used for calibration of the rotameters by the method of fluid displacement.

Meticulous attention was given to all aspects of the calibration and filling processes to reduce both types of error. First, to reduce random errors, the pressure gauges and the levels of the rotameter floats were monitored constantly during calibration and filling; and the pressure valves and metering valves were continually adjusted to maintain the desired settings within specified limits. Careful and, hopefully, unbiased reading of the instruments and timing of the fluid displacement in the graduated cylinder minimized any unavoidable errors. A prism arrangement was used that allowed more precise reading of the graduated cylinder at the line of meniscus at the gas/water interface. The barometric pressure was obtained from the weather

service at Hopkins International Airport where the tests were conducted, reducing the uncertainty of that measurement over that for a mercury barometer.

The random errors that remained included uncontrollable fluctuations in the upstream and downstream pressures and in the levels of the fuel and air rotameter floats. Human error in interpreting the instrument readings was, of course, present. Also, the synchronization of the starting and stopping of the stop watch with the beginning and end of a graduated cylinder filling, respectively, was less exact at higher flow rates. The effects of these errors on the calculated flow rates were reduced by taking multiple readings of the flow rates. Average flow rates for the air rotameter calibration were calculated from six fillings of the graduated cylinder. Average flow rates for the fuel rotameter calibration were calculated from three fillings of the graduated cylinder.

Second, systematic errors could be minimized by employing certain experimental procedures over others or eliminated by applying correction factors. Instruments which enhanced the accuracy of the mixing system as a whole were selected when there was a choice. For example, since the volume flow rate of fuel was small relative to the volume flow rate of air, the rotameter tube sizes and float densities were matched to yield the best possible resolution of the mixture compositions. The value of the back pressure selected was high enough to absorb variations in the down stream flow impedance caused by variations in the number of tubes that could be attached for any given filling. The mercury-in-glass thermometer used for all temperature measurements was calibrated by complete imersion in a bath of distilled water and ice made from distilled water. Temperatures measured with this thermometer were subsequently corrected using the results of the calibration. The temperature of the atmosphere and water bath were monitored for each set of volume flow rate measurements made. The water bath temperature was maintained within 2 °C of the ambient temperature during calibration to make the estimate of the partial pressure of water vapor in the graduated cylinder, using the atmospheric temper-

ature, as accurate as possible. The gas in the cylinder was always assumed saturated with water vapor in the calculations. The pressure gauges were not calibrated, but the pressure measurements were not used to calculate the flow rates, only to set the prescribed upstream and downstream pressures, leaving the only relevant issue that of their precision. Hysteresis error caused by friction in the pressure gauges was reduced by tapping the gauges before each reading. All leaks in the mixing system were eliminated, and connections were checked frequently to make as certain as possible that leaks did not occur.

The systematic errors not accounted for included: pressure gauge hysteresis errors present due to the elasticity of the Bourdon tubes, thermal expansion of the rotameter tubes and floats, and variations in the ambient conditions during a set of graduated cylinder fillings for a given rotameter setting. Also, errors caused by the solubilities of the gases (air, methane, and propane) in the water used for the calibration of the rotameters were not considered. This should have been acceptable for air and methane, but there was concern in the case of propane. Its relatively high boiling point and, thus, low vapor pressure, make propane more soluble than air or methane. Factors affecting the solubility of gases that could not reasonably be estimated included the initial dissolved gas content of the water, the dissolved solid content of the water, and whether or not equilibrium was achieved between the soluble gas and the water [6]. A quantitative treatment of the solubility effects was, therefore, not attempted due to the impracticality of obtaining this information. Furthermore, there was no evidence that solubility effects were significant since the calibration plots of volume flow rate versus rotameter setting yielded straight lines over the ranges of flow rates tested. If solubility effects had been significant, they would have been expected to decrease as the flow rate increased (since the gas was in contact with the water for a decreasing period of time) or as the calibration proceeded (since the water bath would have become saturated with the soluble gas).

The combined effect of these remaining errors on the mixture composition is known as the experimental uncertainty. The systematic and random errors of each instrument during each phase of the research were as follows:

Instrument Accuracies

30 psig upstream pressure gauges (2)	± 2.0% of full scale
50 psig downstream pressure gauges (2)	± 0.1% of full scale
Hand-held digital stop watch	± 0.01seconds
Thermometer (mercury-in-glass)	± 0.05 °C
Graduated cylinder	± 5 cm^3 at 20 °C

Calibration Tolerances

Upstream fuel pressure	± 0.2 psig
Downstream fuel pressure	± 0.1 psig
Upstream air pressure	± 0.1 psig
Downstream air pressure	± 0.05 psig
Timing error	± 0.3 seconds
Reading the graduated cylinder	± 5 cm^3, 1800 cm^3 sample avg.
Fuel rotameter	± 0.5 mm
Air rotameter	± 0.2 mm

Filling Tolerances

Upstream fuel pressure	± 0.2 psig
Downstream fuel pressure	± 0.1 psig
Upstream air pressure	± 0.1 psig
Downstream air pressure	± 0.05 psig
Fuel rotameter	± 0.5 mm

Air rotameter	± 0.2 mm

The combined effect of these errors may be determined by a statistical error analysis. In this case, several simplifying assumptions can be justified. First, all data points are assumed to have an equal probability of occurrence and, therefore, have been assigned the same statistical weight, $w_i = 1.0$. Second, a normal, or Gaussian, distribution of the data points has been assumed. This is reasonable provided the remaining errors are largely random in nature, and they are expected to be so. The relatively small number of flow rate data points collected precluded determination of the true distribution function, but in light of the types of errors encountered, assymmetry or skewness of the data should not be significant. Manipulation of the normal distribution probability function shows that the most probable or "best" reading from multiple experimental samples is given by the numerical average of the samples [7], m, of the n readings defined as

$$m \equiv \frac{\sum_{i=1}^{n} x_i}{n} \qquad [3\text{-}1]$$

where x_i are the observed values of the flow rates for a given rotameter setting. If the best value must be based on this average alone, then statistical theory shows that the most exact value of the standard deviation, s, is obtained from

$$s \equiv \left[\frac{\sum_{i=1}^{n} (x_i - m)^2 f_i}{n} \right]^{\frac{1}{2}} \qquad [3\text{-}2]$$

where f_i is the number of times each x_i is observed. In this analysis, all $f_i = 1.0$.

Each rotameter had an arbitrary scale inscribed on it that corresponded to actual flow rates of a given fluid only after calibration of that rotameter with that fluid at specified upstream

pressure, downstream pressure, and ambient conditions. Unless calibrated against a reference flow rate of known accuracy, the accuracy of the rotameter can only be estimated from the accuracies of each individual piece of calibration equipment. This is true because the residual systematic errors are not perforce indistinguishable from the random errors in the experimental data. For this same reason, all residual errors shall be treated as independent errors in the remainder of the analysis. To determine the propagation of independent errors, consider

$$u = f(x,y)\,, \quad u_i = f(x_i,y_i)\,, \quad u_o = f(\bar{x},\bar{y}) \qquad [3\text{-}3]$$

where u is the desired result, f is any function, x and y are the independent measured properties and the bars signify mean values. If all deviations $\delta s_i = x_i - \bar{x}$ and $\delta y_i = y_i - \bar{y}$ are relatively small, which they are in this case, then the deviation in the result, u_i, is obtained from the Taylor series expansion of u_i [8]:

$$\begin{aligned} u_i &= f([\bar{x} + \delta x_i], [\bar{y} + \delta y_i]) \\ &= f(\bar{x},\bar{y}) + \frac{\partial u}{\partial x}\delta x_i + \frac{\partial u}{\partial y}\delta y_i + \ \ldots \end{aligned}$$

and neglecting higher order terms,

$$\delta u_i = u_i - \bar{u} = \frac{\partial u}{\partial x}\delta x_i + \frac{\partial u}{\partial y}\delta y_i \qquad [3\text{-}4]$$

This result may be substituted into the definition of the standard deviation. Squaring yields

$$s_u^2 = \frac{(\frac{\partial u}{\partial x})^2 \sum_{i=1}^{n} (\delta x_i)^2 + 2\frac{\partial u}{\partial x}\frac{\partial u}{\partial y}\sum_{i=1}^{n} (\delta x_i \delta y_i) + (\frac{\partial u}{\partial y})^2 \sum_{i=1}^{n} (\delta y_i)^2}{n}\,. \qquad [3\text{-}5]$$

As n becomes large, for independent random errors the sum, $\sum_{i=1}^{n} (\delta x_i \delta y_i)$, goes to zero. Since

$$s_x^2 = \sum_{i=1}^{n} \frac{(\delta x_i)^2}{n} \quad \text{and} \quad s_y^2 = \sum_{i=1}^{n} \frac{(\delta y_i)^2}{n},$$

then the standard deviation in the result may be given in terms of the standard deviations of the components,

$$s_u = \left[\left(\frac{\partial u}{\partial x} \right)^2 s_x^2 + \left(\frac{\partial u}{\partial y} \right)^2 s_y^2 \right]^{\frac{1}{2}}. \qquad [3\text{-}6]$$

Equation [3-6] can be generalized to J variables

$$s_u = \left[\sum_{j=1}^{J} \left(\frac{\partial u}{\partial x_j} \right)^2 s_{x_j}^2 \right]^{\frac{1}{2}} \qquad [3\text{-}7]$$

and for the uncertainty interval w,

$$w_u = \left[\sum_{j=1}^{J} \left(\frac{\partial u}{\partial x_j} \right)^2 w_{x_j}^2 \right]^{\frac{1}{2}}. \qquad [3\text{-}8]$$

Equations [3-7] and [3-8] shall be used to determine the cummulative effect of all experimental errors and their effect on the final result. In this case, the result is the flow rate, Q. Thus,

$$\begin{aligned} \frac{\partial Q}{\partial T} &= \frac{nR}{pt} \\ \frac{\partial Q}{\partial p} &= \frac{-nRT}{p^2 t} \\ \frac{\partial Q}{\partial V} &= \frac{1}{t} \\ \frac{\partial Q}{\partial \mathrm{t}} &= \frac{-V}{t^2} \end{aligned} \qquad [3\text{-}9]$$

where t is the time required to fill the graduated cylinder. Applying Equations [3-9] to the flow rate data obtained during calibration yields the values summarized in Table 3-1. Error bars representing the total uncertainty in the flow rates have been included in Figures 2-10 and 2-11. The inaccuracy of the volume measurement is the dominant influence in the overall accuracy of the flow rates, fully one order of magnitude greater than any other accuracy error. The precision, however, is most likely determined by the skill of the person performing the calibration of the rotameters.

In the determination of the mixture composition, M, this approach applied to Equation [2-6] yields

$$\frac{\partial M}{\partial Q_{Fuel}} = \left[\frac{1}{(Q_{Fuel} + Q_{Air})} - \frac{Q_{Fuel}}{(Q_{Fuel} + Q_{Air})^2} \right] \times 100$$
$$\frac{\partial M}{\partial Q_{Air}} = \left[- \frac{1}{(Q_{Fuel} + Q_{Air})^2} \right] \times 100 \qquad [3\text{-}10]$$

where M is in units of volume % fuel. Application of Equations [3-10] results in uncertainties of

Methane	$\pm$ 0.03%
Propane	$\pm$ 0.04%

over the range of mixtures studied. The precision limits, $\pm s$, by definition will include about 68% of the data points. The stated limits of accuracy should include roughly 90% of the measurements made. Therefore, the overall uncertainties in the mixture compositions as listed above are estimated to include approximately 80% of all mixtures. That is to say that only 1 in 5 compositions will show a deviation geater than the stated uncertainty.

Table 3-1. Volume flow rate uncertainties.

Gas	Rotameter Setting (mm)	Average Flow Rate (cm^3/sec)	Accuracy (cm^3/sec)	Precision (cm^3/sec)
Air	60	140.47	± 0.45	± 0.80
	110	268.87	± 0.92	± 1.62
Methane	90.0	7.06	± 0.02	± 0.06
	95.0	7.61	± 0.03	± 0.06
	100.0	8.19	± 0.03	± 0.01
	105.0	8.78	± 0.03	± 0.03
	110.0	9.39	± 0.03	± 0.01
Propane	70.0	4.40	± 0.02	± 0.02
	80.0	5.14	± 0.02	± 0.10
	90.0	5.93	± 0.03	± 0.05
	100.0	6.55	± 0.03	± 0.16
	110.0	7.36	± 0.03	± 0.06
	120.0	8.10	± 0.04	± 0.10
	130.0	8.82	± 0.04	± 0.05
	140.0	9.55	± 0.05	± 0.15

3.3 Flammability Limits

The definition of the fuel-lean flammability limit adopted for the following discussion is one consistent with the literature for SFLT's, namely, that the lean flammability limit is the leanest mixture composition that will allow a flame to propagate the entire length of the tube. To ensure that the limits determined in this study would definitely be flammability limits and not ignition limits, the energy released by each nichrome coil igniter was increased substantially by coating each igniter coil with nitrocellulose. Thus, the total energy released by the igniter was the sum of the energy stored in the capacitor and the chemical energy released in combustion of the nitrocellulose. The energy lost to heating of the nichrome wire coil or to the resistance of the ignition circuitry was small relative to the total energy released and will be neglected. The energy stored in the capacitor is given by

$$U = \frac{1}{2}CV^2 \qquad [3\text{-}11]$$

where C is the capacitance and V is the voltage. Since in these experiments $C = 0.038$ Farads and $V = 28.0$ Volts,

$$U_{\text{Capacitor}} = 14.90 \text{ Joules.}$$

This was essentially constant for all firings. The time constant for the capacitor was 0.20 seconds so that, by definition, half of this energy was released in that amount of time. The energy released from the combustion of the nitrocellulose coating can be calculated if the mass of this coating is known. All igniters had virtually the same size coil with the same number of windings so the coatings have all been assumed to contain approximately the same mass of nitrocellulose. A single igniter was dipped in the nitrocellulose-acetone solution and rinsed in pure acetone twenty different times. After drying, the sample was weighed. The average mass of nitrocellulose applied to each igniter was calculated to be 0.015 gm. The nitrogen content of nitrocellulose will vary, depending upon the application for which it was manufactured, and the heat of combustion of nitrocellulose will vary with its nitrogen content. The nitrocellulose used for these experiments contained from 11.8 to 12.2% nitrogen by weight. The value of the nitrogen content used for these calculations was 12.0%. The heat of combustion of nitrocellulose at constant pressure was estimated from data given in [9] to be 103.8 kJ/gm. Thus, the energy released by combustion of the nitrocellulose was

$$U_{\text{Nitrocellulose}} = 155.7 \text{ Joules}$$

and the total energy released by the igniter was the sum of that stored by the capacitor and that liberated in the combustion of the nitrocellulose or

$$U_{\text{Total}} = 163.2 \text{ Joules.}$$

The combustion of the nitrocellulose was observed from the photographic data to consume approximately 0.15 seconds. The maximum average power released during ignition was then 1,100 Watts. The volume occupied during combustion varied, but averaged about 69.5 cm^3 . The average power density at ignition was then 16.0 W/cm^3 . This value is subject to considerable uncertainty, estimated at + 60% and – 30% about the nominal value, because of variations in the mass of nitrocellulose used for each igniter and the volume occupied by the ignition reaction. However, even at the lower limit, the peak power density should exceed the average by a considerable margin. In any case, the ignition technique used provided orders of magnitude more energy over a sufficiently large volume than the minimum requirements ensuring that the limits established by this research were indeed flammability limits and not ignition limits.

Each experiment was performed at ambient conditions that remained essentially constant during that experiment. However, fluctuations of as much as 20 to 30 °C and 93.1 to 102.1 kPa (13.5 to 14.8 psia) were noted between individual experiments. The influence of the variations in ambient temperature on the limit compositions can be determined from data obtained by Zabetakis [10] for one g upward propagation of methane-air and propane-air flames at atmospheric pressure. The maximum cabin temperature of 30 °C observed during this research was estimated to cause a decrease in the observed limit compositon of not more than 0.02% for methane and 0.01% for propane over the limit composition at the minimum cabin temperature of 20 °C. The influence of variations in the initial pressure on the limit composition was investigated by Ronnie and Wachman for one g upward, one g downward, and zero g propagation of methane-air flames form 50 to 1500 Torr (6.67 to 200.1 kPa) [11] . The zero g data indicated that the maximum cabin pressure of 102.1 kPa caused an increase in the value of the limit composition of 0.07% over the limit compostion for the minimum cabin pressure of 93.1 kPa in the methane-air system. Relevant data for propane at any gravity condition were not found. Zabetakis [10] found that the sensitivity of the propane lean-limit to initial pressure variations is less than that for methane; and since there is less scatter in the propane data than in the

methane data, it probably resulted in limit composition fluctuations of no more than 0.05%. Since the ambient temperature and pressure variations were random and independent of each other, their combined effect is expected to cause variations in the limit composition of at most 0.07% for methane and 0.05% for propane. These large variations in temperature and pressure were only encountered for the zero g cases, that is, only for experiments conducted in the Lear jet. The values of temperature and pressure discussed for zero g are the extremes. On the average, the variations were considerably less. The one g upward and one g downward limits were determined from ground tests conducted in the hangar and were subject to only 20 to 25 °C and 100.1 to 101.4 kPa (14.5 to 14.7 psia) ambient fluctuations. This difference is reflected in the slightly more erratic propagation behavior at the limit for the zero g flames as compared with the one g upward and downward propagating flames. The values obtained by experiment for limit compositons in this research will be discussed in terms of these variations.

Nearly two hundred experiments were performed to determine the one g upward, one g downward, and zero g limits for the methane-air and propane-air systems. These limits were found to be more distinct for the propane-air mixtures, while the methane-air flames behaved much more eratically in the vicinity of the limit. For the methane-air system, flames in mixtures of the same nominal composition were observed to propagate the entire length of the tube on one occasion and not at all on another; this occurred over a narrow range of mixture compositions. The inaccuracy of the mixing system obviously contributed to this behavior. Also, the variations in ambient conditions were important, but the combined error was not sufficient in itself to explain the range of mixture compositions over which the limit methane-air flames of the same nominal composition exhibited both behaviors. Thus, as observed in this study and as cited by other researchers, the limit composition can be indistinct.

Because of the statistical behavior observed for the limit, a statistical weight of 0.0, 0.5, and 1.0 was assigned to each experiment depending upon whether there was no propagation, the

flame propagated some distance from the ignition source, or the flame propagated the entire length of the tube, respectively. The assigned weights were averaged at each mixture composition tested for all results obtained. These values are plotted for the methane-air system in Figure 3-1 and for the propane-air system in Figure 3-2. In some instances, the statistical results were combined to give an indication of the probable behavior of the flames over short ranges of mixture composition. Examination of Figure 3-1 shows that for one g upward propagation and zero g propagation of methane-air flames, there is no significant or consistent difference in the probability of propagation for a given composition. Within the afforementioned uncertainties, the one g upward and zero g limits are the same for methane, 5.25 $\pm$ 0.04% and $\pm$ 0.05%, respectively. This would indicate that gravity has no net effect on the lean limit for upward flame propagation. It is of interest to note that all sub-limit one g upward methane flames were observed to propagate at least some distance from the ignition source. The one g downward limit for methane is 5.85 $\pm$ 0.04%. Figure 3-1 is also indicative of the destabilizing effects of the interaction of the flame front with the buoyancy-induced flow field for one g downward propagation. The one g upward and one g downward limits are consistent with those reported by Strehlow and Reuss [12] . These limits are not, however, entirely consistent with those obtained by Noe [4]. Though he reported the same limit for one g upward propagation, the zero g limit was only 5.10 %. Perhaps the limited number of data points obtained by Noe or the inaccuracy of the mixing system used (but not quoted with his results) could explain the discrepancies.

Figure 3-2 represents the probability of flame propagation as a function of mixture composition for the propane-air system. In this case, the one g upward and zero g limits differ considerably. For one g upward propagation, the lean limit is 2.15 $\pm$ 0.04%. The zero g propagation limit is 2.06 $\pm$ 0.05% indicating a significant influence of gravity on the lean limit for propane-air mixtures. Lastly, the one g downward limit for propane is 2.20 $\pm$ 0.04%. The one g upward, one g downward, and zero g limits for propane occur abruptly, covering only a small range of mixtures which can be explained by the uncertainty in the limit caused by the

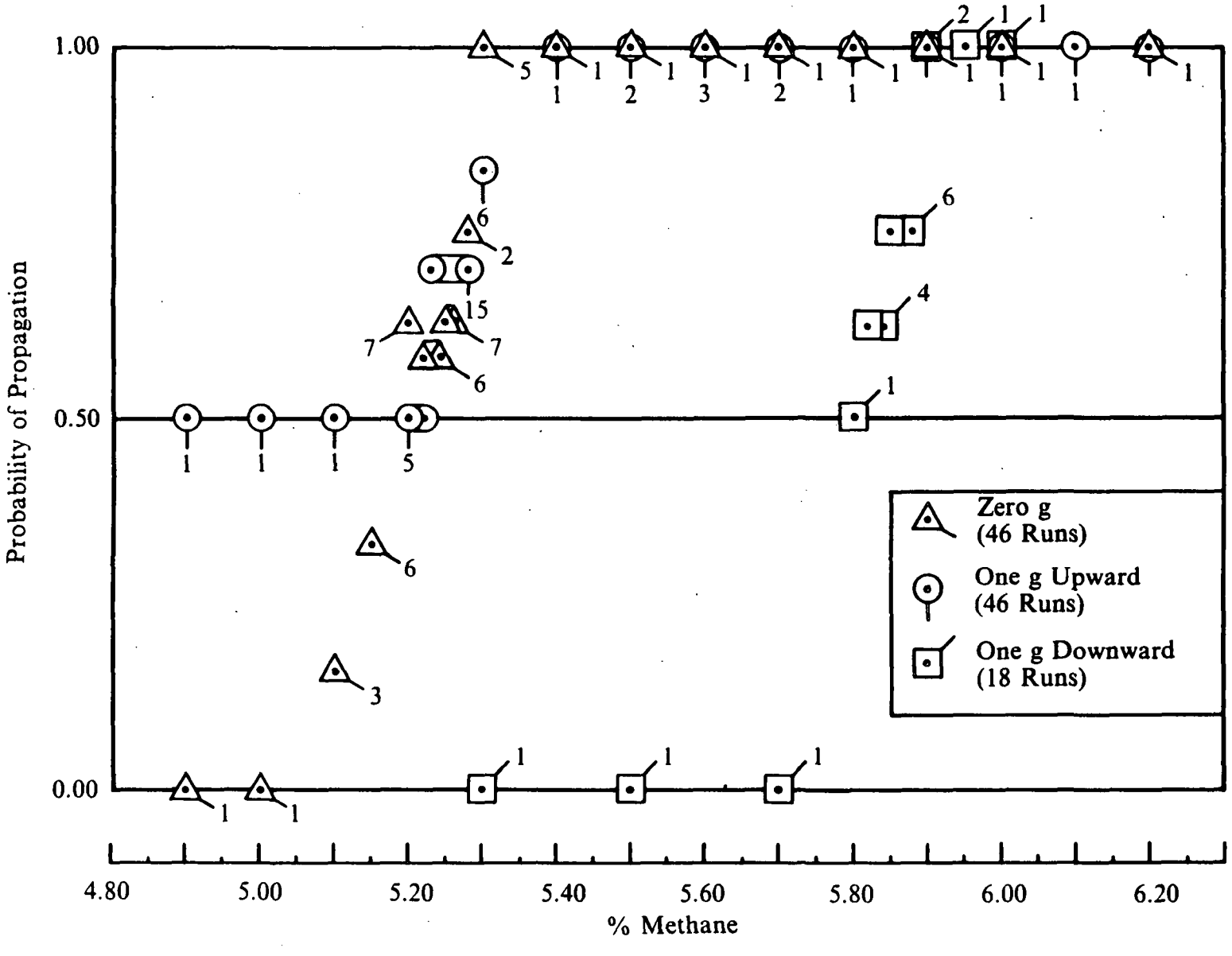

Figure 3-1. Methane limit-mixture-composition diagram. The probability of flame propagation for one g upward, one g downward, and zero g conditions is plotted versus percent methane. Zero indicates no propagation, and 1.0 indicates that the flame always propagated the full length of the tube. Adjacent to each point or group of points is the number of experimental observations that were averaged to obtain that probability.

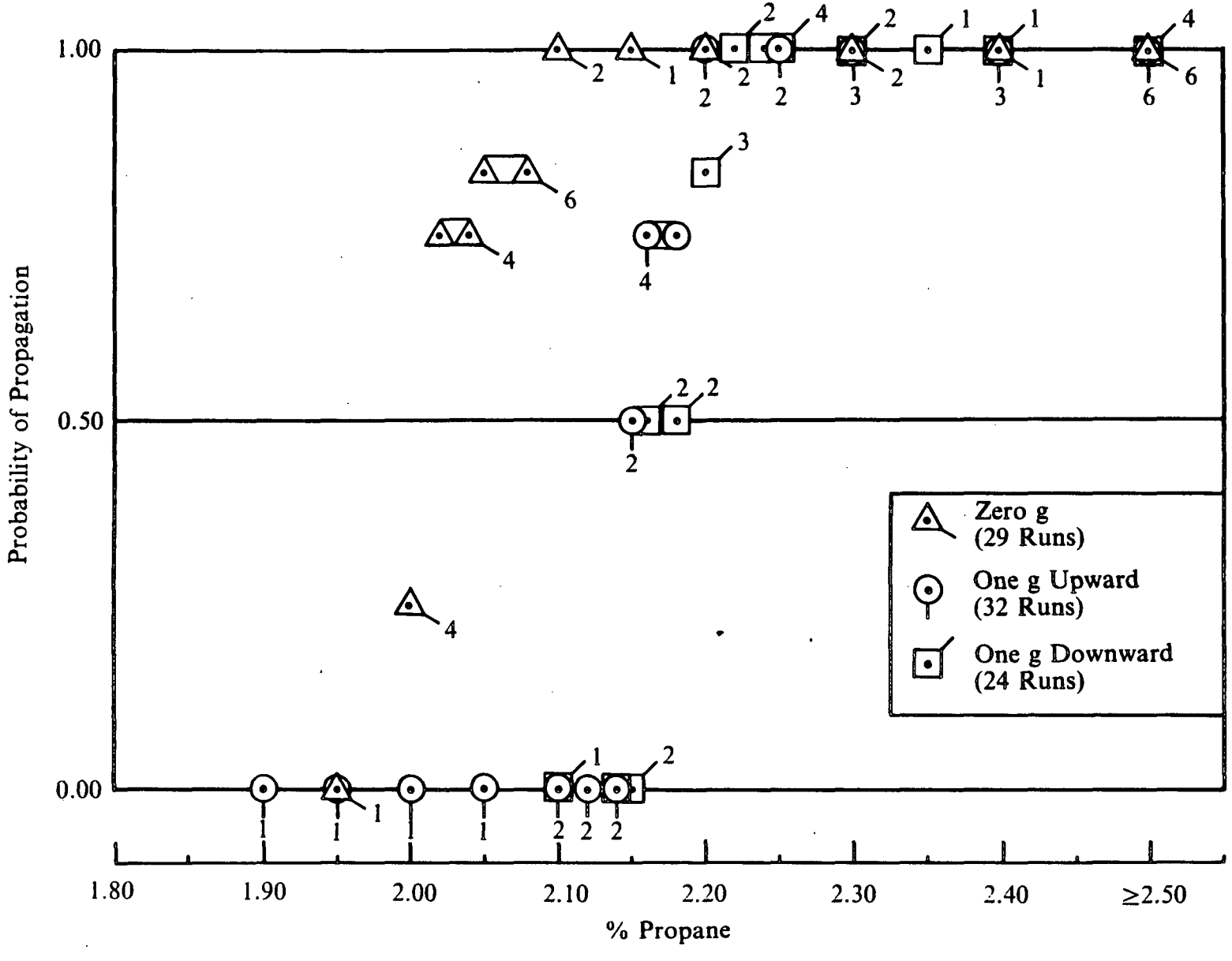

Figure 3-2. Propane limit-mixture-composition diagram. The probability of flame propagation for one g upward, one g downward, and zero g conditions is plotted versus percent propane. Zero indicates no propagation, and 1.0 indicates that the flame always propagated the full length of the tube. Adjacent to each point or group of points is the number of experimental observations that were averaged to obtain that probability.

uncertainty of the mixture composition and the variations in the ambient temperature and pressure. As previously mentioned, all one g upward flames either propagated the full length of the tube or not at all. Partial flame propagation was observed for zero g and one g downward conditions in the vicinity of the limit, but only over a very small range of mixture compositions.

Table 3-2. Summary of flammability limits.

		Wherley	Noe	Strehlow & Reuss	Coward & Jones [13]	Ronnie & Wachman
% CH_4 in Air	One g Upward	5.25	5.25	5.27	5.24	4.70
	One g Downward	5.85	---	5.85	5.85	5.55
	Zero g	5.25	5.10	---	---	5.07
% C_3H_8 in Air	One g Upward	2.15	---	---	2.15	---
	One g Downward	2.20	---	---	2.40	---
	Zero g	2.06	---	---	---	---

3.4 Flame Structure and Behavior

In general, the methane-air and propane-air flames behaved similarly with changing gravity loading and mixture composition, though there were some important differences. The flame caps of zero g flames in both systems were somewhat flattened, curving abruptly away from the unburned gas near the tube wall. The flame skirts were relatively short and asymmetric. Although the maximum and minimum skirt lengths observed were essentially constant with time, the position of these points relative to any chosen reference angle about the tube centerline fluctuated, while the skirt length changed in a "see-sawing" fashion as the flame traveled through the tube. This behavior was particularly common for the methane-air flames. A typical zero g methane-air flame profile is illustrated in Figure 3-3.

Figure 3-3 also shows typical methane-air flame profiles for various constant fractional g loadings for upward propagation. It can be seen that the flame cap loses its flattened shape as the g loading increases, the radius of curvature decreasing steadily due to the increasing bouyancy of the burned gas. The change in the flame skirt length beyond that for zero g is simply related to the change in gravity loading.

Downward propagating flames were studied under transient g conditions for methane-air and propane-air mixtures. Ignited in zero g and propagating while the downward gravity loading was increased, the flame initially had the zero g flame structure shown in Figure 3-3. The flame became increasingly flat as the gravity loading increased with time, its propagation speed decreasing concomitantly. As the downward gravity loading continued to increase, the flat flame front began to propagate in a nonsteady fashion. The specific g loadings at which these behavior changes occurred depended, of course, on the mixture composition. If the circular, nominally flat flame front is imagined as being divided in half along a diameter, then the flame front could be described as pivoting about this line with a "sloshing" motion, deforming slightly as it propagated down the tube. First, one side of the flame front would propagate ahead of the other. Then, the leading half of the flame front would slow, and often stop, while the second half caught up with and passed the first. One g downward limit flames were always observed to propagate in this highly irregular manner for both methane-air and propane-air systems.

For richer mixtures, the skirt length decreased for zero g and one g upward flame propagation. For one g downward propagating flames, mixtures slightly richer than the lean limit produced relatively stable, flat flames and still richer mixtures produced curved flames similar in appearance to the zero g flames. In all cases, the luminosity of the flames and the flame speeds increased as fuel concentration was increased from the lean limit value toward the stoichiometric value. This behavior was common to both fuel-air systems.

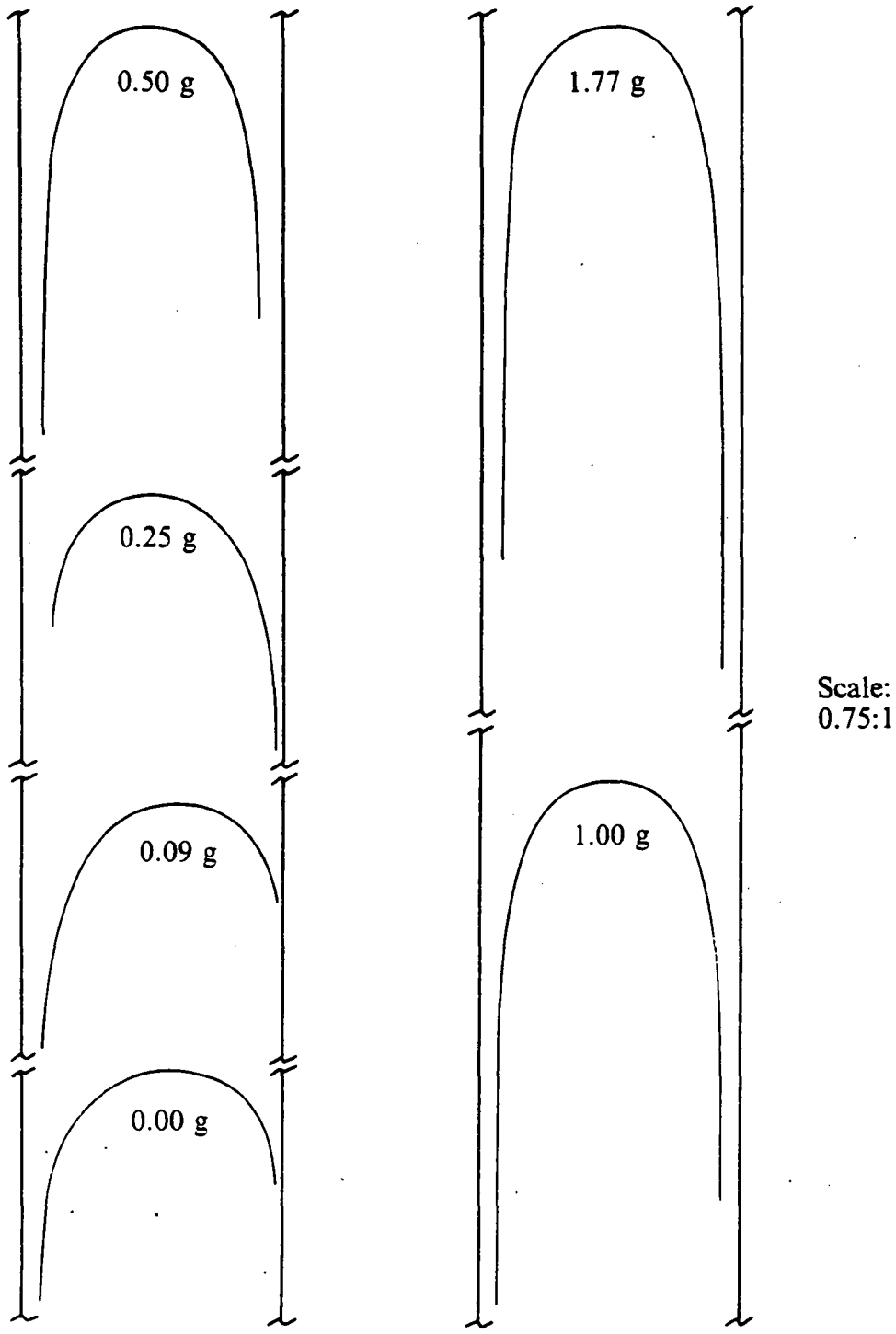

Figure 3-3. Profiles of 5.30% methane-air flames for zero g and upward propagation. Note the effect of gravity loading on the flame skirt length. Visible light photographs taken at 24 frames per second. Some frames omitted. The vertical lines represent the inner walls of the tube.

There was, however, one fundamental difference between the methane-air and propane-air flames studied. Propane-air flames were always observed to be *steady* except for near-limit and limit one g downward propagation, but methane-air flames always propagated in a *nonsteady* fashion. Even flames well above the limit compositions, which readily traveled the length of the tube, did so with fluctuating tip speeds, regardless of the g loading. Maximum tip speeds as large as several times the minimum value for a given mixture composition were observed for the zero g methane-air flames. This was expected for zero g propagation since Noe [4] reported maximum tip speeds for some zero g methane-air flames as large as those for one g upward propagation. This behavior was not, however, expected for one g propagation since Noe and other researchers [12] reported *constant* flame speeds for upward propagation in a SFLT. Mixture composition uncertainty and other sources of error were investigated to determine their effects on flame speed, yet these could not fully explain the flame speed fluctuations. Furthermore, these fluctuations were well outside the limits of what would have been expected for the small variations in gravity loading involved and there was no correlation between flame speed behavior and the g-jitter. The zero g methane-air flames were characterized by an irregular structure as well. The shape of the flame cap, though nominally the same as that observed for propane-air flames, was usually asymmetric, and it undulated along the axis of the tube as it propagated, hence, the variable tip speeds. The cap sometimes stretched, taking on a conical shape, but remaining rounded at the tip. Also, the tip often wandered away from the tube centerline, following a helical path as it traveled through the tube. Occasionally, these flames were observed to produce a cellular flame. Cellular instability is the tendency of the surface of certain flames to spontaneously deform and propagate as a system of troughs and crests rather than remaining smooth. It occurs primarily in fuel-oxidizer systems for which a "sufficiently light species is sufficiently deficient", [14] . In other words, it is usually observed for fuel-lean mixtures in which the fuel has a lower molecular weight than the oxidizer and in fuel-rich mixtures in which the fuel has a higher molecular weight than the oxidizer. Cell formation is a thermodiffusive phenomenon [15] unstable to concave perturbations of the flame front relative

to the unburned mixture. The driving mechanism of cellular instability is the preferential diffusion of mass (the deficient, light species) toward the reaction zone. Normally, in the presence of a concave perturbation, the diffusion of heat into the unburned mixture, caused by the thermal gradient in the preheat zone of the flame, raises the temperature and therefore the flame speed in the concave regions and lowers the flame speed in the convex regions. If thermal diffusivity were the only transport mechanism operating, the flame would be stable to this type of disturbance. However, if preferential diffusion is operating, a concave perturbation at the surface of a flame front will deplete the lighter species (in this case, methane) in the approach flow in the neighborhood of the perturbation. The flame speed is decreased locally in this leaner mixture, causing the disturbance to grow, forming a trough. For the corresponding crests, diffusion of the lighter species toward the convex flame front enriches the mixture ahead of the crest, thus increasing the local flame speed. The result is that the flame propagates as a system of rounded crests and sharp troughs that is usually time variant. There are numerous forms that cellular flames may assume depending on the system geometry, mixture composition, and thermal as well as aerodynamic interactions of the flame front with the gas in which it is propagating. For SFLT's, cellular instabilities were never observed to occur in one g upward propagating flames for this research or for that conducted by Noe [4]. These results are in agreement with those obtained by von Lavante and Strehlow [16] who observed sporadic cellular instabilities in lean methane-air mixtures for one g upward propagation of flames in a 100 mm X 100 mm square tube, but never in a 50 X 50 mm tube. Only a single one g downward flame became cellularly unstable for a 6.00% methane-air mixture. The flame was nominally flat with a cellular structure superimposed. This had the same many-celled structure that Markstein observed for various hydrocarbon-air flames propagating against an approach flow in a transparent tube [17]. Zero g flames were observed to be sporadically cellularly unstable with only a slightly higher probability of occurrence. A cellular, zero g flame is pictured in Figure 3-4 for 5.23% methane in air. When a cell formed, it would grow at the expense of the other cell until it replaced the original front, then continued to propagate as a seemingly stable flame. These flames

were never observed to form more than two cells, and consecutive cellular instabilities in the same column of gas were not observed for the zero g case. An attempt was made to investigate the behavior of cellularly unstable flames in terms of the probability of cell formation and the subsequent behavior of the cells as a function of gravity loading. By observing flames in 5.30% methane-air mixtures at a variety of constant fractional g loadings, it was found that cellular structure never occurred at gravity loadings at or above 0.5 g, but did occur sporadically for gravity loadings at or below 0.4 g. This implies that sufficiently strong gravity-induced flame stretch of an upward propagating flame has the effect of stabilizing an otherwise cellularly unstable flame. Strehlow [14] has noted that if the length of time required for a cell to form at a local disturbance in the flame front is great enough, in the presence of sufficient flame stretch, the disturbance can be washed down the side of the the flame before a cell has time to form. The degree of stretch necessary for this to occur, in the 5.30% mixtures under consideration, must have been attained between 0.4 and 0.5 g. It should be noted that the occurrence of cellular instability was rare, and these gravity values are thus based on a limited quantity of data. Only four instances of spontaneous cellular instability were observed for zero g experiments. Noe reported the occurrence of cellularly unstable flames over the entire range of methane-air compositions tested in zero g. The reason for the discrepancy between this behavior and what Noe reported is not clear. The apparatus employed was the same for both studies; however, the exact purity of the methane and air used by Noe is not known. Perhaps contaminants were present that made the flames more susceptible to spontaneous cell growth. Because of this low probability of occurrence, it was not possible to make any substantial investigation into the effect of gravity loading on cell life. G-jitter was discounted as influencing cell formation in this study since it did not correlate with the occurrence of the instability. The g-jitter for Noe's research was much greater, $\pm$ 0.04 g versus $\pm$ 0.01 g, due to differences in the sensitivities of the cockpit displays used by the pilots. He also reported, however, that no correlation between g-jitter and the formation of cellular flames could be found.

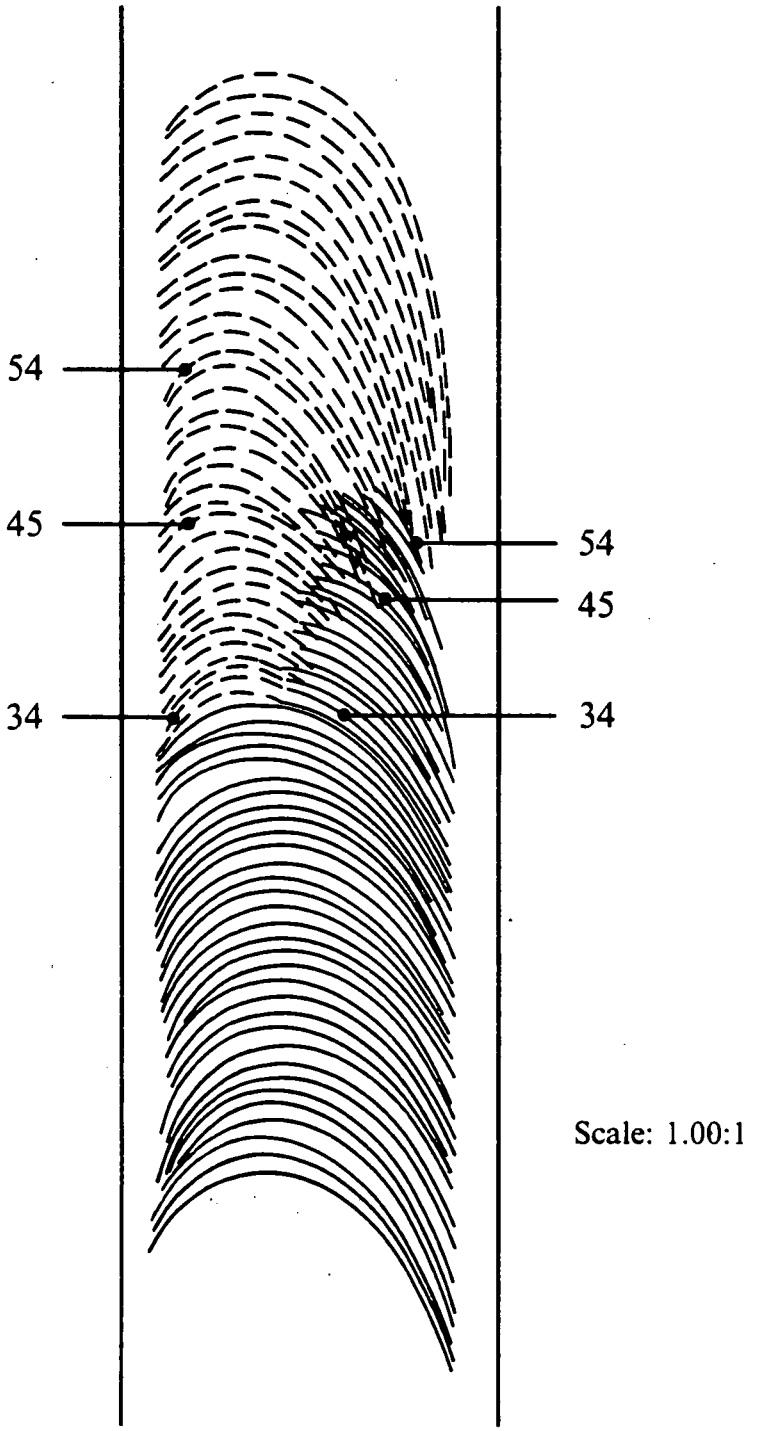

Figure 3-4. Cellular structure of a 5.23% methane-air flame at zero gravity. Visibile light photographs taken at 24 frames per second. Each frame is drawn. The vertical lines represent the inner walls of the tube. The solid and dashed lines denote the different cells in the transition from a stable flame to a cellular flame and back to a stable flame again. Frame numbers are given for clarity.

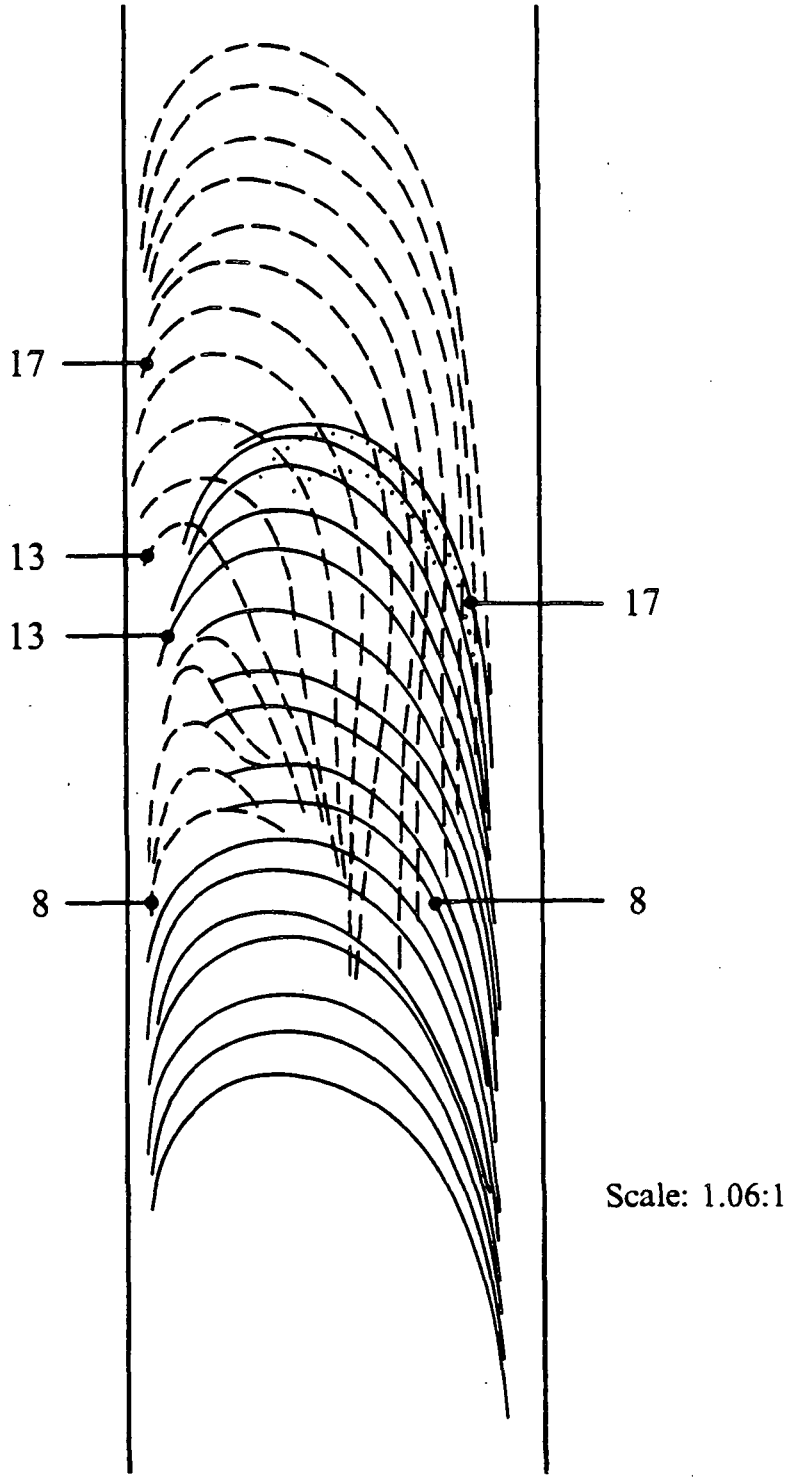

Figure 3-5. Cellular structure of a 5.30% methane-air flame at 0.33 g. Visibile light photographs taken at 24 frames per second. Each frame is drawn. The vertical lines represent the inner walls. The solid and dashed lines denote the different cells in the transition from a stable flame to a cellular flame and back to a stable flame again. Frame numbers are given for clarity. The dotted line denotes the position of the flame front in frames 18 and 19-20 showing that that cell translated downward in the tube before extinguishing.

3.5 Flame Speeds

3.5.1 Method of Data Reduction:

The flame speed is defined for the SFLT simply as the speed, in the laboratory frame, at which the flame front travels through the tube. The tip of the flame was always used in the determination of any flame speed for this analysis. The normal burning velocity is defined as the velocity of a laminar flame front, relative to the unburned mixture, in a direction perpendicular to itself. The two are equal only for an adiabatic flat flame. The behavior of the flames as a function of mixture composition and gravity level will be discussed quantitatively in terms of flame speeds rather than burning velocities. There are two reasons for this approach. Strehlow [14] describes a method of determining the burning velocity of a flame that is propagating inside a tube. The equation for burning velocity, S_u, is given as

$$S_u = \frac{A_{\text{Tube}}}{A_{\text{Flame}}} S_b \qquad [3\text{-}12]$$

where A_{Tube} is the cross-sectional area of the tube, i.e., of a flat flame having the same area as the tube, A_{Flame} is the surface area of the flame and S_b is the flame speed. The first reason, then, is that there are obvious difficulties in accurately determinimg the surface area of a three-dimensional flame from a two-dimensional image because the flames were seldom truly symmetric in shape. The caps were sometimes flattened, as in the zero g case, or the skirts may not have been symmetrical in length, as observed for flames in all but the strongest propane-air mixtures studied. Even if the surface area of the flames could have been calculated satisfactorily from the two-dimensional images, the apparent area of the flame fronts would have differed for different methods of observation, for example, by visible light photography or by Schlieren photography. Second, since heat losses to the walls of the tube have been shown to occur only for that portion of the flame in contact with the tube, at least for methane-air flames [18], the amount of heat lost will vary with mixture composition and gravity loading, thereby affecting

the burning velocities in these regions to varying degrees. Regions of the flame undergoing stretch, caused by the flow field ahead of the flame, will also propagate with different burning velocities depending upon the degree of stretch. Thus, if the entire surface area of the flame is used in the calculation, the value of burning velocity determined will be an "average" of the effects of heat loss and flame stretch. For these reasons, flame speeds have been reported rather than burning velocities, consistent with the findings reported by other researchers for SFLT's.

The collection of data using 16 mm movie cameras allowed the determination of flame speeds as a function of mixture composition and gravity loading. The method of data reduction involved first projecting the image of a flame onto a sheet of paper using a 16 mm analytical movie projector. As the film was advanced frame by frame, successive locations of the flame front were marked on the paper. This type of projector allowed slow-motion and fast-motion viewing of the flame histories in both forward and reverse speeds, as well as single-frame advance of the film. The reference dimension used was the external diameter of the tube. Since the cameras were operated at 24 frames per second, the interval and average flame speeds could easily be calculated. The flame speeds were extracted in this manner for all photographic data obtained during this research. A complete log of the fuel type, mixture strength, gravity conditons, and the results of the experiment for a given tube number and flight was kept for reference and has been included as an appendix. In addition, the cabin pressure and Z-axis gravity loading were recorded adjacent to each marked position of the flame front location, when applicable, so that g-jitter could be studied and so the time rate of change of the gravity loading could be determined. Typically, the cabin pressure was constant during a trajectory, though a variation of 0.7 kPa (0.1 psi) was occasionally observed. The cabin temperature was not subject to significant fluctuations during any one trajectory.

3.5.2 Discussion of Uncertainties:

The figures and tables that follow present flame speed data as a function of mixture com-

position and gravity loading for methane-air and propane-air flames. During data reduction, it became apparent that the interval flame speeds were not constant for any of the constant gravity conditions, particularly in the case of the methane-air flames. Consequently, maximum and minimum values of the flame speeds are plotted in most figures. There were a number of factors suspected of contributing to the flame speed fluctuations. The first source of these fluctuations was variations of the position of the film in the cameras used to photograph the flames and in the projector used in reduction of the data. This film positioning error was kept to a minimum by mounting the cameras on their sides such that the length of the tube, as recorded on the film, ran the width of the film. As explained below, the reason for positioning the cameras in this manner became apparent when the film was reviewed for the extraction of the flame speeds. The analytical projector employed for data analysis was prone to inconsistent vertical positioning of the film during frame-by-frame advance analagous to the initial framing error that occurs when any film is loaded into a projector. The elasticity of the film loops above and below the film guide inadvertantly caused the film to slip under the pressure plate. By positioning the cameras on their sides, the images of the propagating flames advanced horizontally across the screen and so were not subject to this framing error. Only the lateral position of the film in the guide could have influenced the flame speed data. This was ruled out since it was found that, after recording the advances of a flame on a sheet of paper, it was possible to return to the same film at a later date and match up the original marks with the corresponding projected image of the flame for every frame of film.

The second possible cause of the flame speed fluctuations was the inherent variations in the speed of the electric motors in the 16 mm movie cameras. This had no significant influence since the quoted accuracy of the camera motor speeds would have resulted in apparent flame speed fluctuations that were insignificant relative to the observed flame speed fluctuations. Also considered were camera motor speed fluctuations caused by variations in research power onboard the aircraft. This seems a viable explanation since the electrical loads placed on the

aircraft power system no doubt varied during flight, but nonsteady flame speeds of similar magnitude were observed for ground tests as well. Because these tests were performed using the same equipment as used onboard the Lear jet, but with wall outlet power, this would imply that fluctuations in Lear jet power did not contribute to the fluctuations in flame speed.

Third, since the flame speed differentials were observed to be similiar in magnitude for all three gravity conditions in either fuel-air system, even though the magnitudes of the variations in the ambient temperature and pressure were not, the effects of these variations on the flame speeds were relatively small.

There were, however, two factors found to contribute significantly to the flame speed fluctuations. The first of these was the uncertainty in the mixture compositions characteristic of the mixing system ($\pm$ 0.03% for methane-air mixtures and $\pm$ 0.04% for propane-air mixtures). It is obvious from examination of Figures 3-6 and 3-7 that near-limit-mixture flame speeds are quite sensitive to variations in mixture composition. For one g upward, one g downward, and zero g propagation, the maximum and minimum flame speeds of all flames observed for a given mixture composition were reported. These maxima and minima occurred for all mixture compositions, the magnitude of the difference varying at random as would be expected for this type of uncertainty. However, by noting the fluctuation of average flame speed with mixture composition for completely stable flames, such as those observed by Strehlow and Reuss [12] for one g upward conditions, it was found that the magnitude of this difference, roughly 1.2 cm/sec, could not in itself account for the observed flame speed fluctuations which were as high as 10.6 cm/sec.

Second, and of even greater significance, was the error in marking the advances of the flame fronts by hand for each frame of film. Precise visual determination of the location of the flame front was hampered by two factors: the finite thickness of the flame sheet (as much as 4

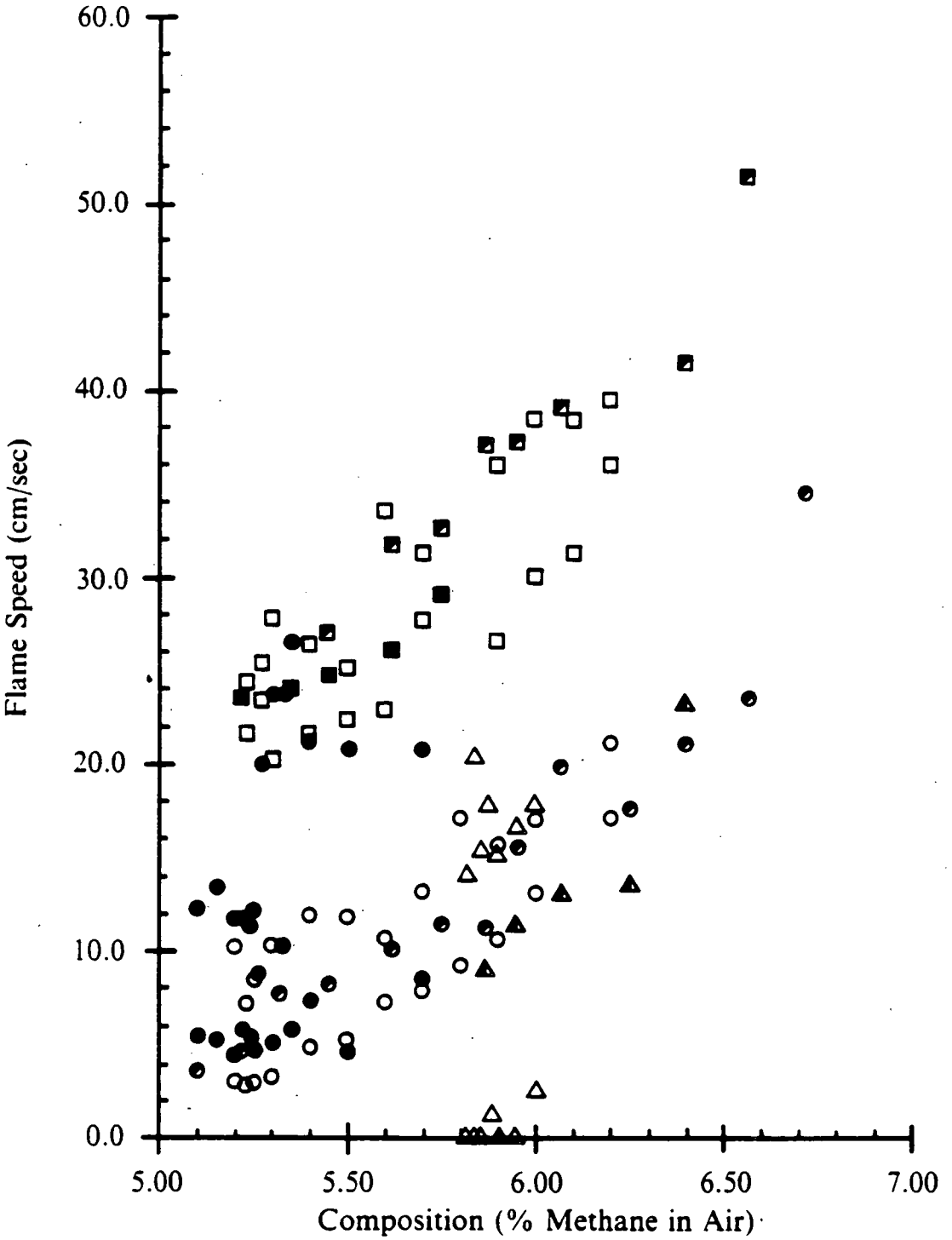

Figure 3-6. The effect of methane concentration on flame speed. Flame speeds are plotted for one g upward, one g downward, and zero g flame propagation versus the percent methane. Symbols: □, one g upward propagation; △, one g downward propagation; ○, zero g propagation. Source: open symbols, this investigation; half-open symbols, Ref. 12, drop-tower SFLT; solid squares, Ref. 12, full-size SFLT; solid circles, Ref. 4, the same apparatus. Maximum and minimum flame speeds are plotted for this investigation and Ref. 4. All others are average flame speeds.

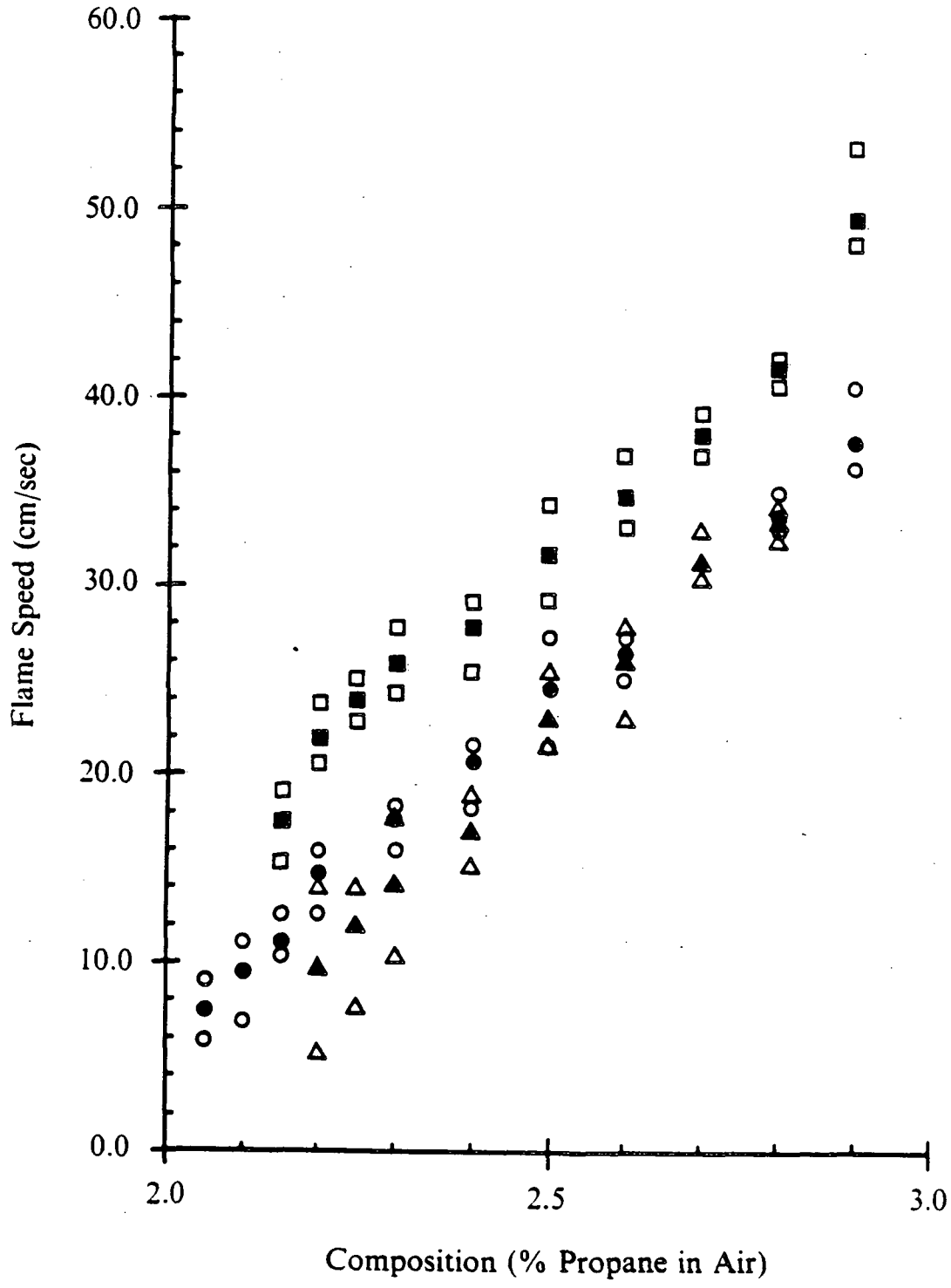

Figure 3-7. The effect of propane concentration on flame speed. Flame speeds are plotted for one g upward, one g downward, and zero g flame propagation versus the percent propane. Symbols: □, one g upward propagation; △, one g downward propagation; ○, zero g propagation. Source: this investigation. Open symbols represent maximum and minimum flame speeds and solid symbols represent average flame speeds.

or 5 mm according to [18]) and the low luminosity of the near-limit flames. Though the flame front location was always marked using the forward-most edge of the flame, the finite thickness of the flame sheet combined with the graniness of the film often made this region indistinct. The problem was compounded by the diminishing luminous intensity of the flame as the limit was approached. Zero g methane-air flames were particularly indistinct, yielding some photographic data that were completely unusable. A considerable effort was made to minimize these errors, but the maximum marking error was still about $\pm$ 0.07 cm when the image of the flame was projected full scale on the screen. This corresponded to an uncertainty in the flame speed of $\pm$1.7 cm/sec or a total variation of as much as 3.4 cm/sec. It might be possible to reduce this error by locating the projector at a greater distance from the screen, exaggerating the dimensions of the projected images. However, the resolution of the flame is fixed by the graniness of the film and the indistinct nature of the flame front such that no net reduction in marking error can be realized.

The differential between the maximum and minimum flame speeds found in this research vary randomly in magnitude. This is as expected for the combined errors in mixture composition and marking of the flame front location. Summing these effects directly yields a maximum variation in flame speed of 4.6 cm/sec. Since both sources of error are independent of each other and random, a more realistic combined variation would be 3.6 cm/sec for the zero g flames. One g upward and downward propagating flames will be subject to slightly smaller uncertainties in the flame speeds since the ambient fluctuations were smaller, but the difference is negligible.

3.5.3 Flame Speed Dependence on Mixture Composition:

The flame speeds were determined for methane-air mixtures for one g upward, one g downward, and zero g conditions. The maximum and minimum flame speeds have been plotted as a function of mixture composition for the three cases in Figure 3-6. Flame speed data as obtained by Noe [4] and Strehlow and Reuss [12] are included for comparison. In all cases the

flame speed decreases directly with the fuel concentration, tending toward a nonzero minimum value at the limit. These results for one g upward propagation generally agree with those of the other researchers. The expected variation in flame speeds of 3.6 cm/sec can account for the flame speed differential for only about half of the data points, the actual fluctuations covering as much as 10.6 cm/sec. Therefore, the fluctuating flame speeds must be the result of nonsteady behavior of the flames themselves.

In the case of one g downward propagation, comparison of the maximum and minimum flame speeds for this research with the single values reported by Strehlow and Reuss [12] is virtually impossible since these flames commonly propagated with a very nonsteady "sloshing" motion. The flame speeds were never constant, nor was there any indication that they ever would become steady for near-limit methane-air mixtures. Strehlow and Reuss also noted that, in lean-limit mixtures, a steady downward propagating flame does not exist.

The results obtained by Noe [4] and those obtained here under zero g conditions, for the same apparatus, are in marginal agreement. Noe encountered the same nonsteady behavior of the flame speeds though much more pronounced. The disagreement is most likely due to the difference in mixture composition uncertainty between this research and Noe's. Though the equipment used was basically the same for both researchers, modifications to improve the mixing system were implemented prior to this phase of the project. The results obtained by Strehlow and Reuss [12] are plotted as well and found to be in very good agreement. Whether or not the flame speeds would ever stabilize for the limit methane-air flames at zero g is not certain. No other SFLT data collected in extended periods of zero g for methane-air mixtures are known to exist.

Figure 3-7 summarizes the maximum and minimum flame speeds obtained for propane-air flames as a function of mixture composition. As observed for methane, all one g upward, one

g downward, and zero g flame speeds decreased with mixture strength toward a nonzero minimum value. In the case of one g upward propagation, the combined uncertainties in mixture composition and flame location account for about 4.4 cm/sec variation in the flame speeds. Almost all flame speed differentials fall within this range, indicating that the apparent nonsteadiness of the one g upward propane-air flames was not the result of any actual physical behavior. Therefore, the average flame speeds are meaningful and have been included in the figure. One g upward propagation flame speeds for a given mixture composition were always observed to exceed the one g downward and zero g flame speeds at the same mixture.

One g downward flame speeds were generally quite stable above 2.40% propane in air. Below this value, the flames behaved similarly to the one g downward methane flames, sloshing about the tube as they propagated. This is reflected in the larger flame speed differential below 2.40%. It is interesting to note that the one g downward and zero g flame speeds for the propane-air system are approximately the same except very near the one g downward limit where the flame front has been destabilized by its interaction with the induced flow field. In methane-air flames, the zero g flame speeds were slightly higher than the one g downward flame speeds for the same mixture.

3.5.4 Flame Speed Dependence on Gravity Loading:

Figure 3-8 summarizes the maximum and minimum flame speeds obtained for 5.30% methane-air mixtures burned under constant fractional gravity loadings ranging from 0.00 g to 1.77 g. The propagation is again nonsteady, but appears to be stabilizing as the gravity load increases. It should be noted that the amount of data supporting the high g point is limited compared with that for the other points. The flame speed generally increases with the gravity loading, but because of the nonsteadiness, an exact relation cannot be determined. The flame speed fluctuations also prevented any useful comparison of constant g flame speeds to transient g flame speeds.

Figure 3-9 shows similar data for propane-air flames. In this plot, however, the average flame speeds have been plotted since the scatter of the data was not due to any actual behavior of the flames for the propane-air system. The figure includes average flame speeds as a function of gravity loading for 2.30% propane in air at constant, fractional g conditions and at the corresponding g loadings for flames propagating under transient g conditions. The rate of change of gravity loading has been plotted as a function of gravity loading at the top of the figure. The constant g data ranges from 0.00 g to 1.77 g. Unfortunately, the transient g data does not exceed 1.00 g. The difficulty with collecting this kind of data was that a flame propagated quite quickly up the tube as the gravity loading was increased, reaching the end of the tube before the aircraft could attain the higher g loadings. It may be possible to collect the higher g data by igniting a flame later in a trajectory at a higher initial g loading, rather than in zero g, but timing this appropriately would be tricky and difficult with the present apparatus. The plot of the time rate of change of the gravity loading indicates the typical performance of the aircraft in such trajectories. The maximum dg/dt achieved was about 1.0 g/sec. The flame speeds observed under transient g conditions were not found to lag those for constant g conditions for the values of dg/dt encountered, and both appear to be increasing with gravity loading, but leveling off. It is expected that if dg/dt were large enough, a lag in flame speed might be observed due the slow change of the flame shape caused by the relatively thick preheat zone. However, this effect could not be investigated, and such a rate of change of gravity loading may not be safely attainable in the Lear jet facility.

Lastly, although transient g data were obtained for downward propagation of methane-air and propane-air flames, the nonsteadiness of these flames in both fuel-air systems for the range of mixtures investigated hindered the analysis. The flame speeds were too eratic to permit useful comparisons of the results. No anomalous behavior was observed for these flames; hence, they will not be discussed quantitatively.

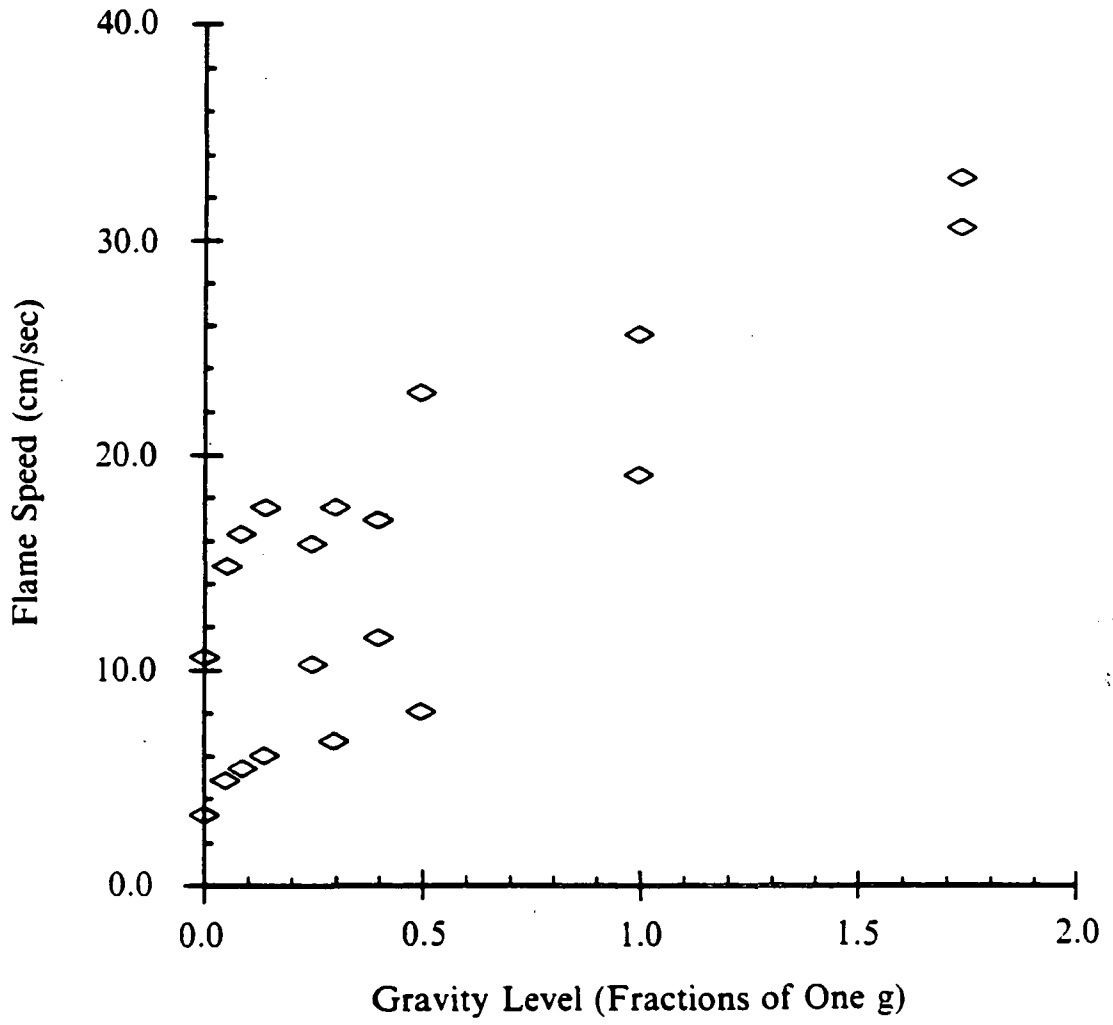

Figure 3-8. The effect of gravity loading on flame speed for flames in 5.30% methane-air mixtures. Flame speeds are plotted for zero g and upward propagation versus g loading. Symbols: ◇, maximum and minimum flame speeds for constant fractional g loadings. Source: this investigation.

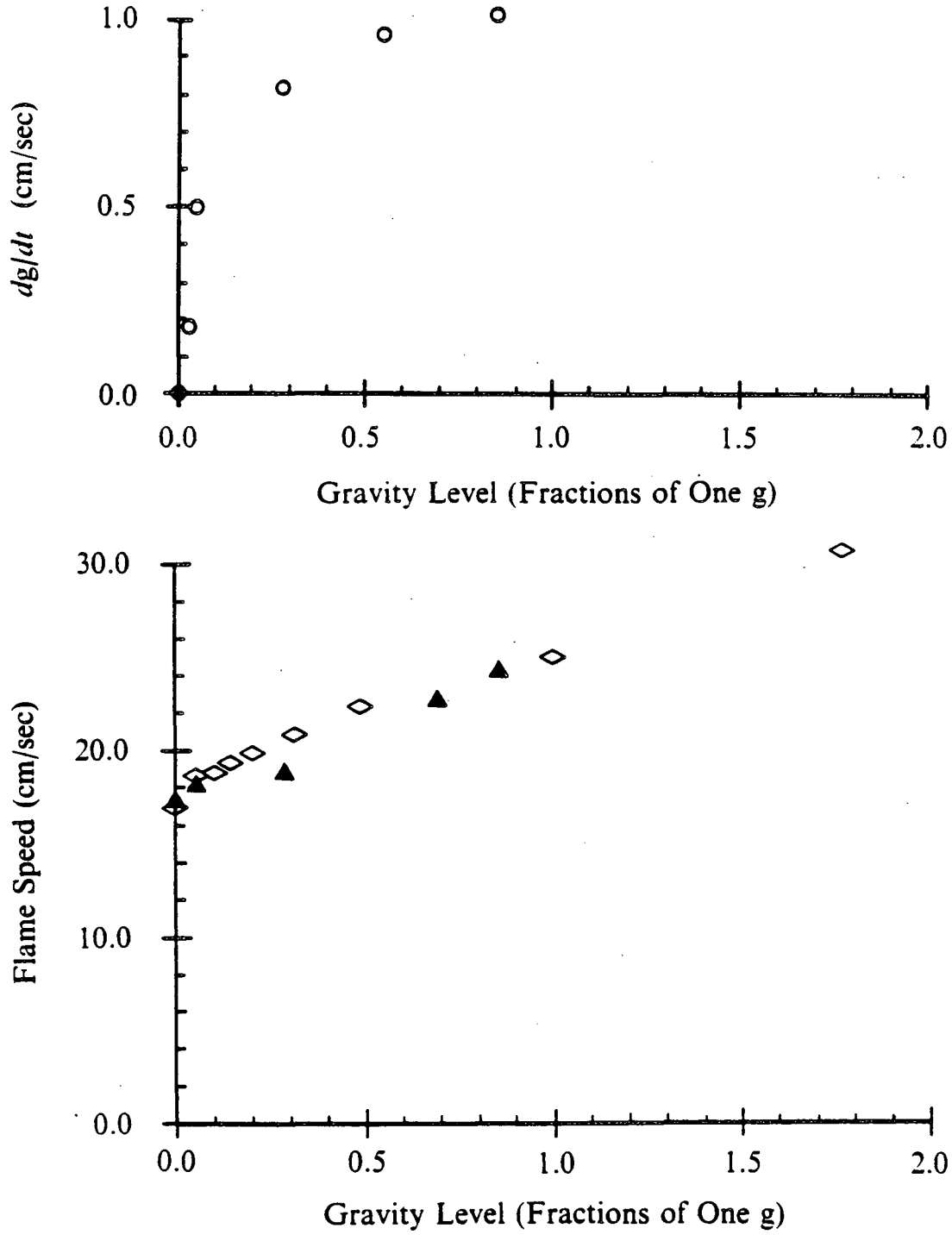

Figure 3-9. The effect of gravity loading on flame speed for flames in 2.30% propane-air mixtures. Flame speeds are plotted for zero g and upward propagation versus g loading. Symbols: ◇, average flame speeds for constant fractional g loadings; ▲, average instantaneous flame speeds for increasing transient g loadings; o, instantaneous *dg/dt* for that g loading. Source: this investigation.

In conclusion, the fluctuations in the calculated values of the flame speeds for propane-air flames were explainable in terms of the uncertainties in the mixture composition and the marking errors inherent in the data reduction process, while the variations observed for methane-air flames were not. All other sources of error have been ruled out. Since the same gas-mixing system was used to produce the mixtures in both cases, the fact that the flame speed fluctuations for propane were explainable in terms of extraneous errors precludes the possibility of incomplete mixing of the gases. Moreover, increasing and decreasing trends in the flame speeds around the maximum and minimum values could be seen on film from frame to frame implying that the flame itself was behaving in a nonsteady fashion. Since steady flame speeds have been observed by other researchers, the only remaining possible explanation of the relatively unstable behavior of all methane-air flames is that the SFLT's employed in these experiments were too short to permit the flame fronts to stabilize completely. It was observed that, subsequent to the very high energy ignition process, some methane-air flames would not attain fully developed structure for as much as one-third of the length of the tube. Achieving what appeared to be stable propagation could require as much as one-half the tube length for upward propagating flames and was usually not observed for zero g methane-air flames. Further investigation of the methane-air system, particularly of the zero g flames, using a longer flammability limit tube may be of interest. It may be for the lean methane-air flames that, in the absence of the stabilizing influence of buoyancy-induced flame stretch, preferential diffusion will never permit the flames to stabilize in zero g.

3.6 Extinction

The extinction process was investigated for constant one g upward, one g downward, and zero g propagation for both fuel-air systems. Extinction processes were also studied for sufficiently lean flames ignited in zero g that were forced to extinguish as the gravity loading was

increased for upward propagation and, then, for downward propagation by inverting the entire flammability limit apparatus within the NASA rack.

One g upward propagating limit and sublimit methane-air flames were observed to extinguish from the tip outward. von Lavante and Strehlow [16] established experimentally for methane-air flames that heat losses to the tube walls could only occur for that portion of the flame in contact with the walls. But since the upward propagating flames were not observed to extinguish at the walls first, heat loss to the walls was ruled out as the cause of extinction. Also, unusually low temperatures of the gas just behind the flame cap for near-limit upward propagating flames were observed by Jarosinski, et al., [18] caused by stretch at the flame tip. Because the flames observed here extinguished at the tip first, excessive flame stretch is believed to be the cause of extinction for upward propagating flames. No extinguishment was observed for one g upward propagation in the propane-air system. These flames either propagated the full length of the tube or did not propagate away from the ignition source at all. In one g downward propagation, however, it seems that the extinction process is initiated by heat loss to the walls, the flames extinguishing from the edge inward. The flame fronts propagated in and unsteady fashion, continually shrinking and slowing, finally rising slightly in the tube before buoyancy-driven extinction occurred. The extinction process for one g downward propagation occurred in the same manner for methane-air and propane-air flames. All observations for one g upward and one g downward propagation of methane-air flames are consistent with those made by Noe [4] for this apparatus and with those made by other researchers for similar apparatus. Zero g extinction was observed for fuel-lean flames in both fuel-air systems studied. Figure 3-10 shows the extinguishment process for a 5.24% methane-air flame. Initially, the flame was observed to fill the SFLT. As it propagated through the tube, the skirt length decreased until only a small cap remained. This cap continued to decrease in diameter as the the flame propagated, extinguishing abruptly as illustrated. The characteristic nonsteadiness of the lean methane-air flames is also visible in the figure.

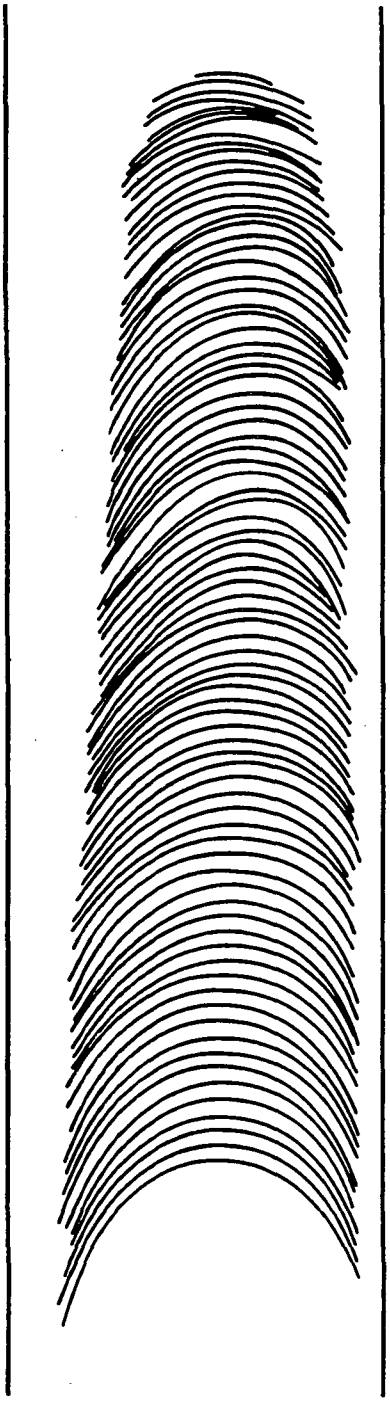

Scale: 1.00:1

Figure 3-10. A 5.24% methane-air flame extinguishing in zero gravity. Visible light photograph taken at 24 frames per second. Every frame is drawn. The vertical lines represent the inner walls of the tube.

Extinguishment of upward propagating flames for transient g loadings occurred essentially in the same manner as that observed for constant one g upward propagation. The skirt length was considerably longer that that of the one g flames, but the flames extinguished from the center, or holding region, outward. Transient g loadings for downward propagation produced extinguishment comparable with that observed for constant one g downward propagation. The slight rise of the flame front typically observed just prior to extinction for one g flames was more pronounced for the transient g flame, as might be expected, due to the increased bouyancy forces acting on the flames at the higher g loadings.

4 Equipment Evaluation

Several equipment deficiencies and malfunctions were encountered in the course of this research project. Modification of the apparatus to correct the deficiencies and to prevent similar malfuncitons in the future should be completed prior to use of this apparatus for further flame propagation studies onboard the NASA Lewis Airborne Research Facility.

4.1 Equipment Deficiencies

First of all, though the gas-mixing system was used successfully to produce the desired mixture compositions, the precision of the system in its present form has been fully realized. The uncertainties determined for the calibration method used were $\pm$ 0.03% for methane-air mixtures and $\pm$ 0.04% for propane-air mixtures which, though improved over that for Noe's research because of hardware modifications, still resulted in variations in the measured flame speeds that complicated data interpretation. Flow rate inaccuracies in this type of continuous-flow system can result from supply-pressure fluctuations with time and temperature, error in reading and difficulty in maintaining the desired upstream and downstream pressures, error in reading the rotameters, and leaks which can occurr at any of twenty-three critical connections or in the mixing chamber itself. After an extensive search failed to locate any new rotameters compatible with this system that could be matched to yield greater resolution of the mixture compositions, it seems unlikely that further improvements of this particular mixing system can be made. Furthermore, this system is time consuming to operate, requiring well over an hour

to fill eight tubes with eight different mixtures, not including the ground test firings for each mixture. Lastly, the methods of calibration available for this type of continuous-flow mixing system were limited and rather inconvenient. The method used in this instance was fluid displacement in a volumetric cylinder. Problems with this method of calibration included error in starting and stopping the flow into the cylinder in exact accordance with the timing device, reading the volume displaced (the single largest source of accuracy error), *assuming* that the gas in the graduated cylinder was saturated with water vapor when it may not have been, and accounting for possible solubility effects. Though the effect of random errors can be reduced by taking multiple readings, the calibration process must be done for each gas used and it is extremely time consuming. In future research, the technique of evacuating the SFLT's and then filling them with fuel and air using the law of partial pressures is recommended over the present arrangement. This would minimize errors because of fewer gauges to read (only one would be necessary, that which measures the pressure of the gases in the SFLT). It would eliminate supply pressure fluctuation errors, rotameters, most of the potentially leaky tube connections, the mixing chamber, and the hazard created by excess combustible gases. The accuracy and precision could be greatly improved over the present system depending only on the accuracy of the pressure gauge. Ronnie [11] reports accuracy of $\pm$ 0.25% which corresponds to $\pm$ 0.013 volume % for the range of mixture compositions studied here. Also, filling times may be reduced, and the practice of confirming the mixture composition with ground test firings would, perhaps, be unnecessary. Overall, the accuracy, precision, and reliability of the system would be superior to that of the existing design. The near-limit flame speeds were found to be extremely sensitve to mixture strength variations, and any improvements made would be reflected in the quality of the data and the integrity of the results.

Second, the DPM's that displayed the accelerometer outputs in all three axes updated the displayed information only three times per second. These should be replaced by DPM's with higher sampling rates that could provide resolution of the changing gravity loading

commensurate with the framing rate of the cameras. This would make possible closer correlation of the g loading with the observed flame behavior.

4.2 Equipment Malfunctions

First, the original design of the mixing system housed both the 28 V dc power supply with the ground-test ignition circuitry and the mixing system components inside a closed stainless steel sheet metal box. The ramifications of combining electrical equipment in a closed container with a flammable mixture of gases are obvious. The stainless steel box was opened at the outset to avoid any mishaps and remained so for the duration of this research. This ignition system eventually failed, however, preventing further ground-test firings. The exact cause of the failure was never determined for to a lack of time.

The flammability limit apparatus itself suffered from numerous mechanical problems. Sticky sliding plate valves were a constant problem, often requiring an inordinate effort on the part of the researcher to manually free the valve during the automatic sequencing cycle after it had failed to open properly. Four additional problems stemmed from the use of a pneumatic cylinder to actuate the sliding plate valves. First, the accompanying pressure tank had to be filled at least every other flight because the plunger approached satisfactory operation only over a small range of tank pressures. Second, because the sliding plate valves offered heavy resistance when seated and very little when useated, excessive tank pressures were necessary unless the valves were manually unseated prior to a tube firing. Even if this was done, the valve opened rapidly under the force of the plunger and halted so abruptly in the fully open position that the plunger was often damaged. Inspection revealed that this component was very near failure at the conclusion of the research. Third, the solenoid valve that controlled air flow to the pneumatic cylinder began to stick during the last few flights. It must be replaced before further use of the apparatus. Fourth, the pressure tank added unecessary weight to an already heavy ap-

paratus that required two people to load it onto the Lear jet. Beside the problems experienced with the pneumatic actuation system, the carrousel arrangement of the SFLT's had many inherent drawbacks. Rotation of the tubes was not always smooth because of misalignment of the slot on the sliding plate valve with the plunger that it was to engage. Also, the knife switches were prone to misalignment and deformation that occasionally resulted in a misfire. Lastly, igniters began failing frequently by the conclusion of the research. This may have been attributable to high atmospheric humidity, but the exact cause remains undetermined.

Slight problems were encountered with the automatic sequencing system timing unit. The allen-head set screws that secured the cam wheels to the timing shaft occasionally worked loose. This caused inaccurate sequencing of the equipment and, in one instance, a set screw came out completely, wedged under another cam wheel, and jammed the entire timing unit. The problem could not be corrected in the air, resulting in an aborted flight. This problem was corrected at the time with Lock-Tite.

4.3 Recommended Improvements

In light of these problems, it is recommended for future research that:

1. The SFLT's should be filled with the desired mixture compositions using the law of partial pressures.

2. A new flammability limit apparatus should be constructed with the improvements already mentioned that can accommodate longer SFLT's.

Such an apparatus could consist of one pair of stationary mounting brackets to support a single SFLT. Each SFLT would be fitted with a sliding plate valve that would engage an electromechanical actuator when properly aligned and locked into the mounting brackets, thus

eliminating the myriad of problems associated with the pneumatic actuator and the carrousel arrangement. A pair of such actuators, one at each end, could make downward propagation experiments as easy to perform as zero g or upward propagation experiments simply by orienting the tube as desired before inserting it in the mounting brackets; the present design is almost unacceptable for this task because the entire apparatus must be removed from the NASA rack, inverted, and reinstalled in the rack, requiring two people and three hours to accomplish. Also, the present flammability limit apparatus contains only eight tubes. This was adequate for zero g experiments since a maximum of six trajectories could be completed on any single flight due to venting of the aircraft's turbine engine lubricating oil in zero g. But for most of the fractional and all of the high g experiments, the maximum number of trajectories could have been much greater. If separate tubes were used, the second NASA rack could be modified to hold perhaps twenty SFLT's that the researcher would remove from the storage rack and install in position manually for photographing. Since the present sequencing apparatus keeps the cameras operating for 23 seconds, the limiting factor would then most likely be the quantity of film. If a separate manual power switch could be installed for the cameras, film would not have to be wasted after the flame had extinguished. Instead of gathering six data points per flight, twenty or more could be collected. This would be a much more efficient scheme considering the limited availability of the Lear jet. More importantly, the cost per data point could be drastically reduced. The new flammability limit apparatus could probably be manufactured for less than the cost of two Lear jet flights, a worthwhile investment. The equipment necessary for the suggested SFLT filling method already exists at NASA and is commonly used for this purpose.

Finally, use of an image intensifier or other form of enhancement should be investigated to make data reduction easier and subject to less error. Installation of further instrumentation, such as thermocouples to determine the thermal structure of the zero g flames, should also be considered. Temporal and spatial temperature information could be used to quantify heat losses

and flame stretch providing detailed insight into the mechanism of extinction for flames under any gravity conditions.

5 Conclusions and Recommendations

The fuel-lean flammability limits were determined for methane-air and propane-air flames for one g upward, one g downward, and zero g propagation using a standard flammability limit tube. The behavior of limit and near-limit flames was investigated for a variety of constant fractional gravity loadings and transient gravity loadings. Three major conclusions have been drawn from this study:

1. The one g upward and zero g lean limits were the same for the methane-air system indicating that gravity has no effect on the upward propagation limit for fuel-lean methane-air flames. However, gravity did significantly affect the lean-limit for upward propagation in the propane-air system.

2. Gravity stabilized an inherently cellularly unstable upward propagating methane-air flame because buoyancy of the hot product gses behind the flame front induced positive stretch at the flame tip, which is qualitatively consistent with previous results and is supported by other quantitative studies.

3. The extinction of upward propagating methane-air and propane-air flames was initiated by excessive gravity-induced stretch at the flame tip. Extinction for one g downward propagation was initiated in both systems by heat loss to the tube walls. The remainder of the flame front was ultimately driven to extinction by differential

buoyancy which forced product gases ahead of the flame [18]. The extinction process for one g downward propagation was augmented by the inherent instability of the fuel-lean methane-air flame which results from preferential diffusion of the fuel toward the reaction zone. Zero g flame extinction was also initiated by heat loss to the tube walls in both fuel-air systems. The extinguishment processes observed agree in all cases with previous experimental results.

Although the observations relative to the propagation behavior and extinguishment processes of these flames were qualitatively explainable in terms of interactions between the SFLT geometry, heat losses, gravity-induced flame stretch, and preferential diffusion, a quantitative study might yield definite relationships among these that would give greater insight into the observed phenomena and make their occurrence quantitatively predictable. Such an analysis would require modification of the existing flammability limit apparatus, or perhaps a completely new design, instrumented to collect temperature and flow velocity data.

References

1. Roskam, J., *Airplane Flight Dynamics and Automatic Flight Controls*, Roskam Aviation and Engineering Corporation, U.S.A., Appendix C (1979).

2. *NASA Lewis Airborne Research Laboratory Experimenter's Handbook*, NASA Lewis Research Center, Cleveland, Ohio (No date available).

3. Strehlow, R. A., "Flammability Limits of Gases Under Low Gravity Conditions," NASA Final Report, NASA Lewis Research Center, Cleveland, Ohio, Nov. (1983).

4. Noe, K. A., "Behavior of the Lean Methane-Air Flame at Zero-Gravity," M. S. Thesis, University of Illinois (1983).

5. Weast, R. C., ed., *CRC Handbook of Chemistry and Physics*, 50th Ed., Chemical Rubber Co., Cleveland, Ohio, Section D-137 (1969).

6. Dack, Michael R. J., ed., *Solutions and Solubilities*, Part 1, in *Techniques of Chemistry*, Vol. 8, John Wiley and Sons, New York, Chapter 7 (1975).

7. Schenck, Jr., Hilbert, *Theories of Engineering Experimentation*, McGraw-Hill Book Company, Inc., New York, New York, Chapters 1-3 and 8 (1961).

8. Parratt, Lyman G., *Probability and Experimental Error in Science*, John Wiley and Sons, Inc., New York, New York, Chapters 1-4 (1961).

9. Fedoroff, Basil T., and Sheffield, Oliver E., *Encyclopedia of Explosives and Related Items*, Vol. 2, Picatinny Arsenal, Dover, New Jersey, Part C (1962).

10. Zabetakis, M.G., "Flammability Characteristics of Combustible Gases and Vapors," Bureau of Mines Bulletin 627, Washington, 121pp (1965).

11. Ronney, P.D. and Wachman, H.Y., *Combustion and Flame*, **62**, 107 (1985).

12. Strehlow, R. A. and Reuss, D. L., "Flammability Limits in a Standard Tube," *Combustion Experiments in a Zero Gravity Laboratory*, Cochran, T. H., ed., *Progress in Aeronautics and Astronautics*, American Institute of Aeronautics and Astronautics, New York, New York, **73**: 61-90, (1981); also NASA CR 3259 (1980).

13. Coward, H.F. and Jones, G.W., "Limits of Flammability of Gases and Vapors," Bureau of Mines Bulletin 503, Washington, 155pp (1952).

14. Strehlow, R.A., *Combustion Fundamentals*, McGraw Hill Book Company, Inc., New York, New York, Chapter 8 (1984).

15. Sivashinsky, G.I., "Instabilities, Pattern Formation, and Turbulence in Flames," *Annual Review of Fluid Mechanics*, **15:** 179-199 (1983).

16. von Lavante, E. and Strehlow, R. A., *Combustion and Flame*, **49**, 123 (1982).

17. Markstein, G. H., *Nonsteady Flame Propagation*, Macmillan. New York, Chapter D (1964).

18. Jarosinski, J., Strehlow, R. A., and Azarbarzin, A., "The Mechanism of Lean Limit Flame Extinguishment in a Standard Flammability Tube," *Nineteenth Symposium (International) on Combustion*, The Combustion Institute. Pittsburgh, Pennsylvania, 1549-1557 (1982).

Appendix. Index of Photographic Data

The following are records of all tube firings performed during this flammability limit study. The mixture compostion (corrected to standard temperature = 273.15 K and standard pressure = 760.0 mm Hg), gravity conditions and results of each firing are listed as a function of the tube number for a given flight or ground test. The film canisters have been labeled according to the flight or ground test number, the date of the test and the time of day it was performed (A.M. or P.M.). This information was included for most of the tests on a placard colocated with the DPM's that is visible in the films. The tube number is also visible on the tube itself.

Ground Test Records

Ground Test 1	Date: 7/25/85, P.M.
Purpose: To establish the one g fuel-lean limit for upward propagation of CH_4-air flames.	

Tube Number	Mixture Composition	Gravity Conditions, Direction of Propagation	Test Results
1	5.60% CH_4	1.00 g upward	misfire
2	5.50% CH_4	1.00 g upward	full propagation
3	5.40% CH_4	1.00 g upward	misfire
4	5.30% CH_4	1.00 g upward	partial propagation
5	5.20% CH_4	1.00 g upward	partial propagation
6	5.10% CH_4	1.00 g upward	partial propagation
7	5.00% CH_4	1.00 g upward	partial propagation
8	4.90% CH_4	1.00 g upward	partial propagation

Note: Top camera was running at 18 instead of 24 frames per second.

Ground Test 2		Date: 7/26/85, A.M.	
Purpose: To establish the one g fuel-lean limit for upward propagation of CH_4-air flames.			
Tube Number	Mixture Composition	Gravity Conditions, Direction of Propagation	Test Results
1	5.20% CH_4	1.00 g upward	partial propagation
2	5.23% CH_4	1.00 g upward	full propagation
3	5.23% CH_4	1.00 g upward	full propagation (no film record)
4	5.27% CH_4	1.00 g upward	full propagation
5	5.27% CH_4	1.00 g upward	full propagation
6	5.30% CH_4	1.00 g upward	full propagation
7	5.25% CH_4	1.00 g upward	full propagation
8	5.25% CH_4	1.00 g upward	full propagation

Note: Top camera was running at 18 instead of 24 frames per second.

Ground Test 3	Date: 7/29/85, A.M.

Purpose: To establish the one g fuel-lean limit for upward propagation of CH_4-air flames.

Tube Number	Mixture Composition	Gravity Conditions, Direction of Propagation	Test Results
1	5.26% CH_4	1.00 g upward	partial propagation
2	5.24% CH_4	1.00 g upward	partial propagation
3	5.24% CH_4	1.00 g upward	skipped it
4	5.20% CH_4	1.00 g upward	skipped it
5	5.26% CH_4	1.00 g upward	misfired
6	5.24% CH_4	1.00 g upward	misfired
7	5.22% CH_4	1.00 g upward	partial propagation
8	5.20% CH_4	1.00 g upward	partial propagation

Ground Test 4		Date: 7/29/85, P.M.	
Purpose: To establish the one g fuel-lean limit for upward propagation of CH_4-air flames.			
Tube Number	Mixture Composition	Gravity Conditions, Direction of Propagation	Test Results
1	5.30% CH_4	1.00 g upward	full propagation
2	5.28% CH_4	1.00 g upward	partial propagation
3	5.26% CH_4	1.00 g upward	partial propagation
4	5.24% CH_4	1.00 g upward	partial propagation
5	5.30% CH_4	1.00 g upward	full propagation
6	5.28% CH_4	1.00 g upward	partial propagation
7	5.26% CH_4	1.00 g upward	partial propagation
8	5.24% CH_4	1.00 g upward	partial propagation

Ground Test 5		Date: 10/4/85, P.M.	
Purpose: To establish the one g fuel-lean limit for upward propagation of C_3H_8-air flames.			
Tube Number	Mixture Composition	Gravity Conditions, Direction of Propagation	Test Results
1	1.90% C_3H_8	1.00 g upward	no propagation
2	1.95% C_3H_8	1.00 g upward	no propagation
3	2.00% C_3H_8	1.00 g upward	no propagation
4	2.05% C_3H_8	1.00 g upward	no propagation
5	2.10% C_3H_8	1.00 g upward	no propagation
6	2.15% C_3H_8	1.00 g upward	no propagation
7	2.20% C_3H_8	1.00 g upward	full propagation
8	2.25% C_3H_8	1.00 g upward	full propagation

Ground Test 6	Date: 10/4/85, P.M.

Purpose: To establish the one g fuel-lean limit for upward propagation of C_3H_8-air flames.

Tube Number	Mixture Composition	Gravity Conditions, Direction of Propagation	Test Results
1	2.30% C_3H_8	1.00 g upward	full propagation
2	2.40% C_3H_8	1.00 g upward	full propagation
3	2.50% C_3H_8	1.00 g upward	full propagation
4	2.60% C_3H_8	1.00 g upward	full propagation
5	2.70% C_3H_8	1.00 g upward	full propagation
6	2.80% C_3H_8	1.00 g upward	full propagation
7	2.90% C_3H_8	1.00 g upward	full propagation
8	3.00% C_3H_8	1.00 g upward	full propagation

Ground Test 7		Date: 10/8/85, P.M.	
Purpose: To establish the one g fuel-lean limit for upward propagation of C_3H_8-air flames and to collect data on richer mixtures.			
Tube Number	Mixture Composition	Gravity Conditions, Direction of Propagation	Test Results
1	2.10% C_3H_8	1.00 g upward	no propagation
2	2.15% C_3H_8	1.00 g upward	full propagation
3	2.20% C_3H_8	1.00 g upward	full propagation
4	2.25% C_3H_8	1.00 g upward	full propagation
5	2.30% C_3H_8	1.00 g upward	full propagation
6	2.90% C_3H_8	1.00 g upward	full propagation

Ground Test 8		Date: 10/8/85, P.M.	
Purpose: To establish the one g fuel-lean limit for upward propagation of C_3H_8-air flames.			
Tube Number	Mixture Composition	Gravity Conditions, Direction of Propagation	Test Results
1	2.12% C_3H_8	1.00 g upward	no propagation
2	2.14% C_3H_8	1.00 g upward	no propagation
3	2.16% C_3H_8	1.00 g upward	full propagation
4	2.18% C_3H_8	1.00 g upward	no propagation
5	2.12% C_3H_8	1.00 g upward	no propagation
6	2.14% C_3H_8	1.00 g upward	no propagation
7	2.16% C_3H_8	1.00 g upward	full propagation
8	2.18% C_3H_8	1.00 g upward	full propagation

Ground Test 9		Date: 10/8/85, P.M.	
Purpose: To establish the one g fuel-lean limit for downward propagation of C_3H_8-air flames.			
Tube Number	Mixture Composition	Gravity Conditions, Direction of Propagation	Test Results
1	2.30% C_3H_8	1.00 g downward	full propagation
2	2.40% C_3H_8	1.00 g downward	full propagation
3	2.50% C_3H_8	1.00 g downward	full propagation
4	2.60% C_3H_8	1.00 g downward	full propagation
5	2.70% C_3H_8	1.00 g downward	full propagation
6	2.80% C_3H_8	1.00 g downward	full propagation

Ground Test 10		Date: 10/8/85, P.M.	
Purpose: To establish the one g fuel-lean limit for downward propagation of C_3H_8-air flames.			
Tube Number	Mixture Composition	Gravity Conditions, Direction of Propagation	Test Results
1	2.10% C_3H_8	1.00 g downward	no propagation
2	2.15% C_3H_8	1.00 g downward	no propagation
3	2.20% C_3H_8	1.00 g downward	full propagation
4	2.25% C_3H_8	1.00 g downward	full propagation
5	2.30% C_3H_8	1.00 g downward	full propagation
6	2.35% C_3H_8	1.00 g downward	full propagation
7	2.20% C_3H_8	1.00 g downward	full propagation
8	2.25% C_3H_8	1.00 g downward	full propagation

Ground Test 11			Date: 10/8/85, P.M.
Purpose: To establish the one g fuel-lean limit for downward propagation of C_3H_8-air flames.			
Tube Number	Mixture Composition	Gravity Conditions, Direction of Propagation	Test Results
1	2.14% C_3H_8	1.00 g downward	no propagation
2	2.16% C_3H_8	1.00 g downward	partial propagation
3	2.18% C_3H_8	1.00 g downward	no propagation
4	2.20% C_3H_8	1.00 g downward	partial propagation
5	2.16% C_3H_8	1.00 g downward	partial propagation
6	2.18% C_3H_8	1.00 g downward	partial propagation
7	2.20% C_3H_8	1.00 g downward	full propagation

Ground Test 12		Date: 10/8/85, P.M.	
Purpose: To establish the one g fuel-lean limit for downward propagation of C_3H_8-air and CH_4-air flames.			
Tube Number	Mixture Composition	Gravity Conditions, Direction of Propagation	Test Results
1	2.22% C_3H_8	1.00 g downward	full propagation
2	2.24% C_3H_8	1.00 g downward	full propagation
3	2.22% C_3H_8	1.00 g downward	full propagation
4	2.24% C_3H_8	1.00 g downward	full propagation
5	5.30% CH_4	1.00 g downward	no propagation
6	5.50% CH_4	1.00 g downward	no propagation
7	5.70% CH_4	1.00 g downward	no propagation
8	5.90% CH_4	1.00 g downward	full propagation

Ground Test 13			Date: 10/8/85, P.M.
Purpose: To establish the one g fuel-lean limit for downward propagation of CH_4-air flames.			
Tube Number	Mixture Composition	Gravity Conditions, Direction of Propagation	Test Results
1	5.80% CH_4	1.0 g downward	partial propagation, (poor film record)
2	5.85% CH_4	1.00 g downward	full propagation
3	5.90% CH_4	1.00 g downward	full propagation
4	5.95% CH_4	1.00 g downward	misfired
5	6.00% CH_4	1.00 g downward	full propagation
6	5.85% CH_4	1.00 g downward	full propagation
7	5.90% CH_4	1.00 g downward	misfired
8	5.95% CH_4	1.00 g downward	full propagation

Ground Test 14		Date: 10/8/85, P.M.	
Purpose: To establish the one g fuel-lean limit for downward propagation of CH_4-air flames.			
Tube Number	Mixture Composition	Gravity Conditions, Direction of Propagation	Test Results
1	5.82% CH_4	1.00 g downward	full propagation
2	5.84% CH_4	1.00 g downward	no propagation
3	5.86% CH_4	1.00 g downward	partial propagation
4	5.88% CH_4	1.00 g downward	partial propagation
5	5.82% CH_4	1.00 g downward	partial propagation
6	5.84% CH_4	1.00 g downward	full propagation
7	5.86% CH_4	1.00 g downward	partial propagation
8	5.88% CH_4	1.00 g downward	full propagation

Ground Test 15	Date: 10/8/85, P.M.

Purpose: To obtain one g fuel-lean upward propagation data for CH_4-air flames in richer mixtures.

Tube Number	Mixture Composition	Gravity Conditions, Direction of Propagation	Test Results
1	5.50% CH_4	1.00 g upward	full propagation (no film record)
2	5.60% CH_4	1.00 g upward	full propagation
3	5.70% CH_4	1.00 g upward	full propagation
4	5.80% CH_4	1.00 g upward	full propagation (no film record)
5	5.90% CH_4	1.00 g upward	full propagation (no film record)
6	6.00% CH_4	1.00 g upward	full propagation (no film record)
7	6.10% CH_4	1.00 g upward	full propagation (no film record)
8	6.20% CH_4	1.00 g upward	full propagation (no film record)

Ground Test 16	Date: 10/11/85, A.M.

Purpose: To collect data points missed in ground test 15.

Tube Number	Mixture Composition	Gravity Conditions, Direction of Propagation	Test Results
1	5.50% CH_4	1.00 g upward	misfired
2	5.60% CH_4	1.00 g upward	full propagation
3	5.70% CH_4	1.00 g upward	misfired
4	5.80% CH_4	1.00 g upward	misfired
5	5.90% CH_4	1.00 g upward	full propagation
6	6.00% CH_4	1.00 g upward	misfired
7	6.10% CH_4	1.00 g upward	full propagation
8	6.20% CH_4	1.00 g upward	misfired

Note: Misfires were caused by a problem with the igniters. The exact cause of the problem was not determined.

Ground Test 17		Date: 10/11/85, P.M.	
Purpose: To collect data points missed in ground test 16.			
Tube Number	Mixture Composition	Gravity Conditions, Direction of Propagation	Test Results
1	5.50% CH_4	1.00 g upward	misfired
2	5.60% CH_4	1.00 g upward	full propagation
3	5.70% CH_4	1.00 g upward	full propagation
4	5.80% CH_4	1.00 g upward	misfired
5	5.90% CH_4	1.00 g upward	full propagation
6	6.00% CH_4	1.00 g upward	full propagation
7	6.10% CH_4	1.00 g upward	misfired
8	6.20% CH_4	1.00 g upward	full propagation

Note: Misfires were caused by a problem with the igniters. The exact cause of the problem was not determined.

Ground Test 18		Date: 10/11/85, P.M.	
Purpose: To collect data points missed in ground test 17.			
Tube Number	Mixture Composition	Gravity Conditions, Direction of Propagation	Test Results
1	5.80% CH_4	1.00 g upward	misfired
2	5.80% CH_4	1.00 g upward	no propagation
3	5.80% CH_4	1.00 g upward	misfired
4	5.80% CH_4	1.00 g upward	misfired
5	6.20% CH_4	1.00 g upward	full propagation
6	6.20% CH_4	1.00 g upward	full propagation
7	6.20% CH_4	1.00 g upward	skipped it
8	6.20% CH_4	1.00 g upward	skipped it

Note: Misfires were caused by a problem with the igniters. The exact cause of the problem was not determined.

Flight Test Records

The records presented here include all tube firings made for all flights. The results of flights 1 through 4 are of little value due to the limited amount of data collected because of difficulties with the apparatus and due to undetermined uncertainties in the mixture compositions that resulted from leaks and design flaws in the mixing system. These data were not used in the final analysis, but may have some qualitative value. The sources of error were eliminated prior to flight 5.

Flight Test 1		Date: 6/19/85, A.M.	
Purpose: To establish the fuel-lean limit for zero g propagation of CH_4-air flames.			
Tube Number	Mixture Composition	Gravity Conditions, Direction of Propagation	Test Results
1	4.80% CH_4	0.00 g	misfire
2	4.90% CH_4	0.00 g	no propagation
3	5.00% CH_4	0.00 g	misfire
4	5.10% CH_4	0.00 g	skipped it
5	5.20% CH_4	0.00 g	misfire
6	5.30% CH_4	0.00 g	skipped it

Flight Test 2		Date: 6/20/85, P.M.	
Purpose: To establish the fuel-lean limit for zero g propagation of CH_4-air flames.			
Tube Number	Mixture Composition	Gravity Conditions, Direction of Propagation	Test Results
1	4.80% CH_4	1.00 g upward	no propagation
2	5.00% CH_4	1.00 g upward	no propagation
3	5.10% CH_4	1.00 g upward	partial propagation
4	5.20% CH_4	1.00 g upward	full propagation
5	5.40% CH_4	1.00 g upward	full propagation
6	5.60% CH_4	1.00 g upward	full propagation
7	5.20% CH_4	1.00 g upward	full propagation

Note: The flight was scrubbed due to an aircraft equipment malfunction and the tubes were subsequently fired on the ground.

Flight Test 3	Date: 6/21/85, A.M.

Purpose: To establish the fuel-lean limit for zero g propagation of CH_4-air flames.

Tube Number	Mixture Composition	Gravity Conditions, Direction of Propagation	Test Results
1	5.00% CH_4	0.00 g	no propagation
2	5.05% CH_4	0.00 g	no propagation
3	5.10% CH_4	0.00 g	partial propagation
4	5.10% CH_4	0.00 g	partial propagation
5	5.15% CH_4	0.00 g	misfire
6	5.25% CH_4	0.00 g	full propagation
7	5.10% CH_4	0.00 g	full propagation
8	5.15% CH_4	0.00 g	partial propagation

Flight Test 4		Date: 6/21/85, P.M.	
Purpose: To establish the fuel-lean limit for zero g propagation of CH_4-air flames.			
Tube Number	Mixture Composition	Gravity Conditions, Direction of Propagation	Test Results
1	5.10% CH_4	0.00 g	partial propagation
2	5.10% CH_4	0.10 g upward	full propagation
3	5.10% CH_4	0.17 g upward	full propagation
4	5.10% CH_4	0.25 g upward	full propagation
5	5.10% CH_4	0.33 g upward	full propagation
6	5.10% CH_4	0.50 g upward	full propagation
7	5.10% CH_4	0.75 g upward	full propagation
8	5.10% CH_4	1.50 g upward	full propagation

Note: All eight tubes were filled simultaneously.

Flight Test 5		Date: 7/3/85, A.M.	
Purpose: To establish the fuel-lean limit for zero g propagation of CH_4-air flames.			
Tube Number	Mixture Composition	Gravity Conditions, Direction of Propagation	Test Results
1	4.90% CH_4	0.00 g	no propagation
2	5.00% CH_4	0.00 g	no propagation
3	5.10% CH_4	0.00 g	no propagation
4	5.10% CH_4	0.00 g	skipped it
5	5.10% CH_4	0.00 g	skipped it
6	5.10% CH_4	0.00 g	skipped it
7	5.20% CH_4	0.00 g	full propagation
8	5.30% CH_4	0.00 g	full propagation

Flight Test 6		Date: 7/3/85, Noon	
Purpose: To establish the fuel-lean limit for zero g propagation of CH_4-air flames.			
Tube Number	Mixture Composition	Gravity Conditions, Direction of Propagation	Test Results
1	5.10% CH_4	0.00 g	partial propagation
2	5.15% CH_4	0.00 g	partial propagation
3	5.15% CH_4	0.00 g	partial propagation
4	5.20% CH_4	0.00 g	partial propagation
5	5.20% CH_4	0.00 g	partial propagation
6	5.20% CH_4	0.10 g upward	full propagation
7	5.20% CH_4	0.17 g upward	full propagation
8	5.25% CH_4	0.00 g	full propagation

Note: The film record of tube 1 appears at the end of the reel for Flight Test 5.

Flight Test 7	Date: 7/25/85, P.M.

Purpose: To establish the fuel-lean limit for zero g propagation and to collect constant fractional g data for upward propagation of CH_4-air flames.

Tube Number	Mixture Composition	Gravity Conditions, Direction of Propagation	Test Results
1	5.10% CH_4	0.17 g upward	misfire
2	5.20% CH_4	0.17 g upward	full propagation
3	5.25% CH_4	0.17 g upward	full propagation
4	5.30% CH_4	0.17 g upward	full propagation
5	5.35% CH_4	0.17 g upward	misfire
6	5.40% CH_4	0.17 g upward	misfire
7	5.30% CH_4	0.17 g upward	full propagation
8	5.30% CH_4	0.00 g	misfire

Note: Originally, tubes 1 through 6 were intended to be fired in zero g, but the cockpit display was inadvertently set on 0.17 g. Tubes 7 and 8 were filled simultaneously. Also, the top camera was running at 18 instead of 24 frames per second.

Flight Test 8		Date: 7/26/85, P.M.	
Purpose: To establish the fuel-lean limit for zero g propagation of CH_4-air flames.			
Tube Number	Mixture Composition	Gravity Conditions, Direction of Propagation	Test Results
1	5.20% CH_4	0.00 g	no propagation
2	5.15% CH_4	0.00 g	no propagation
3	5.10% CH_4	0.00 g	no propagation
4	5.05% CH_4	0.00 g	skipped it
5	5.00% CH_4	0.00 g	skipped it
6	4.90% CH_4	0.00 g	skipped it
7	5.23% CH_4	0.00 g	full propagation
8	5.23% CH_4	0.00 g	full propagation

Note: Top camera was running at 18 instead of 24 frames per second.

Flight Test 9	Date: 7/30/85, P.M.

Purpose: To establish the fuel-lean limit for zero g propagation and to collect constant fractional g data for upward propagation of CH_4-air flames.

Tube Number	Mixture Composition	Gravity Conditions, Direction of Propagation	Test Results
1	5.30% CH_4	0.00 g	full propagation
2	5.28% CH_4	0.00 g	partial propagation
3	5.26% CH_4	0.00 g	full propagation
4	5.24% CH_4	0.00 g	full propagation
5	5.22% CH_4	0.00 g	partial propagation
6	4.20% CH_4	0.00 g	full propagation
7	5.28% CH_4	0.10 g upward	full propagation
8	5.28% CH_4	0.17 g upward	full propagation

Note: Top camera was running at 18 instead of 24 frames per second. Tubes 7 and 8 were filled simultaneously.

Flight Test 10	Date: 7/31/85, A.M.

Purpose: To confirm the results obtained for Flight Test 9 and collect constant fractional g data for upward propagation of fuel-lean CH_4 -air flames.

Tube Number	Mixture Composition	Gravity Conditions, Direction of Propagation	Test Results
1	5.30% CH_4	0.00 g	misfire
2	5.28% CH_4	0.00 g	full propagation
3	5.26% CH_4	0.00 g	no propagation
4	5.24% CH_4	0.00 g	no propagation
5	5.22% CH_4	0.00 g	no propagation
6	4.20% CH_4	0.00 g	no propagation
7	5.28% CH_4	0.25 g upward	no propagation
8	5.28% CH_4	1.00 g upward	partial propagation

Flight Test 11		Date: 8/1/85, A.M.	
Purpose: To collect constant fractional g data for upward propagation of fuel-lean CH_4-air flames.			
Tube Number	Mixture Composition	Gravity Conditions, Direction of Propagation	Test Results
1	5.30% CH_4	0.00 g	full propagation
2	5.30% CH_4	0.10 g upward	full propagation
3	5.30% CH_4	0.17 g upward	full propagation
4	5.30% CH_4	0.25 g upward	full propagation
5	5.30% CH_4	0.33 g upward	no propagation
6	5.30% CH_4	0.50 g upward	full propagation
7	5.30% CH_4	0.75 g upward	full propagation
8	5.30% CH_4	1.00 g upward	misfire

Note: All eight tubes were filled simultaneously.

Flight Test 12		Date: 8/1/85, P.M.	
Purpose: To confirm the zero g fuel-lean limit for upward propagation of CH_4 -air flames.			
Tube Number	Mixture Composition	Gravity Conditions, Direction of Propagation	Test Results
1	5.30% CH_4	0.00 g	full propagation
2	5.30% CH_4	0.33 g upward	misfire
3	5.30% CH_4	0.33 g upward	misfire
4	5.25% CH_4	0.00 g	no propagation
5	5.20% CH_4	0.00 g	full propagation
6	5.15% CH_4	0.00 g	full propagation
7	5.20% CH_4	1.00 g upward	partial propagation (no film record)
8	5.25% CH_4	0.00 g	full propagation

Note: Tubes 1 through 3 were filled simultaneously. The order that the tubes appear in the film record is 1, 4, 5, 6, 8, 2, and 3.

Flight Test 13		Date: 10/1/85, P.M.	
Purpose: To confirm the fuel-lean limit for zero g propagation and to collect transient g data for upward propagation of fuel-lean CH_4-air flames.			
Tube Number	Mixture Composition	Gravity Conditions, Direction of Propagation	Test Results
1	5.15% CH_4	0.00 g	no propagation
2	5.25% CH_4	transient g upward (due to delayed firing)	full propagation
3	5.15% CH_4	0.00 g	no propagation
4	5.25% CH_4	0.00 g	partial propagation
5	5.30% CH_4	transient g upward	full propagation
6	5.30% CH_4	transient g upward	full propagation
7	5.30% CH_4	1.50 g upward	partial propagation
8	5.30% CH_4	1.00 g upward	partial propagation

Flight Test 14		Date: 10/2/85, A.M.	
Purpose: To collect constant fractional g data for upward propagation of fuel-lean CH_4-air flames.			
Tube Number	Mixture Composition	Gravity Conditions, Direction of Propagation	Test Results
1	5.30% CH_4	0.00 g	full propagation
2	5.30% CH_4	0.10 g upward	full propagation
3	5.30% CH_4	0.17 g upward	full propagation
4	5.30% CH_4	0.25 g upward	no propagation
5	5.30% CH_4	0.33 g upward	full propagation
6	5.30% CH_4	0.50 g upward	full propagation (no film record)
7	5.30% CH_4	1.00 g upward	full propagation (no film record)
8	5.30% CH_4	1.50 g upward	partial propagation (no film record)

Note: All eight tubes were filled simultaneously.

Flight Test 15			Date: 10/2/85, P.M.
Purpose: To establish the fuel-lean limit for zero g propagation of C_3H_8-air flames.			
Tube Number	Mixture Composition	Gravity Conditions, Direction of Propagation	Test Results
1	2.00% C_3H_8	0.00 g	partial propagation

Note: The flight had to be aborted due to failure of the solenoid valve on the flammability limit apparatus and the remaining tubes, 2 through 8, could not be fired.

Flight Test 16	Date: 10/3/85, P.M.

Purpose: To establish the fuel-lean limit for zero g propagation of C_3H_8-air flames.

Tube Number	Mixture Composition	Gravity Conditions, Direction of Propagation	Test Results
1	2.00% C_3H_8	0.00 g	no propagation
2	2.10% C_3H_8	0.00 g	full propagation
3	2.20% C_3H_8	0.00 g	full propagation
4	2.30% C_3H_8	0.00 g	full propagation
5	2.40% C_3H_8	0.00 g	full propagation
6	2.40% C_3H_8	1.00 g upward	full propagation
7	2.40% C_3H_8	1.00 g upward	full propagation (no film record)
8	2.50% C_3H_8	0.00 g	full propagation

Flight Test 17	Date: 10/3/85, P.M.

Purpose: To establish the fuel-lean limit for zero g propagation of C_3H_8-air flames and to collect constant fractional g data.

Tube Number	Mixture Composition	Gravity Conditions, Direction of Propagation	Test Results
1	1.95% C_3H_8	0.00 g	no propagation
2	2.00% C_3H_8	0.00 g	no propagation
3	2.05% C_3H_8	0.00 g	full propagation
4	2.10% C_3H_8	transient g upward (due to delayed firing)	partial propagation
5	2.15% C_3H_8	0.00 g	full propagation
6	2.20% C_3H_8	0.00 g	full propagation
7	2.20% C_3H_8	0.10 g upward	full propagation
8	2.20% C_3H_8	0.17 g upward	full propagation

Note: Tubes 6 through 8 were filled simultaneously.

Flight Test 18	Date: 10/4/85, A.M.

Purpose: To establish the fuel-lean limit for zero g propagation of C_3H_8-air flames and to collect constant fractional g data.

Tube Number	Mixture Composition	Gravity Conditions, Direction of Propagation	Test Results
1	2.00% C_3H_8	0.00 g	partial propagation
2	2.02% C_3H_8	0.00 g	full propagation
3	2.04% C_3H_8	0.00 g	full propagation
4	2.06% C_3H_8	0.00 g	full propagation
5	2.08% C_3H_8	0.00 g	full propagation
6	2.10% C_3H_8	0.00 g	full propagation (no film record)
7	2.20% C_3H_8	0.25 g upward	full propagation (no film record)
8	2.20% C_3H_8	0.33 g upward	full propagation (no film record)

Note: Tubes 7 and 8 were filled simultaneously.

Flight Test 19		Date: 10/7/85, A.M.	
Purpose: To collect constant fractional g data for upward propagation of fuel-lean C_3H_8-air flames.			
Tube Number	Mixture Composition	Gravity Conditions, Direction of Propagation	Test Results
1	2.30% C_3H_8	0.00 g	full propagation
2	2.30% C_3H_8	0.10 g upward	full propagation
3	2.30% C_3H_8	0.17 g upward	full propagation
4	2.30% C_3H_8	0.25 g upward	full propagation
5	2.30% C_3H_8	0.33 g upward	full propagation
6	2.30% C_3H_8	0.50 g upward	full propagation
7	2.30% C_3H_8	0.75 g upward	full propagation
8	2.30% C_3H_8	1.00 g upward	full propagation

Note: All eight tubes were filled simultaneously.

Flight Test 20		Date: 10/7/85, P.M.	
Purpose: To confirm the fuel-lean limit for zero g propagation of C_3H_8-air flames and to collect zero g data for richer mixtures.			
Tube Number	Mixture Composition	Gravity Conditions, Direction of Propagation	Test Results
1	2.02% C_3H_8	0.00 g	no propagation
2	2.04% C_3H_8	0.00 g	full propagation
3	2.06% C_3H_8	0.00 g	full propagation
4	2.08% C_3H_8	0.00 g	no propagation
5	2.60% C_3H_8	0.00 g	full propagation
6	2.70% C_3H_8	0.00 g	full propagation

Flight Test 21	Date: 10/8/85, A.M.

Purpose: To confirm the zero g fuel-lean limit, to collect zero g data for richer mixtures, and to collect constant fractional and transient g data for C_3H_8-air mixtures.

Tube Number	Mixture Composition	Gravity Conditions, Direction of Propagation	Test Results
1	2.08% C_3H_8	0.00 g	full propagation
2	2.80% C_3H_8	0.00 g	full propagation
3	2.90% C_3H_8	0.00 g	full propagation
4	3.00% C_3H_8	0.00 g	full propagation
5	2.30% C_3H_8	transient g upward	full propagation
6	2.30% C_3H_8	transient g upward	full propagation
7	2.30% C_3H_8	1.50 g upward	full propagation
8	2.30% C_3H_8	1.50 g upward	full propagation

Note: Tubes 5 through 8 were filled simultaneously.

Flight Test 22		Date: 10/9/85, A.M.	
Purpose: To collect zero g data for richer mixtures and to collect constant fractional and transient g data for CH_4-air mixtures.			
Tube Number	Mixture Composition	Gravity Conditions, Direction of Propagation	Test Results
1	5.40% CH_4	0.00 g	full propagation
2	5.50% CH_4	0.00 g	full propagation
3	5.60% CH_4	0.00 g	full propagation
4	5.70% CH_4	0.00 g	full propagation
5	5.30% CH_4	transient g upward	full propagation
6	5.30% CH_4	0.50 g upward	no propagation (no film record)
7	5.30% CH_4	0.75 g upward	full propagation (no film record)
8	5.30% CH_4	1.50 g upward	misfire (no film record)

Note: Tubes 5 through 8 were filled simultaneously.

Flight Test 23	Date: 10/9/85, P.M.

Purpose: To collect zero g data for richer CH_4-air mixtures and to collect constant fractional and transient g data for CH_4-air and C_3H_8-air mixtures.

Tube Number	Mixture Composition	Gravity Conditions, Direction of Propagation	Test Results
1	5.80% CH_8	0.00 g	full propagation
2	5.90% CH_8	0.00 g	full propagation
3	6.00% CH_8	0.00 g	full propagation
4	6.20% CH_8	0.00 g	full propagation
5	5.25% CH_8	transient g upward	full propagation
6	2.05% C_3H_8	transient g upward	no propagation
7	5.30% CH_8	1.50 g upward	partial propagation
8	5.30% CH_8	1.50 g upward	partial propagation

Note: Tubes 7 and 8 were filled simultaneously.

Flight Test 24		Date: 10/10/85, A.M.	
Purpose: To collect transient g data for downward propagation of extinguishing and nonextinguishing fuel-lean C_3H_8-air flames.			
Tube Number	Mixture Composition	Gravity Conditions, Direction of Propagation	Test Results
1	2.30% C_3H_8	transient g downward	partial propagation
2	2.40% C_3H_8	transient g downward	full propagation
3	2.50% C_3H_8	transient g downward	skipped it
4	2.60% C_3H_8	transient g downward	skipped it
5	2.10% C_3H_8	transient g downward	partial propagation
6	2.20% C_3H_8	transient g downward	partial propagation
7	2.20% C_3H_8	transient g downward	partial propagation
8	2.25% C_3H_8	transient g downward	full propagation

Flight Test 25		Date: 10/10/85, P.M.	
Purpose: To collect transient g data for downward propagation of extinguishing and nonextinguishing fuel-lean CH_4-air flames.			
Tube Number	Mixture Composition	Gravity Conditions, Direction of Propagation	Test Results
1	5.70% CH_4	transient g downward	full propagation
2	5.90% CH_4	transient g downward	partial propagation
3	6.00% CH_4	transient g downward	misfire
4	6.10% CH_4	transient g downward	misfire
5	6.10% CH_4	transient g downward	misfire
6	6.20% CH_4	transient g downward	skipped it
7	6.30% CH_4	transient g downward	skipped it
8	6.40% CH_4	transient g downward	partial propagation

Note: Misfires were caused by a problem with the igniters. The exact cause of the problem was not determined.